Department of Biomedical Engineering

Eindhoven University of Technology

To design a Human Powered Aircraft

Multi-body modelling of recumbent cycling: An optimisation of configuration and cadence

Master's Thesis

Pamela de Jong

E-mail: PameladeJong@gmail.com

BMT1998/ s458398

06/2006

Supervisors:

Dr. K. Meijer	(BW, UM)
Prof. dr. A. Wagenmakers	(BMT, TU/e)
Dr. ir. M. de Zee	(AnyBody, Aalborg)

Committee Members:

Prof. dr. P.A.J. Hilbers	(BMT, TU/e)
Dr. H.H.C.M. Savelberg	(BW, UM)
Prof. dr. ir. F.N. van de Vosse	(BMT, TU/e)

Samenvatting

Doel:

Deze studie is opgezet om een lange-afstand recordpoging in een mens-aangedreven vliegtuig te bevorderen. Het maakt deel uit van 'Team Icarus' dat het huidige record van 115 km wil verbreken. Hierbij is het van belang piloten zo weinig mogelijk energie verspillen. De piloten zijn gepositioneerd in ligfietshouding in een kleine cabine waar warmteproductie direct de prestatie zou kunnen beïnvloeden. Voor de ligfietspositie is weinig bekend over de optimale houding en cadans. De huidige kennis in literatuur beperkt zich tot ergonomie en verdraaiing van biomechanische functies met verandering van de zadelpositie. Daarom wordt er in deze studie gezocht naar de optimale ligfietshouding in combinatie met de optimale cadans, waarbij energieverbruik geminimaliseerd wordt. Een andere benadering voor het voorkomen van vroegtijdige vermoeidheid, is optimalisatie van piekactiviteit van de onderbeenspieren. Hierbij word naar de houding gezocht waarbij niet een enkele spier uitzonderlijk hoog wordt geactiveerd. Deze twee optimalisatie objectieven zullen in deze studie worden vergeleken en experimenteel worden gevalideerd. Daarnaast wordt bestudeerd of achteruittrappen mogelijk een voordeliger traptechniek is met het oog op deze objectieven.

Methodes:

Optimalisatie van de houding en cadans is gedaan aan de hand van een multi-body software pakket 'AnyBody'. Hierin is een ligfietsmodel gecreëerd van het onderlichaam bestaande uit realistische representaties van botten, gewrichten en 35 spieren per been. Het model is gecontroleerd aan de hand van experimentele data verkregen uit een voorgaande studie. Het model berekent verdeling van pedaalkrachten, individuele spierkrachten, spieractivaties, en verkortingssnelheden met behulp van het min-max criterion. Optimalisatie van de piekactiviteit kan direct worden toegepast op dit model. Voor de berekening van het energieverbruik is echter een energie model toegevoegd, gebaseerd op een studie van Umberger. Met behulp van dit aangekoppelde energiemodel, is het mogelijk om de houding en cadans met minst energie verbruik te zoeken.

De gesimuleerde optima zijn gevalideerd met een experimentele studie. Dezelfde proefpersonen als voor model controle, hebben deelgenomen aan het experiment. In het experiment zijn de gesimuleerde optimale houdingen zo goed mogelijk ingebracht. Tijdens iedere houding zijn de volgende variabelen gemeten; EMG activiteit, pedaalkrachten, kinematica en zuurstofgebruik.

Resultaten:

De optimalisatie studie resulteerde in verschillende configuraties voor minimale piekactiviteit en minimaal energie verbruik. Tevens bleken optimale cadans en optimale zadelpositie afhankelijk van elkaar te zijn. Het energie model resulteerde in aannemelijke waarden voor efficiëntie. Verder bleek de optimalisatie van piekactivaties van het onderbeen te leiden tot minimalisatie van extreme spieractiviteiten, zoals verwacht. Achteruit trappen bleek niet efficiënter dan vooruit trappen.

Het onderscheid dat gemaakt is in de simulatiestudie voor energieverbruik en piekactiviteit, bleek lastig te destilleren uit de experimentele studie. Trends zoals gevonden voor energieverbruik en piek activiteit in de simulatie zijn niet teruggevonden in de experimentele setting. Wel bleek het model een adequate voorspeller te zijn voor pedaalkrachten en spier activiteiten.

Conclusie:

Een goede start is gemaakt voor het vinden van de optimale houding tijdens het ligfietsen. Er is een adequate basis gelegd voor het optimaliseren van houding en cadans in het ligfietsen in een 'AnyBody' computer model. Ondanks dat trends zoals gevonden in het simulatie model voor energieverbruik en piek activiteit niet zijn gevonden in de experimentele setting, bleek het model een goede voorspeller te zijn voor pedaalkrachten en activatie tijden. Het is aangetoond dat optimale zitpositie gerelateerd is aan de optimale cadans. Biomechanische functies bleken te transformeren consistent met voorgaande literatuur voor zadelverplaatsing en literatuur voor vooruit en achteruit trappen in de conventionele houding. Tevens resulteerde het gekoppelde energiemodel in waarschijnlijke waarden, maar nadere validatie is wenselijk.

Abstract

Background:

This study has arisen from the aim to break the long distance record by a Human Powered Aircraft. It is part of the work done by 'Team Icarus' that is going to make this record attempt. For this attempt, it is of great importance that the pilots waste a minimum amount of energy. The pilots are positioned in a recumbent configuration in a small cabin, in which heat production could be of direct influence on performance. Current knowledge on recumbent cycling is restricted to ergonomics and tuning of biomechanical functions with seat position. The aim of this study is therefore to find an optimal recumbent position in combination with an optimal cadence by minimising energy expenditure. Another approach for preventing premature fatigue is optimisation of peak activation of lower extremity muscles. With this approach, a configuration is searched for at which single muscles are not activated exceptionally high. In this study, these two objectives will be compared to each other and the experimentally validated. In addition, it is studied whether backwards pedalling might be more efficient with respect to these objectives.

Methods:

Optimisation of configuration and cadence is performed by means of the multi-body software package 'AnyBody'. With this software, a recumbent cycling model is created of the lower extremity, consisting of realistic representations of bones, joints, and 35 muscles. The model is checked with experimental data taken from previous research. The model calculates the distribution of pedal forces, individual muscle forces, muscle activities and shortening speeds by means of the min-max criterion. Optimisation of peak activation can be directly applied to this model. However, to calculate energy expenditure a separate model based on a study of Umberger is implemented in 'Matlab'. With this model, it is possible to search for the configuration and cadence that will minimize energy expenditure.

The simulated optima were experimentally validated. The subjects, whose data were used to test the model check, also participated in the experiments. In the experimental setting, predicted optimal configurations were implemented as accurate as possible. In each configuration, EMG data, kinematics, pedal forces and oxygen consumption were measured.

Results:

The optimisation for minimal energy expenditure and minimal peak activation resulted in different configurations and cadences. Optimal cadence and optimal configuration appeared to depend on each other. The energy model resulted in plausible values for efficiency. Furthermore, optimisation of peak activation resulted in minimisation of extreme muscle activations, as expected. Backwards cycling was not found to be more efficient in comparison to forwards pedalling.

The distinction that was made in the simulation study for energy expenditure and peak activation was difficult to validate experimentally. Trends as found for the simulation study were not seen in the experimental data. Nevertheless, the model appeared to be a good predictor for pedal forces and muscle activations.

Conclusion:

A good start has been made to search the optimal cadence in combination with the optimal configuration. A solid foundation was laid for a recumbent cycling optimisation model. Although trends for energy expenditure and peak activation were not similar between simulations and experiments, the model appeared to be a good predictor for pedal forces and muscle activation. The energy expenditure model that is applicable to all 'AnyBody' models resulted in plausible values for efficiencies, but further research will be necessary. Furthermore, a relation between optimal cadence and optimal configuration was found. Biomechanical functions found for seat transformation and for forward versus backwards cycling were consistent with previous studies.

Contents

General introduction

This study results from the challenge to break the long distance world record of flying a Human Powered Aircraft (HPA). The current long distance record is held by 'Team Daeldolus' of the Massachusetts Institute of Technology. Their single-seated HPA flew over a distance of 115 km in 3 hrs and 55 minutes. The present study is part of the work done by 'Team Icarus', who wants to break the world record by a double-seated HPA. The two main items to focus on when building an HPA are a good aircraft design and an efficient 'human motor'. The efficiency of the human motor is determined by several factors, with thermoregulation, good nourishment, fluid ingestion, optimal physical performance by training and by a proper configuration being the most important factors.

Conquering air resistance costs approximately 80% of the total energy. Therefore, to decrease the drag, the two pilots will be seated in a lying (recumbent) configuration positioned back-to-back, as demonstrated in figure 1. They will drive the propellers by pedalling.

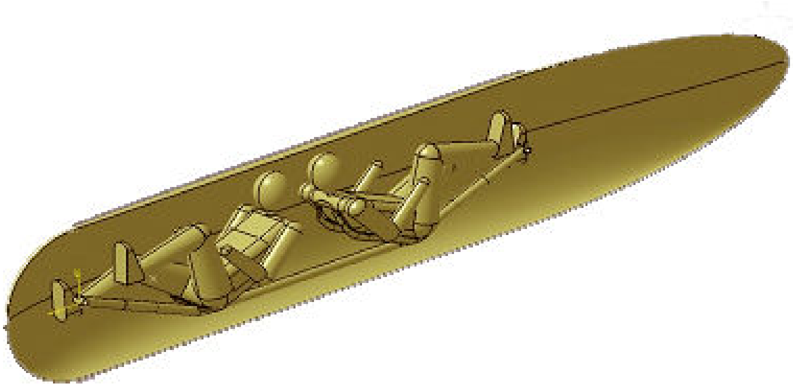

Figure 1 *Recumbent back-to back positioning of pilots in a double seated HPA*

The recumbent configuration might result in changes in the task performance compared to the conventional cycling configuration, because of the change of orientation in the gravity field. The effect of change in configuration on efficiency in task performance has not yet been studied.

The main aim of the current study is to increase human body performance in long endurance recumbent cycling. During the flight, the pilots will be seated in a small closed carbon cabin and they have to pedal for at least 4 hours at 200 W. During this period, which is comparable to a stage in the Tour de France, a lot of heat is produced, since approximately 75% of the total work done by skeletal muscles is lost as heat; only about 25% is mechanical work. Heat reduction can be handled in two ways: a good heat outlet or reducing the heat production. Reducing heat production is the first of the two methods to increase body performance in this study.

Bicycle settings, cadence and muscle build are the factors that influence energy expenditure most. Changes in the bicycle configuration and cadence lead to a different length at which the muscle deliver force, which can cause different energy consumption as will be outlined later on. The current study focuses on searching a proper bicycle configuration and a proper cadence to result in a maximum duration flight with the longest possible reach. Accordingly, the first definition of optimal recumbent pedalling is made as the configuration and cadence with least energy expenditure for a given mechanical output.

Several studies showed that muscle metabolism might not be a key determinant for the optimal pedalling configuration. They found equal energy expenditures between various configurations and cadences or even lowest energy expenditures at configuration and cadences different from those preferred by the cyclists [1-6]. Considering a preferred configuration and a preferred cadence as optimal pedalling, other mechanisms than minimised energy expenditure must play a role in defining optimal configuration. Therefore, a second focus is defined to study. This is the configuration with minimised peak activation level. The peak activation level is defined as the highest value of all maximum activation levels reached by the individual lower leg muscles. Early fatigue of a pilot due to over-activation of a single muscle is thereby minimised.

In addition to studying optimal configuration in recumbent cycling, pedalling technique is considered. Previous research indicated that backwards pedalling has a mechanical advantage over forward pedalling [7]. A dynamic model showed that during the backward movement the power stroke is longer compared to forward recumbent cycling. Whether backward pedalling is also energetically more efficient is questionable and therefore tested in this study.

To find the optimal configurations, a computer model based on AnyBody software is used. This model is a multi-body system that represents skeletal bones and muscles, which is visualised in figure 2.

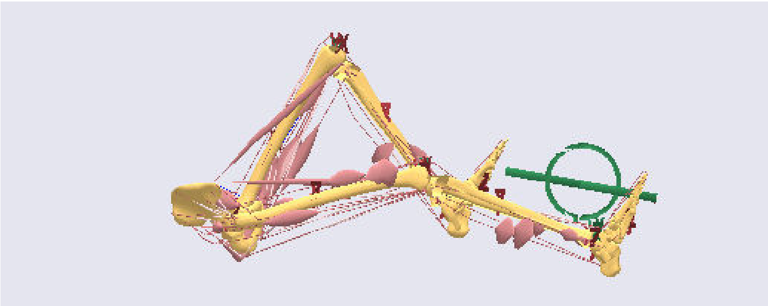

Figure 2 *Visualisation of an AnyBody recumbent cycling model*

A computer model has several advantages over an experimental approach. It can simulate a broad range of configurations without fatigue playing a role in the subject. Unlike the experimental set-up, environmental influences can be kept constant, which allows for changing a single variable. A third advantage is that individual muscle activations can be studied, which is experimentally limited to a few muscles. Moreover, activation amplitudes of individual muscles in an experimental setting are difficult to compare to each other as will be explained later in this study. Individual contributions of muscles to energy expenditures are even impossible to study in an experimental setting. Furthermore, a good simulation model can function as a predictive model that can calculate optimal configurations subject specific.

The model used, consists of 27 muscles per leg. The software calculates individual muscle activation levels relative to the maximal isometric force and also calculates individual muscle force contributions for each configuration. The initial model was a conventional cycling model that had to be translated to a recumbent configuration in this study. To minimise energy expenditure, an energy model by Umberger [8] written in the Matlab language was added to the new recumbent model. At each configuration, energy expenditure can now be calculated, which facilitates the search for an optimal configuration.

The simulation model is a simplification of the human body. To validate the simulation model, an experimental study is performed. The optimal configurations found in the simulation model are applied experimentally and their outcomes are compared to the simulation results.

In summary, the aim of this study is to find an optimal recumbent cycling configuration and cadence. In which optimal is defined as minimised energy expenditure or minimised peak activation level. To achieve this goal, a start is made on creating a predictive model and the predictive characteristics of the model were explored experimentally as well. In addition, an introduction to compare the forward pedalling technique to a backward pedalling technique has also been made.

In Chapter 1 muscle categorisation, muscle synergy, and aspects of conventional cycling will be described. Also, the differences between conventional and recumbent cycling are described to get a good understanding of recumbent cycling. Chapter 2 describes how the characteristics of recumbent cycling are implemented in the simulation model. Chapter 3 describes the optimisation study used to search the optimal bicycle configuration and cadence. The experimental validation of the model is described in Chapter 4. General recommendations and conclusive remarks will complete this report.

Chapter 1: Aspects of and Muscle Contributions to Cycling

This study focuses on muscle use in the lower extremity during cycling. Therefore, the most important leg muscles (27 in total) and their function during propulsion will be outlined. A review of cycling aspects in conventional cycling will be the basis for a solid understanding of the recumbent propulsion. Several variables that have been found to affect metabolic rate and muscle activity in conventional cycling will therefore be described.

1.1 Lower extremity muscle categorisation

Leg muscles can be categorized in several ways. The classic approach based on anatomical position divides muscles in extensors, flexors, abductors, adductors and rotators. Extensors and flexors extend or flex a joint, moving the leg in the sagital plane, whereas abductors and adductors move the leg in the frontal plane. In this study, the main focus will be on the extensors and the flexors since the pedalling cycle can be considered as a two-dimensional movement, mainly directed in the sagital plane. Yet, the abductors and adductors have been taken into account for higher accuracy. This is because during movement, most abductors and adductors have an extensor or flexor component as well.

A functional classification divides the muscles in mono- and bi-articular muscles. Mono-articular muscles flex or extend a single joint by direct power delivery, whereas bi-articular muscles cross two joints. The moment distribution will then be over two joints and thereby align external the force in the favoured direction. [9]. A table of the categorisation of all considered 27 leg muscles can be found in Appendix A.

An alternative functional approach is a categorisation of the muscles in antagonistic pairs. Each of the mono- or bi-articular flexors and extensors contribute to one of these pairs. Figure 3 shows the division of the pedalling cycle in six different biomechanical functions. Each phase represents a state of the leg with respect to the end point, to which the muscles can be assigned. The duration of each phase can be helpful in studying muscle activation during the pedalling cycle. This categorisation was chosen for this study. The six functions are grouped in three functional pairs. These are the extensor/flexor pair (EXT/FLEX), the posterior/anterior pair (POST/ANT) and the dorsal flexor/plantar flexor pair (DORS/PLANT) [10, 11]. The EXT/FLEX extends or flexes the limb (foot accelerated away from and toward the pelvis respectively), the PLANT/DORS flexes the foot plantarly or dorsally, and finally POST/ANT shifts the foot anteriorly or posteriorly relatively to the pelvis [10, 11]. Some muscles can contribute to two functions. The muscles contributing to each phase in conventional and recumbent cycling will be described in sections 1.2 and 1.3 respectively.

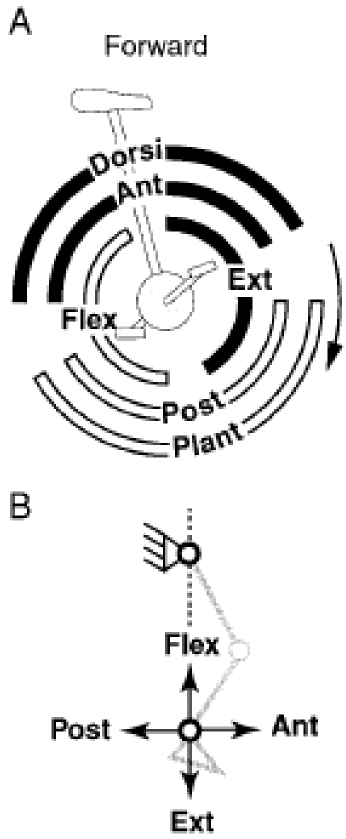

Figure 3 *A. Antagonistic pairs in conventional cycling. B. Extensor/Flexor pair is responsible for moving the foot away or towards the limb respectively. The Posterior/Anterior pair moves the foot posteriorly or anteriorly with respect to the pelivis. The dorsi/plantar pair flexes the ankle plantarly or dorsally [11]*

1.2 Conventional cycling

Definitions and muscle synergy

To investigate maximum performance, several conditions that affect this performance need to be studied. These are thoroughly discussed in literature for conventional cycling, but much less information can be found on recumbent cycling. Subsequently, the effects of changing variables in recumbent cycling are unknown. Since conventional cycling and recumbent cycling are expected to be relatively similar movements, knowledge on conventional cycling can be used to estimate the optimal recumbent cycling movement. The main conditions that affect muscle activity and energy consumption will be highlighted later in this section. These are cadence, trunk angle, seat height and seat distance.

First, conventional cycling needs to be defined. In conventional cycling the body position is upright and thus with leg position perpendicular to the ground.

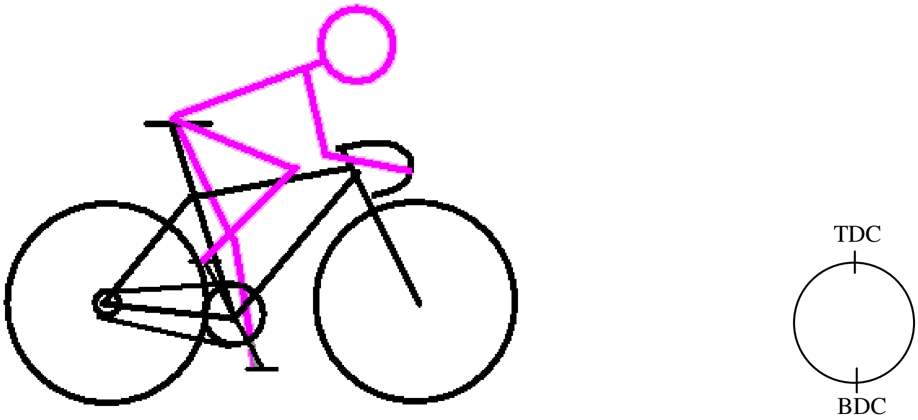

Figure 4 *The conventional cycle position. On the right the top dead centre (TDC) and bottom dead centre (BDC) in the crank cycle. In TDC flexion turns into extension and in BDC the opposite occurs.*

Figure 4 illustrates the conventional cycling position. As can be seen in this picture, the seat is located above the crank. The seat tube angle, which is the angle between seat and crank, differs per bicycle. Support is given from the saddle to the ischium from a single location between the legs. Two dead centres appear during the pedalling cycle: at the top where flexion becomes extension and exactly opposite at the bottom of the cycle. Gravity strengthens dead centre positioning, because in bottom dead centre and top dead centre it is directed parallel to the crank. The dead centres hamper the transitions of the leg through these points. The standard crank length is 17 cm.

Muscle activation during the pedalling cycle is the next important issue to look at. In section 1.1 the categorisation of the leg muscles contributing to each biomechanical function is described. Figure 5 shows the most relevant muscles contributing to the pedalling cycle. Abbreviations of these as repeatedly mentioned in this report are also given.

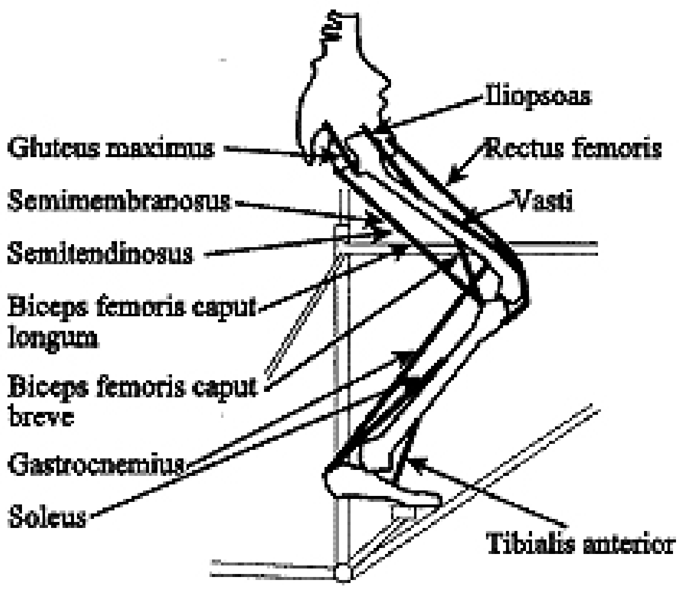

Figure 5 *Position of most relevant leg muscles and their abbreviations as used in this report [12]*

Gluteus Maximus	GM
Semimembranosus	SM
Biceps Femoris caput longum	BF
Gastrocnemius	GC
Soleus	SL
Iliopsoas	PS
Rectus Femoris	RF
Vastus Medialis	VM
Tibialis Anterior	TA

As mentioned, each muscle contributes to one or two of the six biomechanical functions. For conventional cycling these functions were shown in figure 3. The classification of the leg muscles per biomechanical function is shown in table 1.

Table 1 *Muscles contributing to each biomechanical function during conventional cycling. Biomechanical functions are defined as the effect of movement on the end-point of the leg. Ext= extension phase, Flex= flexion phase, Ant= Anterior movement, Post=posterior movement, Dorsi=dorsal flexion, Plant= plantar flexion*

Function	Ext	Flex	Ant	Post	Dorsi	Plant
Muscles	VM	PS	RF	BF	TA	SL
	GM	TA		SM		GC
	SL	GC				
	RF	SM				
	BF					

Changing trunk angle, seat position and cadence can affect these biomechanical functions by changing muscle activation patterns. Subsequently, peak activation, which is a minimisation determinant in this study, is also influenced. Furthermore the other determinant of this study, muscle energy expenditure, is highly dependent on muscle activation [8]. Subsequently, cadence and seat position directly affect muscle efficiency.

Literature uses several definitions of efficiency. Gaesser et al. [4] formulated 4 definitions of efficiency. These are:

- Gross efficiency = mechanical work accomplished/ Energy expenditure
- Net efficiency = mechanical work accomplished/ (Energy expenditure-energy expenditure during rest)
- Work efficiency = mechanical work accomplished/ (Energy expenditure- energy expenditure measured in unloaded cycling)
- Delta efficiency =change in mechanical work accomplished/change in energy expenditure at increased mechanical work delivery measured at increased power output

The effect of seat position and cadence on efficiency has been studied by several researchers and will be discussed below.

In addition to efficiency, variations in seat positions and cadences were also expected to influence the peak activation levels. Each muscle has an optimal fibre length at which it delivers the highest force at a specific activation level. Figure 6 shows the force-length relationship of a muscle.

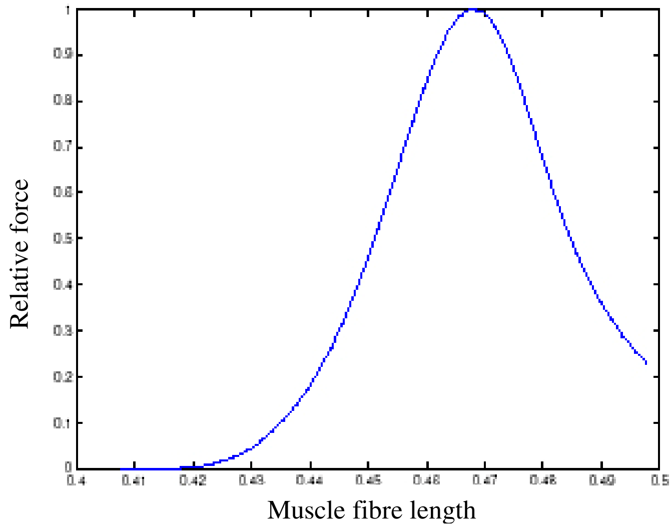

Figure 6 *An example of a force-length curve.*

Trunk angle, seat position and cadence affect the range of motion and shortening velocity of the muscles, thereby changing the length at which these have to deliver force. When muscle lengths lie closer to the optimal fibre length, the needed activation levels to obtain this force will be lower. Subsequently, peak activation level decreases. Both cadence and the individual seat position conditions that affect minimum peak activation and minimum energy expenditure will be separately discussed below.

Cadence

Cadence is the first variable considered affecting energy expenditure and peak activation. Like the force-length relationship as mentioned above, there is also a force-velocity relationship. It is clear that cadence influences the contraction velocity of the muscle. An example of a muscle force-velocity curve is shown in figure 7.

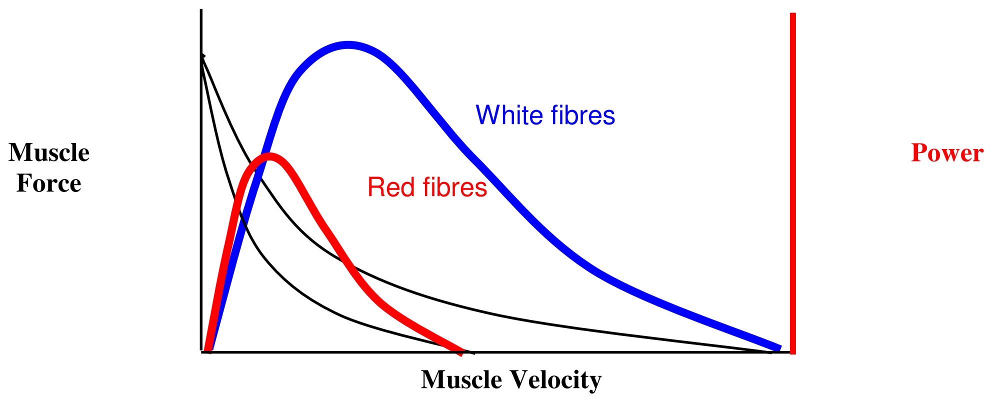

Figure 7 *An example of a force-velocity curve. Steepness and matching power delivery are dependent on fibre type distribution.*

Since power is the product of velocity and force an optimal velocity for maximum power results from this relationship. Each muscle has a contraction velocity at which maximum power can be delivered. Like in the force-length curve, lower activity levels are needed to reach a specific power when close to the optimal contraction velocity. As mentioned activation level directly affects energy expenditure and thus efficiency. This way both peak activation level as energy expenditure are affected by cadence.

Many researchers have studied the factors that determine the preferred cadence by cyclists. Preferred cadence is mostly found around 90rpm independent of training level. [6, 13, 14] Most studies found cadences lower than 90 rpm to be optimal as explained below. However, it needs to be taken into account that preferred cadence by cyclists is not considered optimal in the current study. As explained, for the HPA a minimum energy production and preventing premature fatigue by peak activation levels are.

Gaesser et al. found that when cadence increases (40, 60, 80 rpm), efficiency decreases at power outputs of up to 130W. This was found for all definitions of efficiency [4]. In contrast, Sidossis et al. [5] found a constant gross efficiency level for cadences of 60, 80 and 100 rpm at 80% and 90% $\dot{V}_{O_2\,\max}$ (maximal oxygen consumption), which was equal to 280 W and 300 W respectively. At low power outputs a decrease in gross efficiency was found, as was also seen in Gaesser and Brooks. They also found that delta efficiency increased at these high power outputs with increase of cadence. Sidossis'data were consistent with Faria et al.. The main difference between Gaesser et al. and Sidossis studies was that Sidossis used trained subjects and higher power outputs. It could be concluded that at high power outputs efficiency does not decrease.

Marsh et al. [13] examined the effect of cadence on delta efficiency more closely and included the effect of fitness level. Marsh et al. [13] found no trend for increase or decrease in delta efficiency at increase of cadence (50, 65, 80, 95,110 rpm) at each power output. These findings were regardless of fitness level or cycling experience (power was 75,100,150 W for less trained; 100,150,200W for trained subjects). Since the cyclists could cycle at a broad range of cadences without affecting delta efficiency, it could be said that change in energy expenditure is one-to-one related to power output. Finding optimal cadence at a specific power output should subsequently be searched for in a different way.

Marsh et al. [6] performed a similar experimental study to find the most economical cadence at specific power output. The most economical cadence is defined as the cadence at which oxygen consumption is minimized [6]. The most economical cadence was not influenced by increase in power output (75,100,125, 150 W for less trained; 75,100,150,200W for trained subjects), or fitness level and was found to be 53-60 rpm [6]. The most economical cadence is found to much lower that the preferred cadence by cyclists. For preferred cadence other mechanisms might play a role. Since in this study it is wishful to decrease energy production, this is still one of the determinants chosen for optimisation.

Another method for studying optimal cadence was performed by McIntosh [15], who found that muscle activation was minimised at higher cadences with increase of power output. McIntosh [15] used minimum activation (the root mean square of the EMG data), which appeared to depend on power output. Power outputs studied were high, namely 100, 200, 300 and 400W. The optimal cadences were found to be at approximately 60, 70, 85, 100 rpm for these power outputs respectively. Since it is expected that peak activation level will be determined by multiple muscles in the optimal situation (thus after eliminating the peak), this effect is also expected to be seen when minimising peak activation level. The power output in this study is set to 175 Watt and therefore optimal cadence is expected to be found around 70rpm for minimum peak activation.

All mentioned research studies indicated that the determinants investigated, might not be key determinants. Their findings showed lower rates compared to preferred cadence that was approximately 90 rpm at sub-maximal activity in all studies [4-6, 13, 15]. The high preferred cadence indicates other mechanisms also play a role in preventing premature fatigue. A possible explanation for this high cadence is that peak forces decrease at higher rates. The reduced force requirements can be fulfilled with an increased activation of slow twitch fibres, which have higher mechanical efficiency than fast twitch fibres [16]. That the preferred cadence is found at approximately 90 rpm, is probably because above 90 rpm, negative muscle work increases [5, 17].

Since least energy expenditure is the line of approach in this study, it is expected that the most economical cadence of 53-60 rpm will also be the most optimal cadence with respect to energy expenditure, since oxygen consumption and metabolic demand are directly related. Furthermore, the optimal cadence minimising peak activation is expected to be found at about 70 rpm as explained.

Saddle height and distance

Changing seat position results in change of range of motion in the lower extremity joints, which also affects shortening range and velocities of the concerned muscles [1]. In this study there are different definitions chosen for saddle height and distance in recumbent and conventional cycling. First these variables for conventional cycling have been drawn in figure 8.

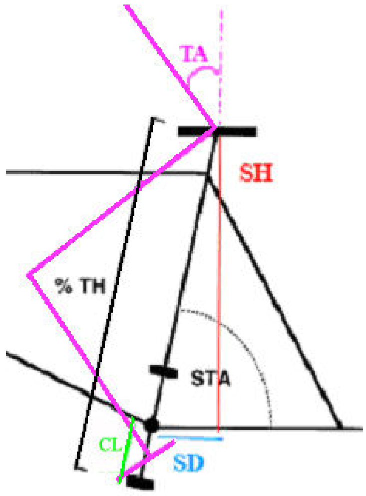

Figure 8 *Conventional cycle defintions, trunk angle (TA), seat height (SH), seat distance (SD), seat tube angle (STA), % trochanter height (%TH), crank length (CL)*

Trochanteric height is defined as the distance between the trochanter and the ground when standing straight. Setting seat position to throchanteric height is measured from the lowest position of the pedal to the saddle. Seat tube angle is the angle between saddle and spindle [1]. Seat height is the vertical distance of the trochanter to the spindle, and seat distance the horizontal distance between the saddle and spindle.

For upright cycling Priceand Donne [2] have performed research on effect on heart rate, oxygen consumption and lower limb kinematics by changing seat tube angle and the percentage trochanteric height (%TH) during submaximal exercise. They concluded that a seat tube angle of 80^{o} (smallest seat distance) was significantly more efficient than 74^{o} and 68^{o}. Welbergen [1] who compared 2 seat tube angles, also found a higher power output at the more vertical position. Oxygen consumption also followed the same trend, although not significant. Furthermore, a percentage trochanteric height of 96-100%TH was found to be most efficient compared to 104 %TH [2].

Overall it can be said, that the optimal seat height for metabolic consumption is 96-100 %TH. Seat tube angle was found to be optimal in the more vertical position, thus at small saddle distance.

Trunk angle

Changing trunk angle affects kinematics and subsequently also has an influence on the force-length distributions of the muscles and thus on activation levels and energy expenditures of the entire lower limb [18]. Effect of trunk angle was studied by Savelberg et. al [18], who compared trunk angles of 18.6^{o} extended backward, upright and 22.3^{o} flexed forward (figure 9) in 8 subjects at 80% maximal power at 70 rpm.

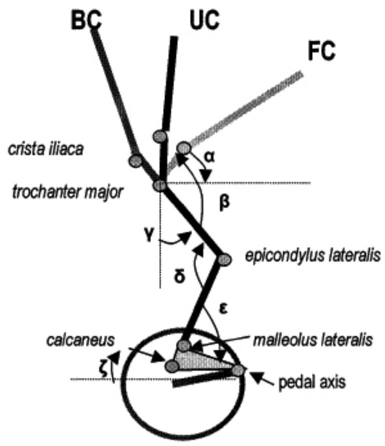

Figure 9 *The three trunk angles tested by Savelberg et al. [18] backward, upright and forward configuration.*

Although they did not draw a conclusion on which trunk angle was ideal, it showed that 6 of the 7 muscles increased activity level and changed timing in the backward trunk angle [18]. The longer activation in the backward angle shows an increased negative muscle work. The upright and forward flexed trunk angles are therefore expected to be more energetically efficient.

Gnehm et al. [19] studied the effect of several cycling configurations among 14 well trained cyclists. Under laboratory, drag free conditions, the crouched position (hands on drops) was compared to upright cycling and hands on aero-handlebars. The results of the study showed an increase in oxygen consumption, heart rate and an increase of energy expenditure for the most aerodynamic position and therefore a loss of mechanical efficiency in this position. The mechanical most efficient position is found to be the upright position, or in other words a trunk angle close to vertical.

Welbergen [1] found similar results for studying the crouched position versus the upright position. Their 6 well trained subjects delivered significantly more power from the upright position, where the hip angle is more stretched than in crouched position. Although, it showed a similar trend as the work of Gnehm [19], no significant differences were found for oxygen consumption [1, 19]. This conclusion was also the same in Ryschon [3], who compared sitting with hands on hoods to hands on drops.

Overall it can be concluded, that when drag is not taken into account, the most mechanically efficient trunk angle is in the upright position, or in other words with trunk angle perpendicular to the ground.

Forward vs. backward pedalling

In addition to optimal configuration, pedalling technique can also influence energy production and muscle activation. Two cycling techniques, forward and backward pedalling will therefore be compared. Backward pedalling leads to different activation patterns of the leg muscles. Muscles are activated at a different length compared to forward cycling. This might result in a difference in energy expenditure of these muscles. Understanding of backward pedalling will first be considered in the upright position.

Backwards pedalling affects the periods of the biomechanical functions. Based on forward dynamic simulation findings of Raasch [20], Ting et al. [11] performed an experimental study to find out whether reversing the ANT/POST pair is sufficient for pedalling backward. They found, as expected, that of the muscles investigated only the muscles contributing to the ANT/POST pair were phase-shifted (BF delay BW 166±74°, RF delay BW 51±38°, SM delay BW107±57°) [11].

Uncertainty remained, however, whether the biomechanical contributions of the bi-articular muscles remained unchanged. Neptune and kautz [21] used a forward dynamic model consisting of 14 muscles to show that the functions of these muscles in forward and backward cycling remained unchanged [21].

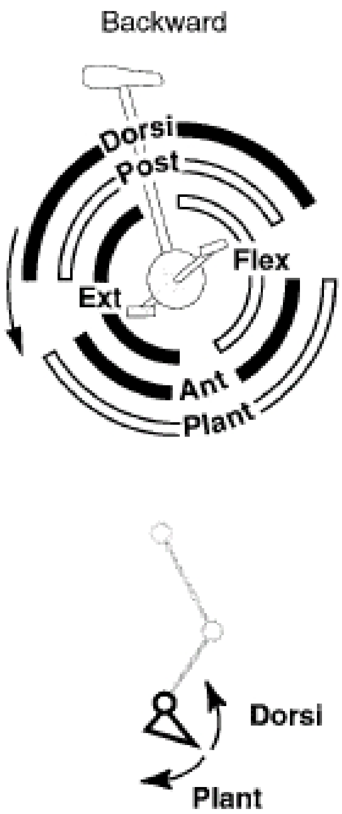

Figure 10 *For defining antagonistic pairs in backward cycling, changing the anterior/posterior is sufficient. [11]*

The Vastii and the gluteus maximus, contributing to the extensor function, produced the largest amount of energy in forward as well as backward cycling [21]. Nevertheless, changes in contraction period were found. Furthermore, integrated EMG values (iEMG) increased for the vastii because of a longer shortening region during backward cycling [11, 21, 22]. Neptune [21] indicated that the vastii during backward cycling directly deliver their energy to the crank. Instead, in forward cycling the vastii deliver their energy to the limbs transfer the energy via the Soleus to the crank. This suggestion would also explain the 10% reduce in iEMG for the Soleus, found by Ting [11]. Ting also found reduction in (iEMG) for Biceps Femoris (32%) and Gastrocnemius (11%) during backward cycling, although the amount of mechanical work for limb extension and flexion in both pedalling directions remained equal. The change in muscle activation might indicate changes in energy consumption. Therefore, forward and backward cycling will in the present study be compared to investigate which pedalling technique is less energy consuming.

Bressel et al. [22] investigated the metabolic consumption during backward cycling. Like Ting [11] they found that the activation times in Biceps femoris and Rectus Femoris were phase shifted. The amplitude and duration of the VM increased. The metabolic consumption, however, did not show any differences. Although no differences can be found for reverse pedalling in conventional cycling regarding energy expenditure, differences are expected in recumbent cycling due to change in gravitational setting. In Section 1.3 the differences expected in forward and backward pedalling during recumbent cycling will be discussed.

1.3 Recumbent cycling

As mentioned before, conquering air resistance during cycling costs a lot of energy. This amount can increase up to 80 percent of the total energy expenditure [3, 23]. Air resistance is determined by frontal area, cycling velocity, bicycle surface texture and design. Recumbent cycling reduces air resistance enormously by reduction of frontal area. Furthermore, reducing frontal area also has a major advantage for the aerodynamics of the human powered aircraft. The change in configuration, however, might influence power output and muscle metabolism. It is therefore important to understand the differences in recumbent cycling and conventional cycling.

Definitions and muscle synergy

The major change for recumbent cycling, compared to conventional cycling, is that the body is positioned parallel to the ground in a lying position (figure 10). In recumbent cycling, the crank is located in front of the body, instead of below, which influences the effect of gravity to the body. Seat distance (SD) is the horizontal distance between crank and trochanter major and seat height (SH) is the vertical distance between these two (fig 10). Furthermore, seat position (SP) is defined as the position of the trochanter with respect to the furthest pedal position. Seat height, seat distance and seat position are all expressed as a percentage of the trochanteric height (%TH). Next, support points are also different in recumbent cycling because the support is given from a seat to the right and left tuber ischiadicum, instead of to a single location on the ischium. Furthermore, the lying position causes large horizontal forces during the pedalling cycle. A back support with trunk angle defined with respect to horizontal is added to encounter this force. It is also needed since the centre of mass is located behind the seat.

No standard configuration exists for recumbent cycles, so many differences in trunk angle and crank height can be found. Practical experience is the main factor to make a choice in these variables. Recumbent cyclists with little experience prefer to sit more upright, since this position lies closer to conventional cycling. The ideal configuration has not yet scientifically been studied [18, 23].

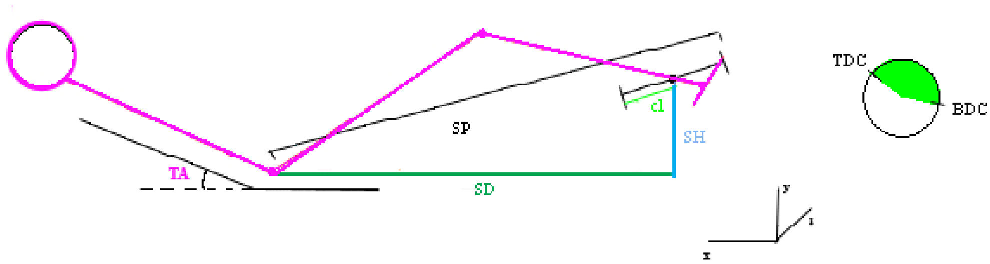

Figure 11 Definitions of recumbent cycling , seat height (SH), seat distance (SD), Seat position which is the distance between crank and trochanter major (%SP) and trunk angle (TA). The circle on the right represents the crank cycle, with the filled region representing the stroke region above the centres.

Another difference between the two positions is force delivery. The top and bottom dead centres from conventional cycling do not appear to translate by 90^{o} for recumbent cycling. An internal report, found the dead centres to be located as shown in green in figure 11. This suggestion was based on a dynamic computer model and might be caused by the change of gravity on the legs [7].

The change in configuration leads to differences in onset and offset timing of the muscles involved. Because of the change in seat configuration, the effect of gravity on the body changes [18]. A correction can be made for the change in gravity similar with the change in seat angle with respect to the crank [24]. After this correction, it appeared that muscle activation patterns are similar for the recumbent and upright position [24]. Thus, the biomechanical functions have been transformed with the same angle as the seat and table 1 remains similar for both conventional as recumbent cycling. Also onset and offset timing react similarly to changes in pedalling rate in both pedalling positions [24]. Moreover, general muscle moment patterns act similarly in conventional and recumbent cycling. Therefore, the same definitions of the antagonistic pairs can be maintained, but they need to be transformed over the change in seat angle as shown in figure 12 [24].

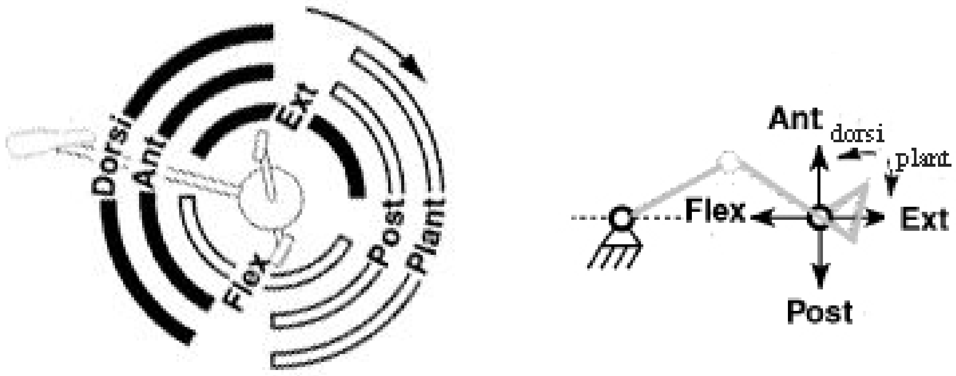

Figure 12 The biomechanical functions rotate with the same angle as the seat is shifted from conventional to recumbent cycling. Functions remain equal in both configurations [24]

Trunk angle

As mentioned, research indicated that the lower limb muscles are used similar in both recumbent and upright pedalling [24]. A translation of the seat position results in a similar translation of the forces in the cycle [24-26]. Therefore, it is hypothesised that the ideal back angle for recumbent cycling is 90 degrees rotated towards the horizontal position. Since the optimal trunk angle was concluded to be in the upright position, the optimal trunk angle is hypothesised to be parallel to horizontal. Since human beings are most accustomed to standing, the muscles are likely to function optimally when the hip is stretched. The horizontal position is a 90^o translation of the position in which the hip is mostly similar to the standing position. A backrest angle below horizontal would not be ideal because of blood flowing towards the head and was already found to be least effective considering muscle activation in conventional cycling [18]. In this study a horizontal backrest angle is expected to be optimal. But since the cyclists need to have a clear view in front of them, a trunk angle of 26^o is chosen in the aircraft, allowing the pilots to look over their knees. In practice, current recumbent bicycles also have trunk angles between 25 and 30 degrees. Twenty-six degrees is the trunk angle at which optimal pedalling in the current study is based.

Seat height/distance

To compare the hypothesised optimal seat height and distance to conventional cycling, trochanteric height can be considered the seat position in recumbent cycling. The optimal seat height in conventional cycling was found to be at 100% TH. The ideal seat position is therefore expected to be at 100% TH.

Price and Donne suggested that the seat tube angles found in conventional cycling were the result of change in ankle pattern solely. The seat tube angle appeared to be optimal in the more vertical positions. This is, when translated 90^o, comparable to a crank height of 0 cm with respect to the trochanter [2]. For these reasons, the optimal seat position is hypothesised to be found at a seat distance of 100 %TH and a seat height of 0 %TH.

Cadence

Hakansson [24] observed whether onset and offset timings reacted similarly to change in cadence in conventional and recumbent cycling. They found absolute differences for onset and offset timings for six muscles, but only at a single cadence each. The phase shift trends for increase in cadence were similar for both configurations. The phase shifted earlier in the crank for the biceps femoris, rectus femoris, and vastus medialis at increase of cadence [24, 27] Gastrocnemius shifted to later in the crank cycle as cadence increased. The similar changes show that the functional roles in change of cadence are similar for conventional and recumbent cycling.

Because the changes were similar in change of cadence, the most economical cadence is also expected to be approximately 53-60 rpm like in conventional cycling. Oxygen consumption is directly related to metabolic demand. Therefore the most economical cadence for conventional cycling is expected to be similar for minimised metabolic demand. For minimised maximal muscle activity cadence is expected to be minimal at minimal peak value of the gluteus maximus.

Forward versus backward pedalling

As mentioned before, research suggested that backward pedalling might be mechanically beneficial over forward pedalling [7]. First muscle functions in this position are considered. For the biomechanical functions during backward cycling, a combination of the change in angle as seen in Hakansson [24], together with the phase reversal of the Ant/Post pair [11] is expected to be seen when pedalling backwards in the recumbent position.

Now, the effect of the backwards cycling the recumbent position can be closer studied. A dynamic model indicated that the dead centres were not positioned exactly opposite to each other in recumbent cycling as is the case in conventional cycling [7]. It can be seen that the region below the dead centres is larger than the region above the dead centres, increasing the extending period (power stroke) during backward cycling (figure 11). The change of dead centre positions seems to be the result of the position of the seat with regard to the crank. It is unclear whether this could also be beneficial considering muscle metabolism[7]. Since power delivery is most efficient during extension phase, reverse pedalling might be more efficient since the extension range is increased in this direction.

Final remark

Now, all variables and definitions are introduced and the changes in the conventional cycling model can be applied to create a recumbent simulation model. However, a final remark needs to be made on the previous studies mentioned in this chapter that search for optimal variables. In these studies the following variables; cadence, seat height, seat distance and trunk angle were separately optimised. However, these variables should be combined to find a proper optimal configuration and cadence. For example, to find the optimal cadence, effects of seat position were not taken into account in the previous studies. Nevertheless, a different seat configuration might influence optimal cadence since a change in seat position changes the range of motion of lower extremity joints [1] and thus the position on the force-length curve. For example a high saddle, increases the length at which force can be delivered. A different distribution of activation over the muscles can now be expected since other muscles will be closer to their optimal lengths. In general it can be said that, change in configuration results in other shortening ranges and shortening velocities in the muscles. Therefore, to find an optimal situation, seat position should be studied along with cadence, which will be done in the current study by optimising all of these variables at once. In the following chapters the search for the optimal combined set of variables is outlined.

Chapter 2: The Recumbent Model

2.1 Introduction

As mentioned in the introduction a conventional bicycling model made in the AnyBody Software is adapted to simulate recumbent cycling. The AnyBody conventional bicycling model is a multi-body system, consisting of bones, joints, muscles and external segments (for example pedals). AnyBody calculates for each configuration the individual muscle forces, joint forces, tendon elastic strain energy and contains a simple version metabolic expenditure. Since energy expenditure is to be minimized to reduce heat production in the HPA, a more complex metabolism model is added and described in Section 2.4. Both the AnyBody recumbent cycling model and the metabolism model are based on the Hill-type muscle model, which consists of a contractile element, a serial elastic element, a parallel elastic element and a tendon unit (figure 13).

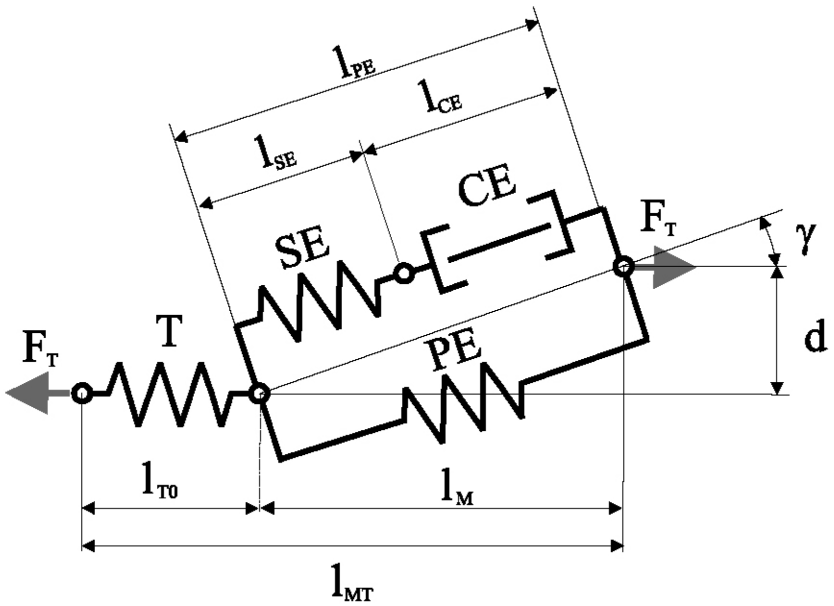

Figure 13 *Hill-type muscle model on which the AnyBody software and energy expenditure model are based [28]*

The contractile element is the force producing unit of the muscle model, which is specified by force-length and force velocity properties. The serial elastic element will take up length changes during rapid and small length variations, while the contractile element remains at constant length. The parallel elastic element represents the passive properties of the muscle. The tendon unit is represented by a linear spring with a specific stiffness. Like in human muscle, the muscle fibre is inserted with a specific pennation angle (γ) [8, 28, 29].

The AnyBody software uses inverse dynamics to predict movement kinematics and the Hill-type muscle's activation patterns. An input/output scheme for the AnyBody model is given in figure 14.

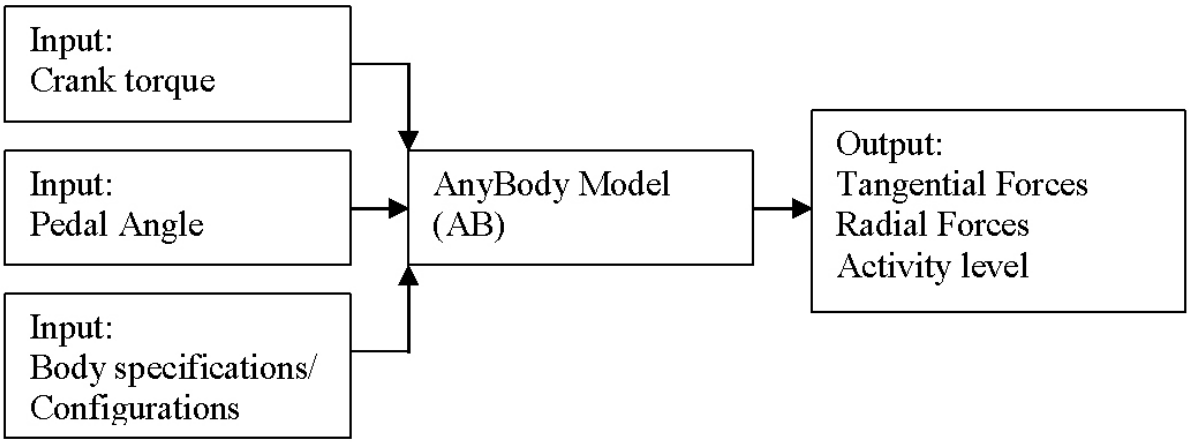

Figure 14 S*chematic overview of the in and outputs of the AnyBody model.*

Input materials for the model are external forces and kinematic movements; crank torque, crank movement, pedal angle, as well as subject segment lengths and seat position. Experimental data obtained from an internal study [7] were used as initial input data for the model. The experimental data consisted of pedal force measurements, EMG data and video analysis (for detailed information on these methods, see Section 4.3).

From the input data, muscle forces and activity levels are calculated with the min-max criterion. In the model, an activation level of 1 is the maximal activation level which results in maximal isometric force. Thus, all activation levels in the model are levels relative to the maximal isometric force per muscle. The individual activation levels and muscle forces are determined with the input crank torque, pedal movement and seat configuration. The internal forces and activation levels are calculated by the min-max criterion. This criterion minimizes the maximal activation of all muscles for the given crank torque. This way, the criterion distributes external load over all muscles that contribute to each part of the propulsion, which results in activation of as many muscles as possible with the lowest possible activation level [28, 30]. For example, the vastus medialis, vastus intermedius and the vastus lateralis can each perform knee extension, the model chooses to activate all three muscles with the lowest possible activation level instead of let one of these muscles do all the work.

Outputs of the model that will be compared to the experimental data are tangential forces, radial forces and muscle activation times. The resemblance between experimental and simulation data will be a measure for determining whether the model is acceptable. The goodness of the energy model will be studied in chapter 4, since no energy data were available from the experimental data used as input [7].

First, the conventional cycling model configuration was changed into a recumbent cycling position. The change in configuration led to a change in need of support, since a recumbent cycle supports from the back and below instead of a single saddle point like in conventional cycles. Experimental data [7] were used to define crank torque, pedal angle and the subjects' segment length.

Scaling of the model is needed to adjust muscles masses and strengths to these lengths. Furthermore, the fractions of fast twitch fibres were changed into values based on literature findings, which will be explained in this chapter. The choices and assumptions made to adapt the model for recumbent cycling will be discussed in this chapter. The created recumbent cycling model will be used to optimise the seat position and cadence in forward and backward pedalling. The AnyBody model output was used for validation purposes as well as input for the energy expenditure model.

2.2 Definitions

For a good understanding of recumbent cycling the definition of a few terms, which are mentioned repeatedly in this report will be explained in this section. The relevant variables used in the model are drawn in figure 15. First, a definition of the crank cycle needs to be made. The top of the crank cycle is determined as the $0^o/360^o$ point. Dependent on the cycling direction ‘a’ is 270^o or 90^o. In forward direction a= 270^o and in backward direction a=90^o. Furthermore, time (t) is defined zero (0s) at the top of the cycle.

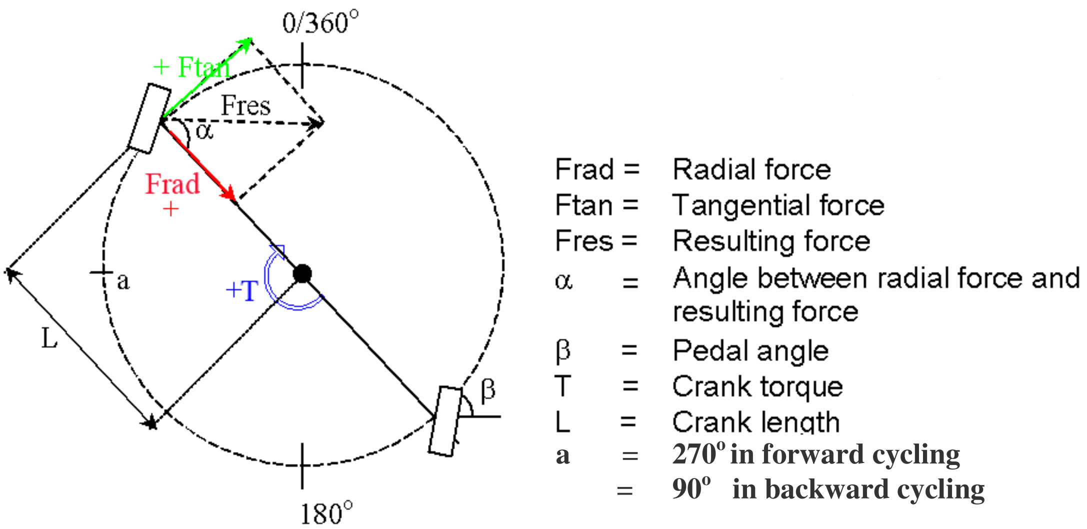

Figure 15 *Definitions as used during pedalling cycle*

Second, definitions of the forces need to be made. The radial forces are the forces parallel to the crank and the tangential forces are the forces delivered perpendicular to the crank (fig 1.1). Tangential (F_{tan}) and radial forces (F_{rad}) contain important information for the validation of the model. These forces can directly be extracted from the computer model. Experimentally these can be derived from the resultant force (F_{res}) measured on the crank. The angle α between the resulting force and the crank is needed for the derivation.

By means of the tangential forces, crank torque (T) over a cycle can be determined. The crank torque is an important input for the model, described in this chapter. Crank torque is calculated by means of multiplying tangential force by crank length (L):

$$T = F_{\tan,left} \cdot L + F_{\tan,right} \cdot L \qquad eq(1)$$

T = crank torque

F_{tan} = tangential force

L = crank length

The torque is defined positive when directed clockwise.

Furthermore, the pedal angle (β) is an important factor in the cycling movement, it functions as input for the computer model as will be described in section 2.3.2. The pedal angle affects the ankle angle directly and therefore determines the subject's movement.

Optimal pedalling with minimizing energy expenditure and minimizing peak activity will also be mentioned repeatedly in this report. Metabolism is defined in this report as muscle metabolism of the lower extremity muscles. Peak activity is the activation level of the muscle with the highest activity level of all maximum activation levels of the lower limb muscles. The corresponding configuration and cadence with the lowest values for energy expenditure or the lowest peak activation is searched for in this study.

2.3 Changes of cycling model

The changes made in the conventional cycling model are threefold. First, changes were made in the cycling model that can be applied to all subjects. Second, subject-specific changes were made. Third, the model is adapted to simulate backward cycling. The changes made in the cycling model are changes in support, changes in percentages of fast twitch fibres, changes of scaling and driver directions. The subject specific changes concern input values like, crank torque, pedal angle and configuration. All changes made will be discussed in this section.

2.3.1 General changes

Support

The recumbent cycling configuration requires supporting points different from the conventional bicycle configuration. The support used in the initial model, is a fixed hip, pinned to the saddle. For the recumbent cycling model this might not be the best simulation. An alternative support has therefore been created. A choice between the two supports will be made, based on the tangential force and radial force results compared to the experimental findings.

A major difference between support for recumbent cycling and conventional cycling is the addition of a back support in recumbent cycling. A back support is necessary since the recumbent cyclist experiences a large horizontal backward force when pushing the pedals. The centre of mass of the trunk is a second reason for creating a back support because it is located behind the hip support. Nevertheless, trunk and trunk angles were not taken into account in this study, and back support was limited to a restricted backward movement.

A second difference in practical recumbent cycling is the seat. The conventional bicycle model has only one supporting point that is from the saddle to the pubic bone. In recumbent cycling, support is given by a flat seat, creating two supporting points, from the left and right tuber ischiadicum. To simulate the seat in recumbent cycling, constraint forces were applied to these points. In the initial situation the subject model had complete translational and rotational freedom. This situation is comparable to cycling on a recumbent ergometer by sitting on a seat on wheels. With the applied movement, the subject has to keep himself in place by increasing lower limb muscle activity. To create a more realistic support, constraint forces were defined to fixate the chair. First, constraint forces placed horizontally from behind on the points of support of the hipbone prevented the subject to slide further backward. Second, constraint forces placed vertically upward prevented the subject to go below the given height. The subject is, however, still allowed to move upward and forward. More subtle forces also influenced the subject during pedalling. The subject encounters friction from the seat which only allows a limited hip rotation. To simulate friction, small forces from the left and right side and on the front and back of the supporting points are placed. All forces are drawn in figure 16.

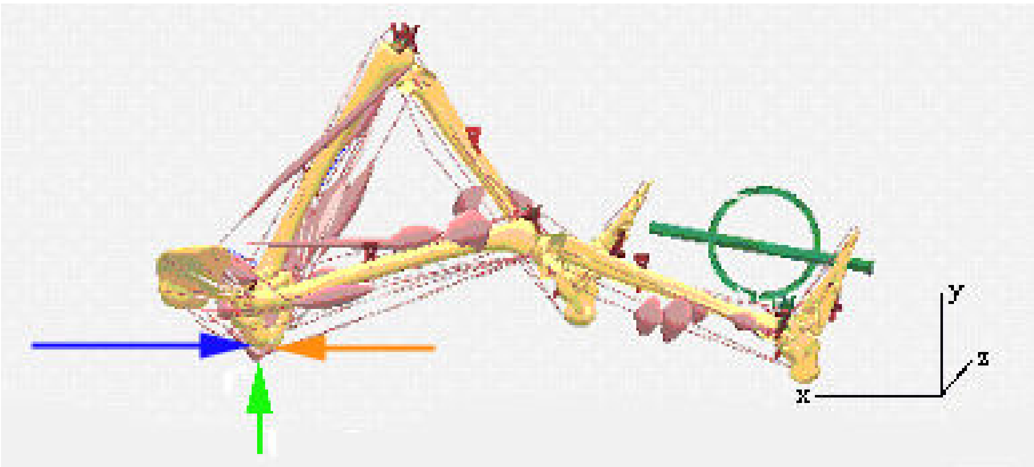

Figure 16 *Representation of the alternative support. The green arrow simulates the seat support, the blue arrow back support and the orange arrow friction values. Support is placed on both sides of the body on the left and right side of the tuber ischiadicum.*

The constraint force levels determine the amount of force that can be delivered to a mass before it starts moving. The model also determines the constraint activity by the min-max criterion. The force level is important for its activation level; a low force will easily result in over-activated constraints, which the body needs to neutralize by activating the leg muscles. A high force minimizes influence on muscle activation. The saddle constraint forces are set to a high level (20 000N); with the result that the subject cannot move downward and the constraint force is minimally activated. For the horizontal forces (friction and back support), constraints 3 & 4 (F=900N) have been given a higher force than constraint 5 & 6 (F=300N), since back support restricts the backward movement. In AnyBody the friction can be set to a random value and is subsequently independent of mass, thus suitable values need to be found. Values used for the alternative support are chosen by estimation only. The support should be expanded with more proper values.

Scaling

Two scaling methods have been developed by AnyBody that can be applied to make the subject's muscle mass fit to their segment lengths. In this study the subjects' segment lengths are extracted from the experimental data [7]. Their masses have been estimated from their percentile contribution to total body mass according to Winters [31].

A longer segment length results in different muscle attachment nodes in the co-ordinate system. To scale for this properly, a linear scaling method is used. The scaling method can be formulated as [32]:

$$s = S \cdot p + t \qquad eq(2)$$

p= original nodal location

t= translation

s= position vector of the node in the (segment –fixed) local coordinate

S= 3x3 scaling matrix

Scaling matrix S, determines how the scaling of the relative nodal position is performed. When this diagonal matrix is defined as,

$$S = k \cdot I \qquad eq(3)$$

then k is the scaling ratio, equal in all 3 directions, with

$$k = L_1 / L_0 \qquad eq(4)$$

L= AnyBody segment length

Subscript $_1$= new

Subscript $_0$= reference

This is called a uniform scaling of the nodes. Uniform scaling is based on the idea that muscle strength depends on cross sectional areas and body mass depends on volume. Muscle volume is thus scaled with the same factor in all directions as well. For the uniform scaling, the muscle strength results in:

$$F = F_0 {k_m}^{2/3} \qquad eq(5)$$

F_0= maximal isometric force

$$k_m = m_1 / m_0 \qquad eq(6)$$

m= AnyBody reference segment mass

This method is relatively easy to apply, but scaling in all directions with the same factor can make a small person relatively strong.

Therefore, a length-fat- mass method is applied. This method scales the matrix S in all directions with each having different values with respect to segment mass and strength, taking the subject's fat percentage into account. This method divides the body in muscle, fat and other tissue.

The contribution of this last group was estimated to be 50%. Thus the percentage of muscle is calculated as [32]:

$$R_{muscle} = 1 - R_{other} - R_{fat} = 0.5 - R_{fat} \qquad eq(7)$$

R_{other} = percentage, blood, organs, bones etc.

R_{fat} = percentage fat

R_{fat} can be directly measured for an individual or it can be estimated from the Body Mass Index (BMI). The R_{fat} is estimated by Frankenfield [33] for man to be:

$$R_{fat=} -9.00 \cdot 10^{-2} + 2.03 \cdot 10^{-2}\ BMI - 1.56 \cdot 10^{-4}\ BMI^{2} \qquad eq(8)$$

This approach was tested in this study, but appeared not reliable for his study. It appeared that for the new calculated strength:

$$F = F_0 \frac{k_m}{k_L} \frac{R_{muscle,1}}{R_{muscle,0}} \qquad eq(9)$$

F became too weak. The muscles got activated for 200%, which is obviously incorrect (figure 17).

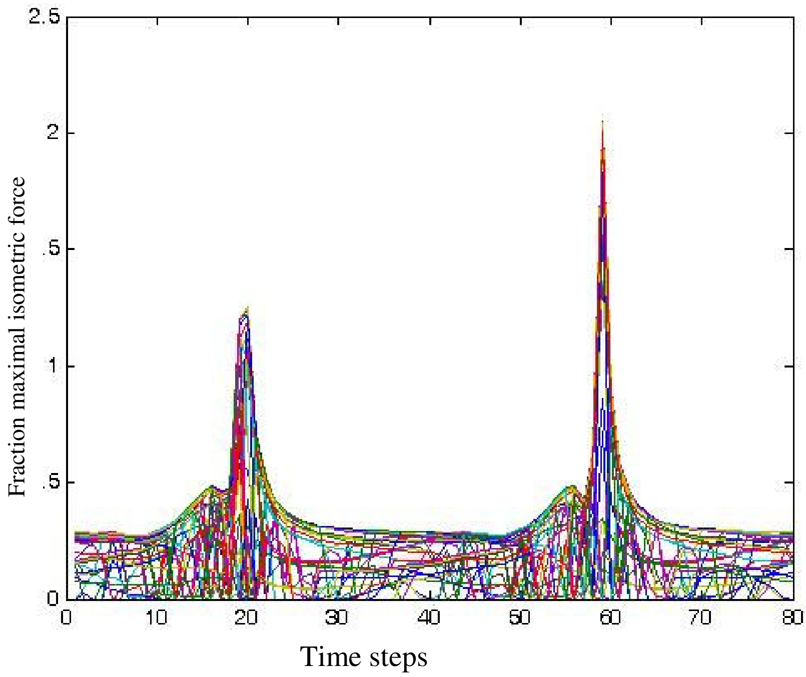

Figure 17 *Isometric force during cycle with length fat mass scaling, 1 represents maximal isometric force.*

Frankenfield and Rasmusssen [32, 33] both mention that the approach is not very reliable for individuals with BMI values below thirty. In this study both subjects have BMI values of approximately twenty-one. Therefore, uniform scaling method was the scaling method used in the present study.

Percentages fast twitch fibres

In the original model the fractions of fast twitch fibre were set to 0.4 in all muscles. In this study the values where set to values found in literature for each muscle [31]. This literature table summarizes the fibre type distributions found in different studies. The different fast twitch fibre fractions used in the current study are listed in Appendix C. In this table most of the data were taken from Johnson et al. [34], who measured fibre type distribution from six male adults in the age between seventeen and thirty years old. Muscle specimens were taken at autopsy within twenty-four hours after death. Of the muscles they measured in both surface and deep tissue, mean values were used in the current study. They measured the most important muscles contributing to the pedalling cycle, but lacked data of smaller muscles. Of those muscles lacking in this study, data of White that were reported in the tables of Multiple Muscle systems [31] were inserted. The data of fast twitch fibre type distribution measured in both these studies were consistent with each other, and ranged from 0.25 for the Soleus to 0.62 for the rectus femoris. The fractions of fast twitch fibre affect activity level and steepness of the force-velocity relationship. Furthermore, fractions of fast twitch fibres directly affect the muscle metabolic rate. Good values are thus important for calculating energy expenditure.

2.3.2 Subject specific changes

Crank torque

To calculate the muscle activation properly, the crank torque and pedal angle are of great importance. The crank torque (T) has been calculated from experimentally measured tangential forces as seen in Section 2.2.

Since only the right leg has been measured, the left leg forces need to be estimated by performing a phase shift of the right leg tangential forces similar to 180 degrees. The sum of left and right leg tangential forces is the resultant crank torque. This resultant torque is fit with a Fourier curve fit to approximate the sinusoidal course, which is shown in figure 18.

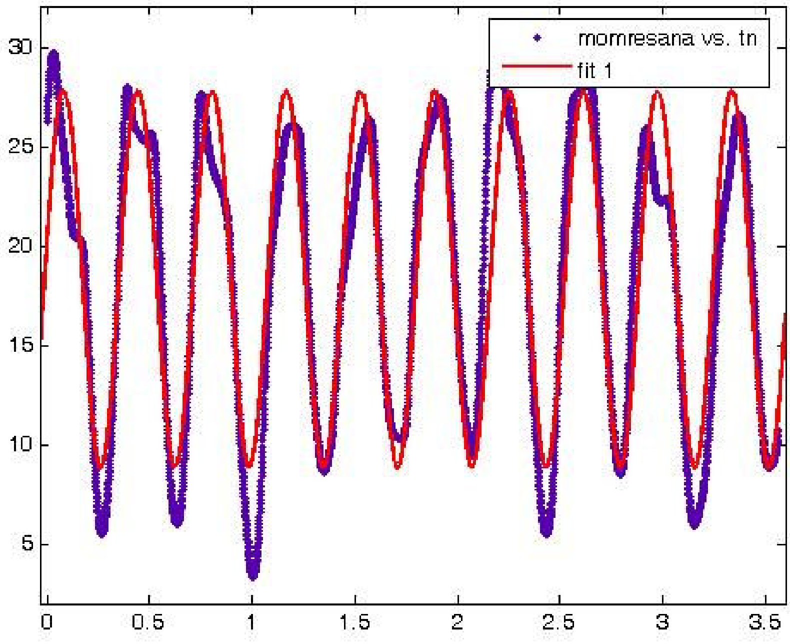

Figure 18 *Fourier fit through the experimental torque.*

The Fourier curve fit that was calculated, resulted in the following variables:

$$T = a_0 + a_1 \cdot \cos(w \cdot t + b) \qquad eq(10)$$

T = crank torque

a0 = offset value

a1 = amplitude

t = time (s)

b = phase shift

w = angular velocity (rad/s), Torque is determined by two legs, thus in this case: = 2· w_{crank} (rad/s)

The goodness of these fits ranged between r^2= 0.80 and r^2= 0.96, which are considered good fits. Irregularities in the fits were seen mostly in amplitude. The Fourier variables are direct input for the AnyBody model. In this study the optimal configuration at a constant power output is searched for. So when changing one of the input variables, the power is kept constant, with power defined as:

$$P = \int \frac{T \cdot \theta}{t} \qquad eq(11)$$

P = power (W)

θ = crank angle (rad)

To achieve constant power output, the surface beneath the torque versus time needs to remain equal.

From figure 19 it can be seen that:

$$W = T \cdot \theta = a_0 \cdot 2\pi \qquad eq(12)$$

W = work (J)

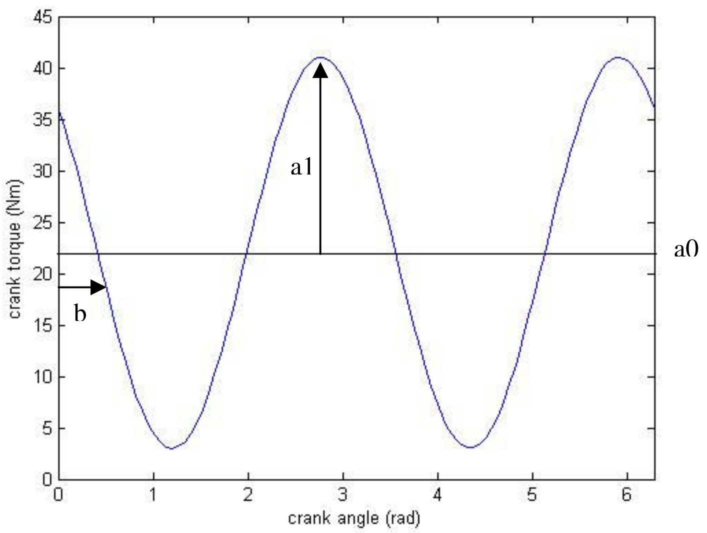

Figure 19 *Input crank torque. The cosine function allows the surface to be calculated as a square surface (2π·a0).*

Since the valley on the right side can be exactly filled in with the heap on the left side, a square surface remains. Now, power output can be redefined to:

$$P = \int \frac{T \cdot \theta}{t} = \frac{a_0 \cdot 2\pi}{t_{end}} \qquad eq(13)$$

with $$t_{end} = \frac{2 \cdot 2\pi}{w} \qquad eq(14)$$

Power (P) can be rewritten as:

$$P = \frac{a_0 \cdot w}{2} \qquad eq(15)$$

which immediately shows, that a change in angular velocity (w) should lead to a linear change in offset (a_0). This also creates the opportunity to give in a chosen power at a specific cadence. Subsequently, to keep the power output constant, a factor of w_{ini}/w is added to a_0 to the torque formula; in which w_{ini} is the initial input angular velocity:

$$T = a_0 \cdot \frac{w_{ini}}{w} + a_1 \cdot \cos(w \cdot t + b) \qquad eq(16)$$

Each of the variables in this equation can be used separately and can be used as optimisation variables as will be explained in Chapter 3.3. The Fourier variables were also used to calculate other variables of importance for the pedalling cycle. For example, the amount of cycles per second that a subject pedals, in other words the frequency (f) in Hertz, can be calculated from:

$$f = \frac{w_{crank}}{2 \cdot \pi} = \frac{w/2}{2 \cdot \pi} = \frac{w}{4 \cdot \pi} \qquad eq(17)$$

From which again another important variable for this study can be calculated. In the AnyBody model cadence in cycles per minute is calculated by means of:

$$cadence = \frac{60 \cdot w_{crank}}{2 \cdot \pi} = \frac{60 \cdot w}{4 \cdot \pi} = 60 \cdot f \qquad eq(18)$$

Pedal angle

For the pedal angle, a similar Fourier fit is performed. From experimental observation, the pedal angle also appears to have a sinusoidal course and can therefore be fit by the same equation as crank torque. Again to calculate the course, the data have been shifted to a crank angle that equals 360 degrees at t = 0s. For the left leg a phase shift has been performed on the right leg data by shifting the crank torque 180 degrees. To do so the Fourier variable amplitude (a_1) is set to negative. The pedal angle fit is shown in figure 20. In this figure, 0 represents a foot parallel to horizontal and ½ π represents a vertically placed foot. The goodness of the fits ranged between r^2= 0.75 and 0.98. Backwards cycling showed slightly less well fits between 0.75 and 0.92 whereas forward ranged from 0.96-0.98. However, the backward fits were still considered very acceptable fit values.

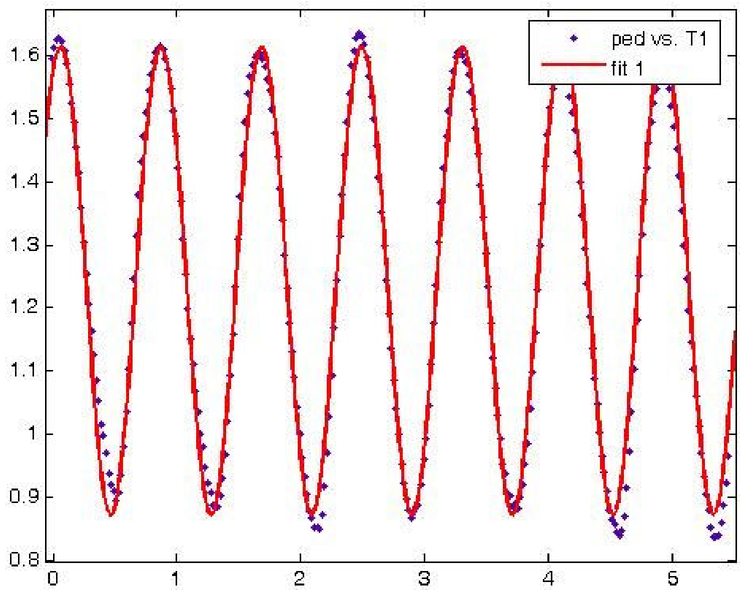

Figure 20 *Pedal angle Fourier curve fit.*

Again changing cadence affects other Fourier variables. In this case angular velocity of the pedal angle needs to be adapted to fit the course in the changed time course. This is why the angular velocity of the pedal (w_{pedal}) should be multiplied by a factor w/w_{ini} to keep the angular course of the pedal angle within the time course of the crank torque. Resulting in a pedal angle equation of:

$$\tau = a_0 + a_1 \cdot \cos(w_{pedal} \cdot \frac{w}{w_{ini}} \cdot t + b) \qquad eq(19)$$

τ = pedal angle (rad)

a0 = offset value

a1 = amplitude

t = time (s)

b = phase shift

w = crank angular velocity (rad/s)

w_{ini} = input crank angular velocity (rad/s)

w_{pedal} = pedal angular velocity (rad/s)

Seat Configuration & Body specifications

The recumbent model is not only made subject specific by pedal angle and crank torque course. Also seat configurations and body specifications are of great importance. As mentioned in Chapter 1, the main variables for seat configuration are seat height and seat distance with respect to the crank. These distances have been taken from the experimental marker distances of the pedal centre and Trochanter major. As explained in Chapter 1 the trunk angle is set to 26^o.

In addition to seat configurations, subject segment specifications are put in. The lengths of the thigh and lower leg have been extracted from the marker data of the experimental measurements. The experimental thigh length was measured from Maleolus to the Trochanter major, while in the model this length was measured from Maleolus to Caput Femoris. To compensate this difference, 0.042m is added to the measured thigh length. Foot length has been measured by hand, from ankle to toe. The masses of the segments, compared to the standard body model in AnyBody are scaled with segment specific factors taken from Winter [35]. Furthermore, 0.03m has been added to the seat distance to include the pedal thickness for all subjects.

2.3.3 Backwards cycling

The changes for simulating backward cycling concern the crank torque and angle velocity. For determining the crank torque fit and pedal angle fit, it has to be taken into account that the angle course in the experimental measures has to be reversed. Instead of moving the crank from 0-360^o, it now moves from 360-0^o. The angle is redefined for backwards cycling as was shown in figure 15 represented by 'a'.

Only two changes to reverse pedalling are needed. The first change to be made is reversing angular velocity, which can be done by setting the driver angle velocity to negative. The second change to be made is reversing the crank torque. The crank torque to be delivered has changed direction, and consequently is changed into negative.

2.4 Model additions: Energy metabolism

A good energy model is essential to find the configuration with minimum energy expenditure. Not only mechanical work, but also thermal energy needs to be taken into account. The AnyBody model only contains a very simple muscle metabolism model, in which the mechanical work has been considered 25% of the total energy. The mechanical work during shortening is multiplied by a factor 4 to estimate the total amount of energy expenditure. This approach is very inaccurate since it neither accounts for the contribution of relative amount of fast twitch and slow twitch fibres nor does it divide heat production in several stages. Several researchers have created more reliable simulation models for muscle metabolism [8, 29, 36]. The simplest approach is an empirical muscle mechanics model based on the Hill-type muscle model. Based on this research an energy model written in Matlab is added to the recumbent model for more accuracy.

Energy production can be divided in two terms, namely mechanical work and thermal heat. Mechanical work ($\dot{w}_{CE}$) is calculated by the Hill-type muscle model, but is only a small part of the total energy produced by muscles during movement. The main part of energy produced consists of heat, but this thermal heat is not computed by the standard Hill-type muscle model.

Both energy models of Umberger and Bhargava are based on forward dynamics. In contrast to Bhargava, Umberger can easily be adapted to be coupled to an inverse dynamics model. To do so stimulation and activation level had to be considered equal. Between stimulation and the actual contraction there is a small time delay, this includes a small difference for the outcome but is considered negligible [37]. Umberger [8] has been chosen as the energy expenditure model to be implemented in the current study. Not only is it easy to adapt to inverse dynamics, it is also considered a reliable model, since variables used were all based on mammalian muscle and human muscle where possible instead of on amphibian muscle. It is an empirical muscle mechanical model, based on the Hill-type muscle model. Results had a good correlation with experimental validation for walking one step, isolated muscle actions and single joint movement [8]. Moreover, only a few variables available from the recumbent model described in section 2.2 are needed as input.

The equations used in the Umberger model [8] were taken from previous research and were based on maximal activity. Umberger [8] developed scaling factors to make these equations applicable to submaximal activation as well. Submaximal activity is of great importance when studying duration exercise as is studied in the present study. Therefore, these scaling factors have also been adapted in the current study. Below the equations used per heat source are listed, al heat rates are given in W/kg.

Thermal heat can be divided into three sources [8, 29]. The first is activation heat ($\dot{h}_A$), which is defined as the initial energy liberation independent of tension. The second type is called maintenance heat ($\dot{h}_M$), which is the heat rate produced during isometric contraction. Umberger [8] combined activation and maintenance heat in one equation, which is adapted for the current study. And finally, the third source is heat produced beyond maintenance heat by the shortening/lengthening heat ($\dot{h}_{SL}$). Resulting in the main equation, for total energy expenditure in (W/kg):

$$\dot{E} = \dot{h}_A + \dot{h}_M + \dot{h}_{SL} + \dot{w}_{CE} \qquad eq(20)$$

The Activation/Maintenance heat rate ($\dot{h}_{AM}$) equation is strongly dependent on the percentage of fast twitch fibres (%FT). The energy expenditure model is sensitive to fibre type distributions. Fibre type distribution is muscle specific and important to account for since slow twitch fibres (ST) produce up to four times less heat and are consequently much more economical than the fast twitch fibres [8, 38]. In the recumbent multiple muscle model, fractions of fast twitch fibres have been defined for the individual muscles, as was described in section 2.3. As can be seen in the following equations, these fractions are of great importance for determining heat production. The Activation/Maintenance heat rate ($\dot{h}_{AM}$) is defined as:

$$\dot{h}_{AM} = 1.28 \cdot \%FT + 25 \qquad eq(21)$$

$\dot{h}_{AM}$ = activation /maintenance heat rate

$\%FT$ = fraction of fast twitch fibre.

The Shortening heat rate is given by:

$$\dot{h}_{SLS} = -\alpha_{S(ST)} \tilde{V}_{CE} (1 - \%FT/100) - \alpha_{S(FT)} \tilde{V}_{CE} (\%FT/100) \qquad eq(22)$$

h_{sls} = shortening heat rate

$$\alpha_{S(ST)} = \frac{4 \cdot 25}{\tilde{V}_{CE(MAX-ST)}} \qquad eq(23)$$

$$\alpha_{S(FT)} = \frac{1 \cdot 153}{\tilde{V}_{CE(MAX-FT)}} \qquad eq(24)$$

$\tilde{V}_{CE}$ = the shortening velocity (fibre length/s)

The maximal contraction velocity for fast twitch fibres ($\tilde{V}_{CE(MAX-FT)}$) is assumed to be three times greater than the maximal contraction velocity for slow twitch fibres ($\tilde{V}_{CE(MAX-ST)}$), $6s^{-1}$ and $2s^{-1}$ respectively [39]. Lengthening heat rate is only dependent on the shortening velocity and given by:

$$\dot{h}_{SLL} = \alpha_L \tilde{V}_{CE} \qquad eq(25)$$

in which

$$\alpha_L = 4\alpha_{S(ST)} \qquad eq(26)$$

h_{sll} = lengthening heat rate

Mechanical work rate is defined by contraction force (*Fce*), contraction velocity (*Vce*) and the individual muscle masses (*m*):

$$\dot{w}_{CE} = -\frac{F_{CE}V_{CE}}{m} \qquad eq(27)$$

$\dot{w}_{ce}$ = mechanical work rate

F_{ce} = contraction force (N)

m = muscle mass (kg)

The final equation for individual muscle metabolism is a combination of the individual energy types multiplied by the scaling factors. A list of inputs for the metabolism model is muscle activation level, contraction force, contraction velocity, muscle mass, fibre length and pennation angle. The final energy expenditure equations are [8]:

If L_{ce}<= L_{ce}(opt)

L_{ce} = fibre length

opt = optimal

$$\dot{E} = \dot{h}_{AM}\, A_{AM}\, S - \dot{w}_{CE} \qquad eq(28)$$

$$+\begin{cases} \dot{h}_{SLS}\, A_S S & \text{If } \tilde{V}ce <= 0 \\ \dot{h}_{SLL}\, AS & \text{If } \tilde{V}ce > 0 \end{cases}$$

in which

A = activation level,

A_{AM} = scaling factor for $\dot{h}_{AM}$ = $A^{0.6}$

A_S = scaling factor for $\dot{h}_S$ = $A^{2.0}$

S = scaling factor for submaximal activity= 1.5 (aerobe activity)

If Lce>Lce(opt)

$$\dot{E} = (0.4x\dot{h}_{AM} + 0.6x\dot{h}_{AM}\ F_{ISO})A_{AM}S - \dot{w}_{CE} \qquad eq(29)$$

$$+\begin{cases} \dot{h}_{SLS}\ F_{ISO}A_S S & \text{If } \tilde{V}ce <=0 \\ \dot{h}_{SLL}\ F_{ISO}AS & \text{If } \tilde{V}ce >0 \end{cases}$$

F_{ISO} = isometric force

The complete model description of Umberger can be found in the Journal of Computer methods in biomechanics and biomedical engineering [8].

2.5 Model validation

Two male recreational cyclists were simulated in AnyBody. They were chosen from a pool of five possible subjects, whose data were available from former experimental data [7]. The current two were chosen because of their difference in body height, which is 17 cm, would be useful in studying more extreme measures Anthropometric data were subtracted from the former study kinematics' data, and are shown in table 2 below.

Table 2 *Anthropometric data of subjects*

	Subject 1 FW	Subject 2 BW
Gender	Male	Male
Age	23	23
Length (m)	1.98	1.81
Weight (kg)	82	75
Foot length (cm)	22.5	21.5
Thigh length(cm)	48.2	40.8
Shank length (cm)	43.3	41.0

Before optimisation studies are performed, first the model as mentioned above is validated. Previous experimental data [7] are used to determine all input values, as crank torque, pedal angle and segment specifications. The input values will be compared to the output data for tangential forces, radial forces and muscle activation levels. Furthermore, the effect of chosen support and scaling differences will be studied. Both experimental and simulated data were based on a mechanical output of 175 W.

Prediction of Forces

The tangential forces are the first model output values to be compared to the experimental data. In figure 22 the experimental tangential forces are plotted in one figure with the calculated tangential forces of the recumbent AnyBody model.

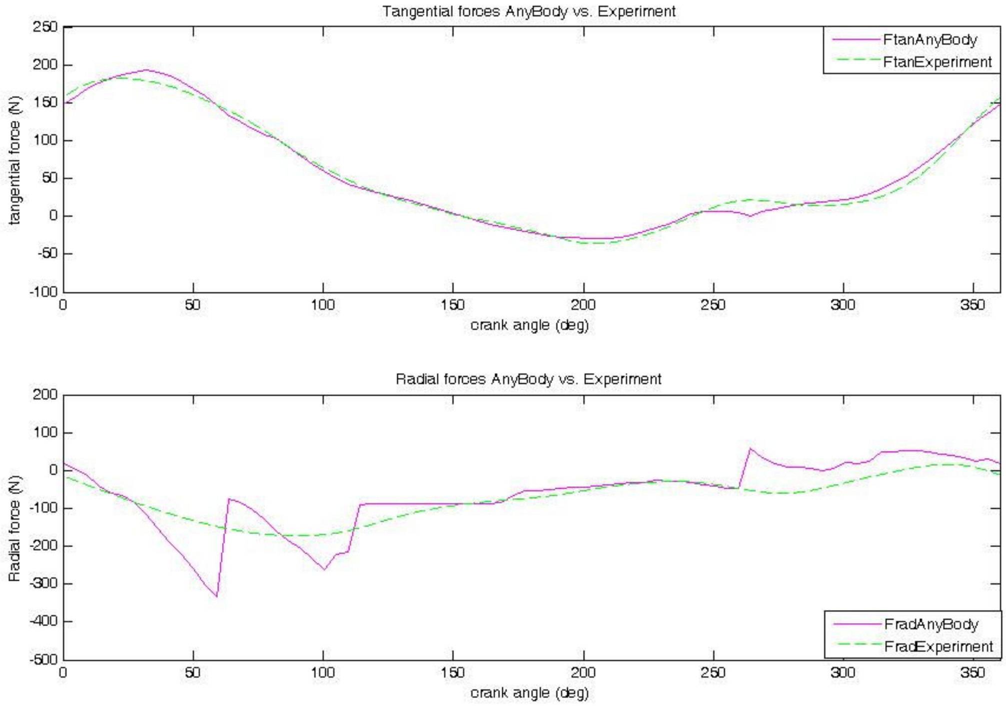

Figure 21 above) *tangential forces as found in the experimental data versus the calculated tangential forces of the recumbent model, subject 1 during forward cycling.* ***below)*** *the corresponding calculated and experimental radial forces.*

This figure shows that resemblance between the calculated and experimental tangential forces is very good. In addition, the correlation coefficient was calculated to express this resemblance in numbers. The correlation values are shown in table 3. The correlation coefficient is a measure to show the goodness of a linear relation of the experimental tangential force compared to the calculated tangential force. It is calculated as follows:

$$corr = \frac{\sum (A-\overline{A})(B-\overline{B})}{\sqrt{\sum (A-\overline{A})^2 \cdot \sum (B-\overline{B})^2}} \qquad eq(30)$$

Table 3 *Correlation coefficients of the tangential and radial forces of the recumbent model versus the experimental forces.*

		Correlation	Corrected correlation
Subject 1	Ftan FW	1.0	
	Frad FW	0.85	0.94
	Ftan BW	0.98	
	Frad BW	0.75	0.88

		Correlation	Corrected correlation
Subject 2	Ftan FW	0.94	
	Frad FW	0.90	0.93
	Ftan BW	0.95	
	Frad BW	0.73	0.90

For the interpretation of the correlation, it is helpful to consider the square of the correlation coefficient. This value represents the fraction of the variation in one variable that can be explained by the other variable [40]. This means that correlation coefficients of 0.71 can be explained by at least 50% of the other variable. Therefore, correlations of 0.71-0.8 ($50\%<r^2<64\%$) are considered reasonable, 0.8-0.9 is considered good correlation (($64\%<r^2<81\%$)) and 0.9-1 ($81\%<r^2<100\%$) is considered very well.

The tangential forces of both subjects during forward as well as backward cycling all resulted in correlations in the range 0.94-1, whereas one represents a rounded of correlation of 100%. The correlation of forward cycling of subject 1 has a 99.6% correlation and is therefore rounded off to one. The correlations of subject two were slightly lower compared to the correlations of subject 1 but still very well correlated.

One of the inputs of the model was the crank torque determined by both legs. The model can divide the crank torque into the individual leg tangential forces freely. Since the input crank torque is directly determined from the experimental tangential forces, good resemblance between the experimental and simulated data was expected. The second type of model output values are of greater importance. The radial forces are not directly related to the input values, but were calculated by the simulation model independently. For the radial forces as well, correlation coefficients were determined. It can be seen in Table 3 that for these radial forces, correlation was much less, with correlations in the range of 0.73-0.90, or as explained between reasonable to good correlations.

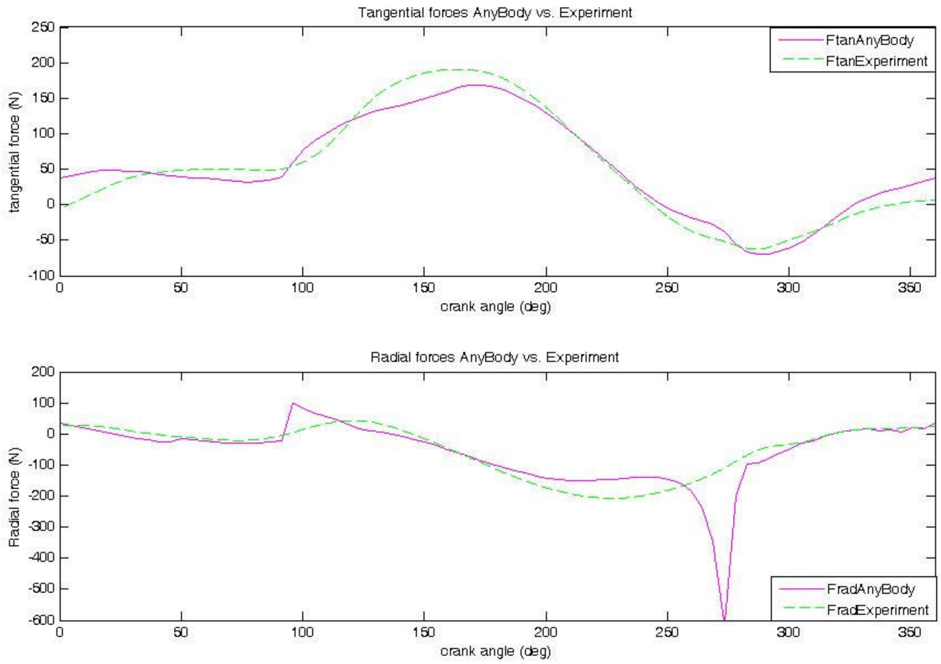

Figure 22 ***above****) tangential forces as found in the experimental data versus the calculated tangential forces of the recumbent model, subject 1 during backward cycling.* ***below****) the corresponding calculated and experimental radial forces.*

At first sight, the correlations seemed to be better for forward cycling compared to backward cycling. Nevertheless, when looking at figure 23, it can be seen that during backward cycling the model contains larger peaks compared to the radial forces during forward cycling. These peaks are probably the result of difficulties of the model at the dead centres where flexion becomes extension and the other way around. The reason of these difficulties is probably because of the instantaneous switch on/off of the muscle activation in the model, which occurs in reality more gradually. For this reason a polynomial fit (9^{th} degree) was drawn through the calculated radial force, which excluded the peaks. In figure 24 this fit is illustrated.

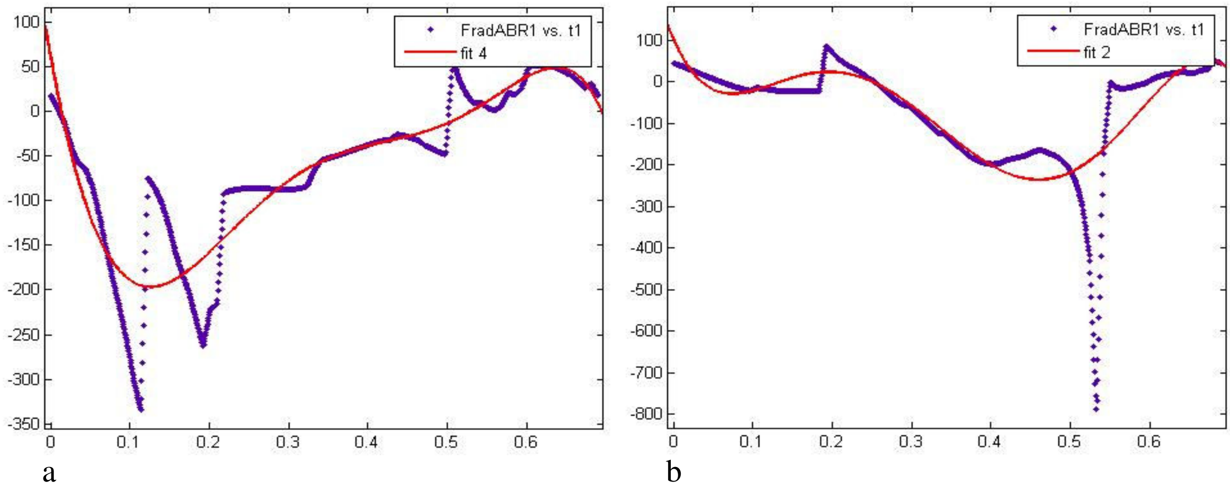

Figure 23 ***a)*** *The 9th degree polynomial fit through the radial forces (N) versus time (s) of the modelled subject 1 during forward cycling.* ***b)*** *The 9th degree polynomial fit for backward cycling, excluding the peaks around the dead centres.*

When the correlation coefficient is now calculated again, values increase up to a range of 0.88-0.94, from good to very well correlations. Subsequently, the model force calculations were considered very acceptable.

Choice of support

As mentioned, two types of support can be chosen from, the fixed hip support and the alternative support. Although, the alternative support allows for hip movement in the seat and therefore simulates reality better, good friction values should be added. The values chosen now were not determined properly.

The choice of support is based on the comparison of the calculated radial and tangential forces to the experimental data. Looking at the results for radial forces of both methods in figure 24, it can be seen that the minimal value of the peak at 80 degrees with the alternative support is much lower than in the fixed hip support. Patterns were similar for both supports. For simplification and because of the lack of good friction values, the fixed hip support is the chosen support in this study.

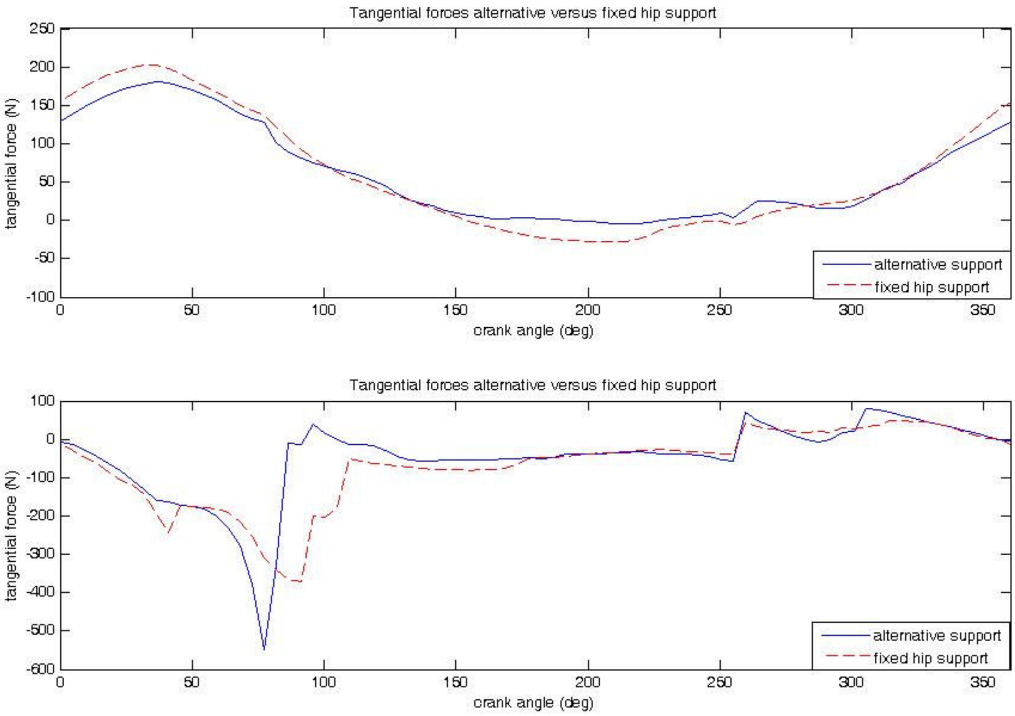

Figure 24 *Above) tangential force results of the fixed hip support versus the alternative support. Below) the corresponding radial forces.*

EMG versus Activation

The final validation of the recumbent model has been done by studying the muscle activation. However, the calculated activation levels cannot directly be compared to EMG data. The amplitude of the EMG data is dependent on many factors, for example on the placement of the electrodes, with respect to the muscle belly, the depth at which the muscle is located, the amount of measured muscle fibres. Because of these factors, there is no direct relationship between amplitude and force delivery as is the case with the simulation muscle activation level. For these reasons, activation time is the only variable that can currently be compared to the EMG data. Later on in the experimental validation of the optimisations in chapter 5, amplitude will be taken into account to determine peak activity since between the different tested configurations the EMG electrodes will be left in place and amplitudes then can be compared.

To compare the simulation data activation times to the experimental activation times, the muscles in the experiment were considered active when activation reached a threshold. This threshold was equal to 20% of the maximal activation per muscle. Since AnyBody has instant activation, the threshold was set to 10%, so that small peaks were filtered. In figure 25, activation times of the experimental data of subject 2 during forward cycling are compared to its simulation equivalent.

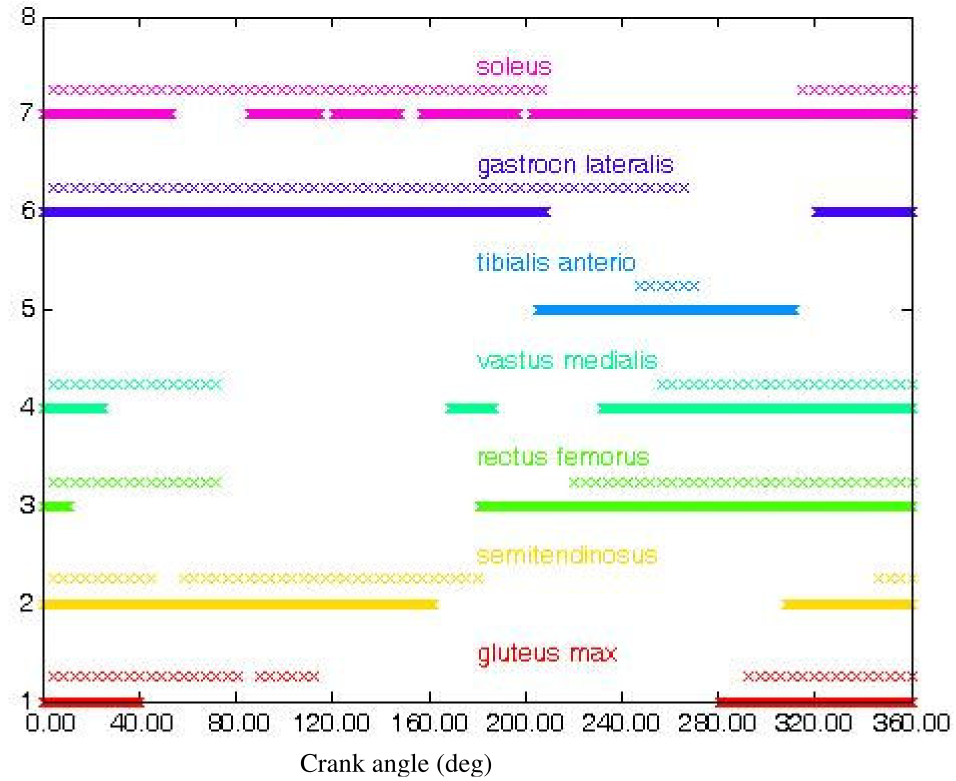

Figure 25 *Activation times of subject 1 during forward cycling. The crosses xx represent the simulated activation times. The continuous lines represent the experimental data.*

All modelled activation times occurred in the same regions as the experimental activations. The extensors and flexors were found to be slightly phase shifted with later activation and de-activation compared to the experiments. The soleus was least well predicted by the model. The experimental soleus activation pattern, however, was also found to be very irregular which explains the almost constant activation time. The threshold also has an effect on the experimental activation times, as will be shown in the overlap values below.

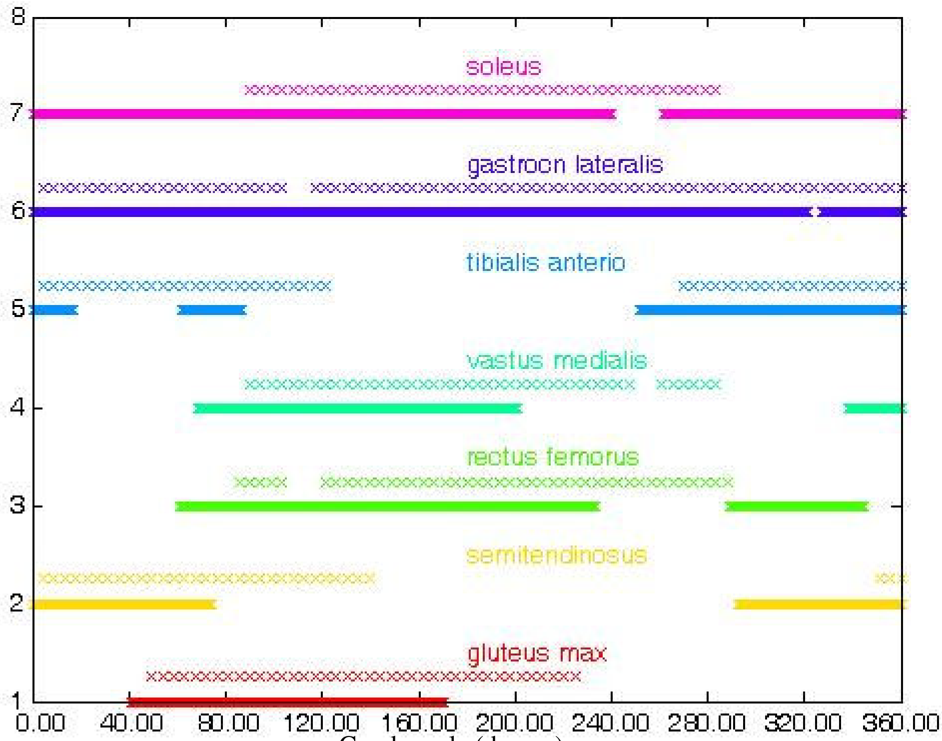

Figure 26 *Activation times of subject 1 during backward cycling. The crosses xx represent the simulated activation times. The continuous lines represent the experimental data.*

At first sight the activation times look more phase-shifted in figure 26 in comparison to forward cycling. Therefore, to quantify the similarities between the model and experiment, overlaps will also be calculated later on. The activation times in backward cycling also shows a shorter prediction for the soleus activation time. As mentioned, threshold plays an important role in activation period which might explain the temporary gaps as seen in the rectus femoris activation and gastrocnemius lateralis.

To refine the visual findings, the percentages of overlap between the experimental and model activation times have been calculated. These are calculated as:

$$\frac{time\,both\,'on'}{(total\,time\,'on'\,\mathrm{model} + total\,time\,'on'\,\mathrm{exp})/2} \qquad eq(31)$$

The mean overlap in forward cycling was found to be 72.5% and 70.4% for subject 1 and subject 2 respectively. The values per muscle are shown in table 4.

Table 4 *Overlap percentages model activation times and experimental activation times*

subj1	FW ini (%)	BW ini (%)	
	74.9	81.4	gluteus maximus
	84.6	58.9	semitendinosus
	76.5	66.0	rectus femorus
	75.8	67.4	vastus medialis
	42.6	74.5	tibialis anterior
	80.9	98.0	gastrocnemius lateralis
	72.4	66.5	soleus
mean	72.5	73.3	
SD	13.8	13.9	

subj2	FW ini (%)	BW ini (%)	
	54.6	82.6	gluteus max
	91.9	62.8	semitendinosus
	81.3	61.6	rectus femorus
	71.9	72.8	vastus medialis
	40.1	79.4	tibialis anterior
	66.3	91.8	gastrocnemius lateralis
	86.5	77.8	soleus
mean	70.4	75.5	
SD	18.4	10.8	

The tibialis anterior shows least overlap with 42.6% (subject 1) and 40.1% (subject 2). The activation periods of this muscle did fall within the middle of the experimental activation periods. For backwards cycling, this muscle is much better predicted with 74.5% (subject 1) and 79.4% (subject 2). The overall overlaps in backwards cycling are of the same order with 73.3% and 75.5% respectively.

As mentioned several times before, the height of the threshold plays a role in the amount of overlap. For example a threshold of 10% of the maximum value of the EMG's instead of 20% for subject 1 in forward cycling, leads to a decrease of overlap for five of seven muscles of up to 9% for the vastus medialis and an increase of overlap for the soleus of 11%. This increase for the soleus is caused by the value of the threshold now allowing for continuous activation throughout the pedalling cycle. A threshold of 30% of the maxmum EMG leads to less well overlaps for four of the seven muscles of up to 16% for the semitendinosus and increase of overlap of only up to 7% for the vastus medialis. For these reasons, the threshold of 20% of the maxmum EMG value seems reasonable.

It has to be taken into account that the activation times, are influenced by several factors. First of all, the activation times are dependent on the chosen thresholds. A differently chosen threshold can increase or decrease the activation times of the experimentally found activation times. Furthermore, the model has instant activation, whereas the human body experiences an electromechanical delay. This is the temporal delay of 26ms to 131 ms between the detected muscle activity and the realisation of the contraction [41]. During this period the change in potential can already be measured, and thus influences activation times. Finally, the experimentally measured activation times can also be influenced by other muscle activations positioned close by. With all of these considerations, the overlap between the experimental activation times and the model activation times is considered reasonable.

Acceptance of the model

In conclusion, on the basis of the observed correlation between model predicted and experimentally determined data the model is considered to be an adequate simulation model. The tangential and radial forces correlate well with the experimental data. Also the activation times observed with EMG data were in reasonable agreement with the simulated activation times. With the acceptance of the model, the study can be continued with optimisation of the model.

Chapter 3: Optimisation

3.1 Introduction

Many factors influence the recumbent cycling model. For long endurance exercise, it is important to find the optimal conditions to prevent premature fatigue and to decrease heat production. The optimisation method used in this study is the golden section method, which will be explained in this chapter. A variable study is used to find good initial guesses and prevents ending up in local minima. Below, a schematic overview is given of the optimisation procedure in figure 27.

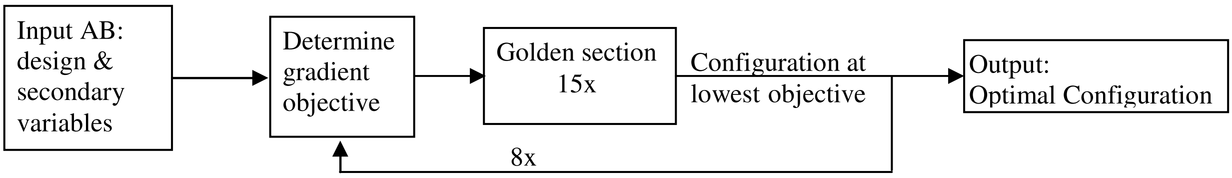

Figure 27 *Schematic overview of the optimisation procedure*

3.2 Objective Function

The objective function is the function that is going to be minimized. The choice of this function is therefore of great importance. To minimize fatigue for endurance exercise, minimizing total energy expenditure would be a logical choice. In Chapter 2.4 it is shown how the metabolism of each muscle can be calculated in W/kg. The lower limb energy expenditure over time is the sum of these individual muscle energies multiplied by the individual muscle masses. The sum of the individual values is the total amount of energy taken as the objective function.

However, this objective does not account for high activity levels. Possibly, the activity in a specific muscle is very high at an optimal metabolism objective, thereby causing local fatigue which becomes a bottleneck. From recumbent cycling experience it is noticed that although heartbeat and oxygen consumption are not maximal, muscle fatigue occurs. Following from these findings, the minimised muscle activity can also be considered a good objective function. The maximal activity can directly be taken from the AnyBody model. It is the highest activity value delivered during the cycle considering all calculated muscles. To prevent a specific muscle to become the bottleneck, the maximum of all individual maximal muscle activities is used as the second objective function. The configuration at the minimum of this objective does not necessarily result in minimum energy consumption. Possibly the activity is better distributed, but combined with higher energy consumption compared to the configuration of least energy expenditure. For both objective functions, the optimal configuration will be searched. The results will be validated experimentally in chapter 4 and a choice for the best objective will be made.

3.3 Design Variables

Optimal pedalling depends on many variables. The most important ones were chosen for optimisation, as were also described in section 1.4. As explained in the same section trunk angle is set to a fixed chosen value.

The first two chosen design variables are seat height and seat distance. The seat position with reference to the crank position is very important. Everyone can imagine that if the seat is too high and too far, it is difficult to keep in place and the subject needs to compensate for these horizontal forces by delivering more muscle force, which increases energy consumption. Likewise, a too low seat position costs the subject much muscle power to keep its legs up. These are examples of extreme positions and easily to imagine. But also small changes can affect the energy consumption in a more subtle way and therefore seat height and distance need optimisation.

The third variable chosen for optimisation was cadence. Is it more efficient to pedal at a low cadence at a high mechanical output or to pedal at a high cadence with low mechanical output? Since the pilots in the record attempt must deliver a power output of 200W, the optimal cadence at high power output will be searched for. As explained, higher cadences lead to lower peak forces changing the activation pattern as well as energy consumption, but too high cadences lead to increased negative muscle work. Subsequently, optimisation of cadence is also very useful. An optimal combination of seat height, seat distance and cadence is searched for in this chapter.

Furthermore, change in design variables can lead to changes in other variables. These are called the secondary variables and are automatically changed other optimal values at changes design variables. For example, it is easy to imagine that sitting far away from the crank leads to a different ankle angle compared to a close position with respect to the crank. This is why pedal angle offset had been chosen as a secondary variable and was also optimised for. For the same reason crank torque phase is chosen as secondary variable for the optimisation study. The optimised values can be compared to experimental data, which can be used as a control.

3.4 Variable study

A variable study calculates the objective value of a series of design variable values. With a stepwise change of the design variables, all values of the objective function are calculated. The minimum of the objective can now be visualised. The variable study can be performed with a single variable or with two variables. If the objective function is a smooth function a 2-dimensional variable study can be done. Now, a surface plot can be made, as illustrated in figure 28. The minimum value can be estimated from the plot.

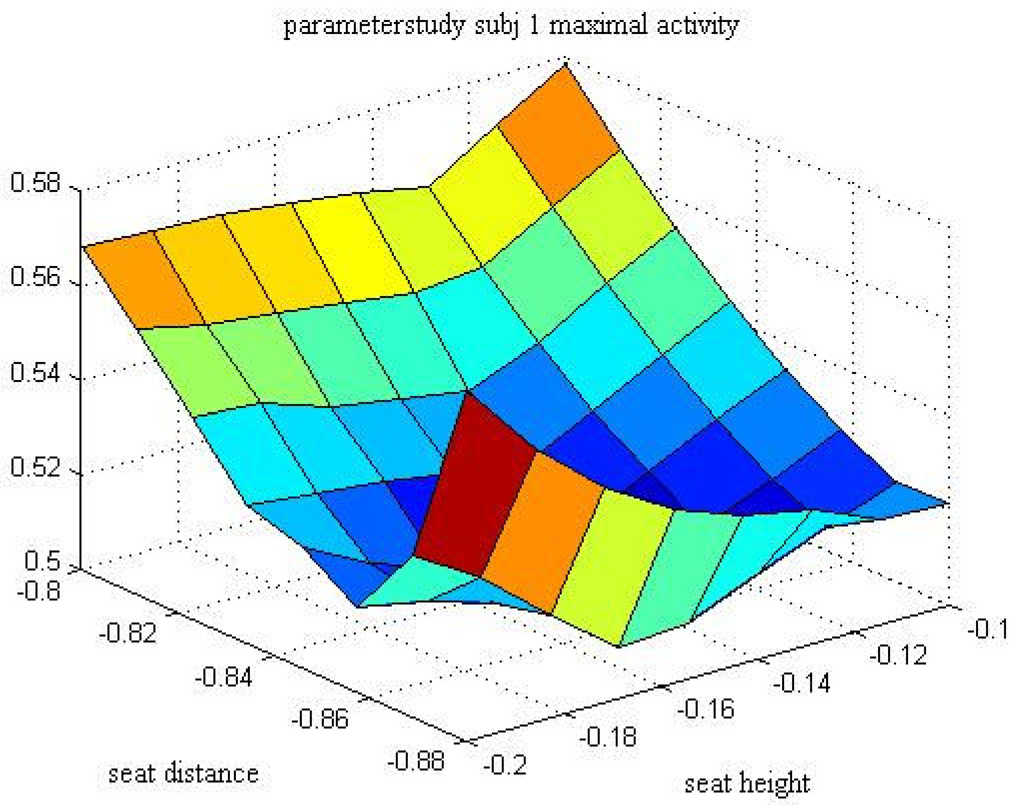

Figure 28 *A minimum can be seen in the variable study of seat height and distance with respect to activity.*

Nevertheless, the disadvantages of variable studies are, however, multiple. Estimation of the minimum is not very accurate. In addition, a variable study is not practical when optimizing more than two variables. All design variables can influence each other, but variable studies can only be visualised when calculating two at a time. Another disadvantage is that the variables study is very time consuming. In figure 28 only two variables have been calculated, but in this study there are 6 variables and it takes subsequently a lot of time to calculate all the values. In figure 28 the objective function has been calculated in 8 steps, which means that the Matlab routine combined with the AnyBody simulation need to be repeated for 64 times. So if you want to do this for 6 variables with each 8 values, the routines should be repeated for 8^6= 262144 times, which would clearly take a lot of time to calculate.

In spite of all the disadvantages the variable studies can be very useful. Local minima can easily be seen and this way the optimisation domain can be restricted so that these are excluded. Moreover, it is very useful for finding initial guesses to start the optimisation study from, again preventing the optimisation to end up in local minima.

In conclusion, the variable studies alone are not sufficient for finding the exact objective minimum. The variable study can obviously be very useful for determining whether the objective function is a smooth function or contains local minima. It shows the approximate minimum location and gives the opportunity to set closer boundaries. An additional optimisation is needed to find the exact minimum.

3.5 Optimisation

In the optimisation study all design variables can be minimized at the same time. The optimal combination of all design variables will be calculated. Calculation is performed with the 'golden section method' [42]. Since it is a numeric minimisation, it can be compared to standing on a mountain blindfolded. To find the valley a person will search for the steepest gradient to go down. Logically, the search direction is the direction with the steepest downward slope. In the objective function this is the direction with the biggest negative gradient. The risk, however, is to end up in a local minimum, a deep valley can be located behind a small hill. By means of the variable studies, boundaries and initial guesses were set to prevent ending up in a local minimum. From the point of the initial guess the gradient in each direction is calculated. The first direction to search the minimum along is the direction with the steepest slope, until a minimum is reached in that specific direction. In this new point, all new gradients are calculated again and the second search direction will be the one with the new steepest gradient. Again the minimum in this direction is searched for. This is repeated until the valley is found. This method is called the golden section method and will be explained below.

Golden section method

The xmax (x1) and xmin (x4) define the interval to search the minimum within. It must be chosen so, that local minima are excluded [42]. Figure 29 shows the golden section method.

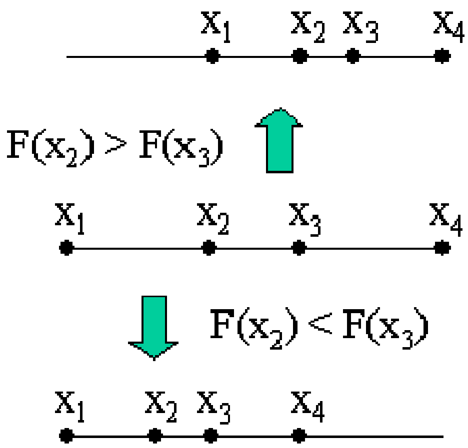

Figure 29 *An illustration of reaching the minimum by means of the golden section method. [43]*

The golden number (0.61803) calculates new values in a narrower interval (x2 and x3) around the minimum, by [42]:

$$x2 = x4 - 0.618 \cdot (x4 - x1) \qquad eq(32)$$

$$x3 = x1 + 0.618 \cdot (x4 - x1) \qquad eq(33)$$

Now, the part of the graph next to the highest value can be excluded in the next calculation since it is known that all values in that part are higher than the minimum. In this example all values right from x3 are excluded when F(x2)<F(x3), with F the value of the objective at the x-values. Now the x3 can be renamed as the new x4. From x1 and x4 again the golden section narrows the interval around the minimum. Because of the golden section number only the new x2 needs to be calculated. The first x2 can be renamed as the new x3, since the new interval (61.803% times 61,803%) is equal to 38.196% which is equal to the position of x2 [42]. If this method is repeated sufficiently enough times, each time the part of the plot next to the highest value is excluded and finally, a reasonable small interval can be assumed a point in the minimum. In this study it is repeated 10 times so the minimum value can be approximated up to 0.8%. The optimisation in this study will be done for all design variables mentioned above for each objective.

3.6 Optimisation Results

In Section 2.5, two subjects of whom experimental data were available from a previous study were implemented in the recumbent model, which was validated with these data. These are also the subjects that have been optimised. The subjects differ 17cm in body height and 7 kg in body weight. Thigh length is 8cm longer for subject 1 and shank length 2cm. All anthropometric data were shown in table 2. Mechanical output was set to 175W. Since there were only two subjects, these will be descriptively studied instead of statistically. Another reason why this method was chosen was that subjects had two different inputs for crank torque amplitude, crank torque offset, pedal angle phase and pedal angle amplitude. Therefore, differences in output values for the two subjects were difficult to ascribe to a single variable effect. Differences in energy expenditure and peak activation might as well be caused by the variations in input data. Therefore, subjects' results will not be compared to each other.

As expected, activation levels were lowest for maximal activation optimisations for each subject, in forward as well as backward cycling. In turn, all energy optimisations resulted in configurations with lower metabolism levels compared to the metabolism levels at the configurations of optimised maximal activity. An overview of the objective values at optimal configurations is shown in figure 30.

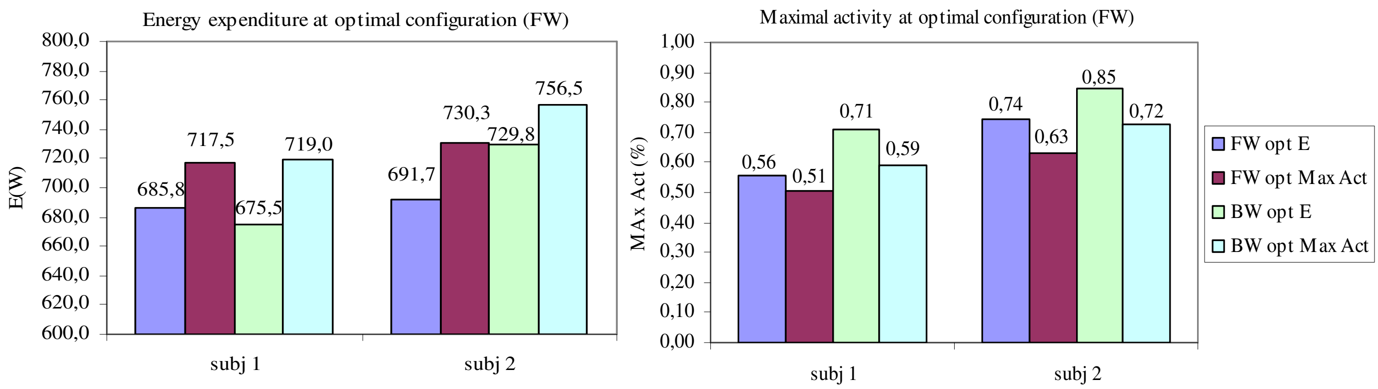

Figure 30 *The activation levels and energy values at each optimal configuration in forward (FW) as well as backward (BW) cycling for both subjects. opt E= optimal energy expenditure, opt A= optimal peak activation*

In forward cycling, activation levels are 8.9% and 14.9% lower for the maximal activity optimisation compared to optimal energy for subject 1 and subject 2 respectively. The total activation has also been calculated for subject 2, since this subject showed the largest difference. The total (integrated) activation was lowest for the energy expenditure objective with 10.9 opt (E) versus 13.9 opt (A)). The optimised energy levels increase for subject 1 from the optimal energy configuration to the optimal activation configuration with 4.6% and for subject 2 with 5.6%. Trends seem to be similar in both subjects.

Subject 1 and subject 2 can also be compared to each other. For each situation (including backward cycling), activation levels and energy levels are lower for subject 1. When compared to subject 1, activation levels are up to 32.1% higher for subject 2. A similar comparison shows higher energy levels up to 8%.

Backward cycling shows similar trends when comparing activation levels and energy levels at each optimal configuration. Although these trends are similar as for forward cycling, maximal activation levels were found to be between 14.3%-26.8% higher for backward cycling compared to forward cycling. Optimal activity levels at optimal maximal activation compared to optimal energy expenditure decreased by 17.2% and 14.22% for subject 1 and subject 2 respectively. The corresponding energy levels are again increasing and are 6.4% and 3.7% respectively. Energy level is also increased for subject 2, with 5.5% and 3.5% for optimal energy expenditure and optimal maximal activity respectively. The only deviation from the trends can be seen in energy expenditure of subject 1. For subject 1 energy expenditure is slightly lower for backward cycling compared to forward cycling for optimal energy expenditure. The decrease is slight, 1.5%. For optimal maximal activity increase is slight as well with 0.2%.

Maximal activity

The objective maximal muscle activity was determined as the peak value of the activations of all lower limb muscles. To determine which muscles are responsible for this maximal value, the individual muscles' maximal activity value has been determined. In Appendix D, it can be seen that the maximal activity value of the lower limb is not determined by a single muscle. Many muscles reach the maximum value. This was found for both objectives. Not the major muscles solely, like gastrocnemius, vastii, semitendinosus, biceps femoris longus, gluteus maximus, are responsible for the maximal activation level. Also many small muscles, like the peroneus brevis, extensor digitorum longus, sartorius and iliopsoas, reach the maximum.

Variable sensitivity

Each design and secondary variable affects the objective values. By means of the variable studies, the individual variable sensitivities have been determined, to investigate which variable influences the objective most. The variable study surface was used to determine the proportional objective increase with respect to the minimum objective value. To do so, objective values in forward cycling were determined at a 10% variable step left from the minimum and at a 10% variable step right from the minimum.

$$slope = \frac{\Delta objective \;\; value(\%)}{param \;\; step 10\%} \cdot 100 \qquad eq(34)$$

In some cases smaller steps were taken because the physical boundaries were reached. For subject 2 in one case, seat height, a 20% step left and right were taken, since the minimum value was so close to zero, that a 10% step was too small. The deviated values are shown left from the found slopes. Table 5 shows the individual variable sensitivities.

Table 5 *Variable sensitivity study.*
The right columns show the step sizes taken and were less than 10% when physiological boundaries were reached. Variable abbreviations are: d=torque phase, offL= left ankle offset, offR= right ankle offset, dist= seat distance, hght=seat height

subject 1 E	slope +	slope -	step size	step size
d	2.2	4.8	10%	10%
offL	8.7	8.7	10%	10%
offR	16.6	8.7	8%	10%
Dist	268	27.1	7%	6%
hght	1.5	4.4	10%	10%
cadence	5.8	14.5	10%	10%

subject 2 E	slope +	slope -	step size	step size
d	1.0	1.1	10%	10%
offL	0.000	7.2	10%	10%
offR	7.2	11.5	10%	10%
Dist	105	21.3	10%	1%
hght	2.1	1.4	10%	10%
cadence	16.5	6.9	10%	10%

subject 1 Act	slope +	slope -	step size	step size
d	78.9	52.6	10%	10%
offL	33.5	47.2	10%	10%
offR	33.5	33.5	10%	10%
Dist	633	141.7	1.1%	8%
hght	19.9	6.0	10%	10%
cadence	45.4	76.9	10%	10%

subject 2 Act	slope +	slope -	step size	step size
d	32.3	27.4	10%	10%
offL	51.7	69.0	10%	10%
offR	258.6	34.5	10%	10%
Dist	2812	17.2	1.6%	10%
hght	2.6	2.6	20%	20%
cadence	85.5	80.3	10%	10%

All values show that a 10% percent variable step affects the objective peak activity values much more in comparison to at the objective energy expenditure energy expenditure. The order of variable sensitivity is for both subjects similar when considering the design variables. The subject is most sensitive to changes in seat distance, followed by changes in cadence and least sensitive to changes in seat height. Considering seat distance, the subject is much more sensitive to positions further away from the optimal position compared to positions closer to the crank. For cadence and seat height such a difference was not found. The sensitivities of the secondary variables vary, but are all of the same order; which secondary variable the objectives energy and maximal activity are most sensitive to cannot be identified. These secondary variables' sensitivities lie in the same order as the sensitivities for cadence except for the crank torque phase in the objective energy expenditure. Sensitivity was for this variable in the order of the sensitivity of the crank height and thus very small.

Optimal configuration

Now it is clear which variables are of the biggest influence, it can be studied which variable caused the differences in the objective values at the optimisation studies. Again comparisons per subject will be made between both objectives and between forward and backward cycling for each objective. Figure 31 shows the optimal configurations per subject in a stick diagram that represents the leg. The zero position is the hip position, from which the thigh and shank positions can be seen respectively. The third stick in the diagram is the length from the ankle to the middle of the pedal. Subsequently, the real ankle angles are smaller than de shown angles. From the stick diagram it can be seen that for both objectives, the hip angles for the objective energy expenditure are smaller compared to the maximal activity objective. The hip angles for forward compared to backward cycling lie closely together per objective.

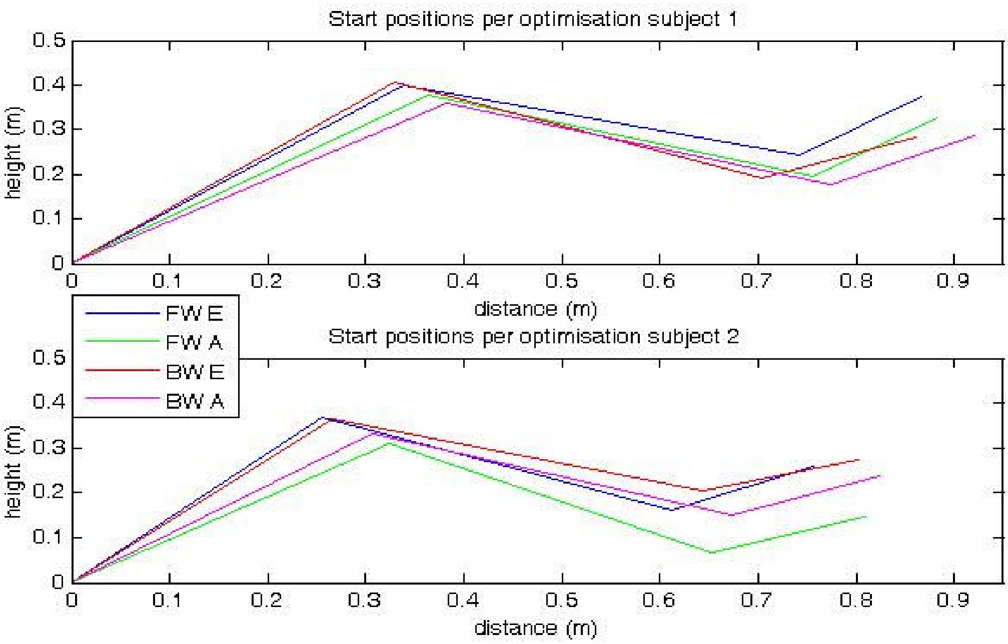

Figure 31 *The starting positions per objective.The zero postion represents the hip. Th ethird stick represents the distance from ankle to the middle of the pedal. FW= forward, BW= backward, E= at optimal energy expenditure, A= at optimal peak activation*

Table 6 *Optimal configurations (in %TH) and cadences (rpm) per subject.*
E= optimal energy expenditure, MA= optimal peak activity, FW = forward, BW= backward

			cadence (rpm)	Seat position (%TH)	seat distance (%TH)	Seat height (%TH)
FW	E	*subject 1*	74.4	100.9	82.2	19.5
FW	*A*	*subject 1*	73.9	101.4	83.7	15.2
BW	*E*	*subject 1*	80.5	98.7	81.6	11.0
BW	*A*	*subject 1*	67.8	104.4	87.3	11.3
FW	*E*	*subject 2*	87.7	102.2	82.7	9.8
FW	*A*	*subject 2*	71.7	107.5	88.6	-2.8
BW	*E*	*subject 2*	67.8	107.6	87.9	11.6
BW	*A*	*subject 2*	64.4	109.4	90.2	7.5

The most remarkable result in the combination of optimal configurations and optimal cadence is that further optimal positions are combined with lower optimal cadences. Furthermore, optimal configurations for the least energy expenditure appear less far in comparison to their optimal peak activation equivalents.

From table 6 it shows that subject 1's seat position resulted for both objectives in forward cycling in 101 %TH, despite the difference in crank height (8% TH (opt E) vs. 19%TH (opt A)). Cadences were also found to be similar at 74 rpm. The main difference in design variables is thus caused by seat height; however, in the previous section it was shown that seat height had least affect on both objectives. The 4.6% higher energy expenditure and 8.9% lower peak activation in comparison to the objective values in the energy expenditure must therefore be caused by the secondary variables. The ankle offset differed for the left ankle with only 2.6% and less than 1 % for the right ankle. So for subject 1 the difference in energy expenditure and peak activation must be caused by the crank torque phase. Crank torque phase indeed increased by 11.7 %. For energy expenditure crank torque phase was found to be of little influence in the variable studies. The small energy expenditure difference was probably caused by a combination of the different saddle height and the different crank torque phase.

In contrast, crank torque phase and seat height were found to be constant between the two objectives for backwards cycling of subject 1, as can be seen in table 6 The main cause of the 17.2% lower peak activation and 6.4% higher energy expenditure was probably seat distance, which increased by 6% for the optimal peak activation. Also cadence and ankle offset showed big changes of more than 10% as can be seen in table 6 and table 7. For this reason, it was difficult to assign the change in energy expenditure and peak activation to a single variable. Taking into account the variable sensitivity, it can only be said that the order of the variables having the largest influence was probably seat distance, followed by cadence and ankle offset.

Table 7 *Secondary variable values after optimisation. Opt E= optimal energy expenditure, opt MA= optimal peak activity, FW = forward, BW= backward, d= crank torque phase, offL/R= left and right ankle offset.*

			d	OffL	OffR
FW	E	subject 1	1.79	1.15	1.19
FW	A	subject 1	2.00	1.18	1.18
BW	E	subject 1	-0.74	1.01	1.01
BW	A	subject 1	-0.73	1.18	1.13
FW	E	subject 2	-1.82	0.99	1.01
FW	A	subject 2	-1.10	0.99	0.89
BW	E	subject 2	0.10	1.08	1.01
BW	A	subject 2	-0.34	1.08	1.12

As can be seen from tables 6 and 7 it was even more difficult to ascribe the change in objective values to specific variable changes. The most striking differences between the two optimal configurations in forward cycling were twofold. First of all, seat positions increased from 102%TH to as far as 107%TH. Second, seat height changed from below the crank for the optimal energy expenditure to above the crank for optimal peak activation. No further specifications have been made for which variable was responsible for the changes in objective values other than the order found in the variable sensitivity study.

For backward cycling, the variables that caused the change in objective values were also ordered as followed from the variable sensitivity study, as seat distance, right ankle offset and crank torque phase. Seat distance increased from 107%TH to an even further 109% TH, caused by both a change in seat distance as a change in seat height.

To compare forward to backward cycling it is impossible to compare crank torque phase since these are calculated from different input crank torque profiles. This is also true for the ankle angle. Therefore, only the configurations and cadences will be compared. The results show different outcomes in the design variables in all cases. No major trends were seen.

Gross efficiency

The gross efficiency can be helpful in understanding the effects of the changed configurations on muscle use. The gross efficiencies are therefore studied for each configuration. The lower limb total efficiencies are plotted below (figure 32).

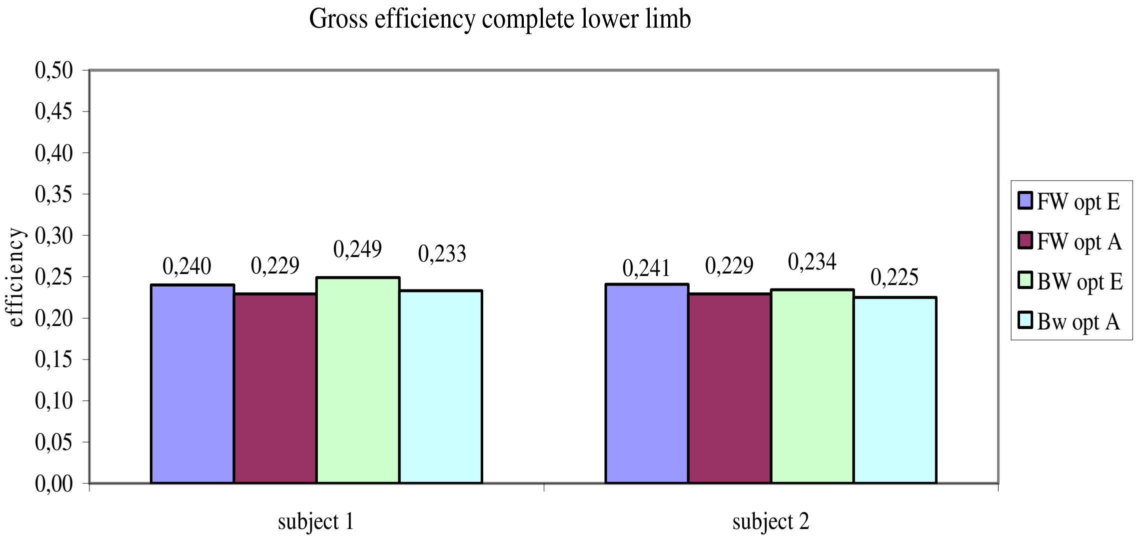

Figure 32 *Gross efficiencies at each configuration of the two subjects.*

Human skeletal muscle is mostly found to be efficient up to 25 % [44]. The total lower limb efficiencies after optimisation show results of the same order. The energy expenditure optimisation resulted in the highest lower limb efficiencies for both subjects and pedalling techniques, as expected. Approximately, 1% in efficiency is won by optimising energy expenditure in comparison to optimising peak activation level. For forward cycling the optimal energy expenditure efficiency was 24% for subject 1, which was less than the 24.9% of backward cycling. The optimal maximal activation resulted in efficiencies of 22.9% and 23.3% for forward and backward cycling respectively. Subject 2 resulted in the same lower limb efficiencies for forward cycling as subject 1, 24.1% (opt E) and 22.9% (opt MA) respectively. Backward cycling resulted in lower efficiencies, namely 23.4% (opt E) and 22.5% (opt MA), which is in contrast to subject 1.

Individual muscle efficiencies

Differences in lower limb efficiencies are small and values are all of the same order, despite differences in configurations and thus expected differences in muscle use. Since the subjects are optimised for energy and activation levels, each configuration is expected to lead to high muscle efficiencies. In addition to total lower limb efficiency, individual muscle efficiencies have been studied as well. The individual muscle efficiencies per configuration have been listed in Appendix E.

Individual muscle efficiencies are calculated to study whether the individual contribution of the muscles was similar for each configuration. The eight most relevant muscles contributing to the pedalling cycle as described in the synergistic categorization (Section 1.3) were studied. Of these muscles, the vastii, semimembranosus and the biceps femoris appeared to be most efficient in all configurations and in both subjects (between 35.8%-40.8% subject 1 and 30.5-35.9% subject 2). The least efficient muscle was the gastrocnemius (between 1-15%).

Differences in the efficiencies of the relevant muscles, comparing the two objectives to each other, are small in both forward and backward pedalling. Differences were taken into account when larger than 10%. Subject 1 shows no changes for individual muscle efficiencies between the two objectives. Subject 2 only show change in efficiency for two muscles, the soleus and the tibialis anterior. The efficiency of the soleus was 11.2% higher for optimal peak activation compared to optimal energy expenditure in forward cycling. The tibialis anterior showed an increase in efficiency of 44% in forward cycling, with a change from negative to positive efficiencies for the peak activity objective. This indicated a change from negative muscle work (eccentric force delivery) to positive muscle work (concentric force delivery). For backwards cycling, the tibilais anterior didn't show negative efficiencies, but in the peak activity objective, efficiency was again higher (11%) for opt A.

Comparing forward cycling to backward cycling, more remarkable changes were seen. For backward cycling, the vastii, semimembranosus and biceps femoris were again the most efficient and even slightly more efficient with efficiencies ranging from 37.0-43.6% for subject 1 and 33.6%-38.9% for subject 2. Of the relevant muscles, changes are found in the tibialis anterior efficiencies of both subjects. Tibialis anterior increased efficiency with 13.3% (opt E) and 11.4% (opt MA) for subject 1 and for subject 2 change from negative to positive muscle work was seen in the energy expenditure objective and an increase of 29.7% in the peak activity objective. In contrast, the gastrocnemius was found to decrease efficiency for backward cycling. Subject 2 decreased efficiency with 12.5% and 11% for optimal energy expenditure and optimal peak activation respectively. Although slightly less than 10% this tendency was also seen in subject 1 which showed decreases of 8.4% (opt A) and 8.9% (opt E) respectively. A final difference in individual muscle efficiencies was found for the soleus in subject 2. Subject 2 increased soleus efficiency with 12.6% for the optimal energy expenditure objective.

Work-loops

Work-loops can be helpful in studying the muscle functions at the different configurations. For this purpose, work-loops of the most relevant muscles for the cycling movement have been looked at. From the efficiency section, it followed that the muscles contributing to plantar and dorsal flexion, gastrocnemius, the soleus and the tibialis anterior, changed efficiency most between forward and backward cycling. Subsequently, these muscles are expected to change their work-loops. Muscles that did not change their efficiencies between forward and backward cycling were not expected to change their functions between forward and backward cycling, and subsequently no major differences were expected to be seen in their work-loops. The work-loops of the rectus femoris, soleus, tibialis anterior and the gastrocnemius are shown in figures 33-36 for each configuration of subject 1. Also the corresponding figure of the length and force of the rectus femoris during the crank cycle is illustrated.

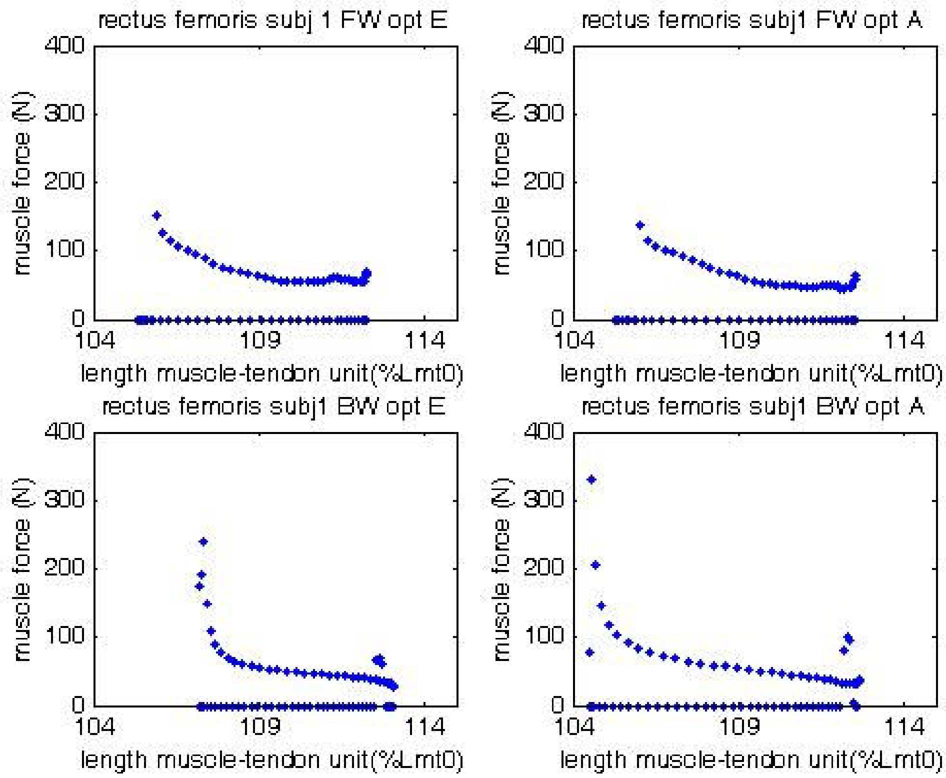

Figure 33 *a) Workloops of the rectus femoris. The upper work-loops are the loops for forward cycling and the lower figures are the loos for backward cycling. The left figures are the loops for optimal energy expenditure and on the right are the loops of optimal peak activation.*

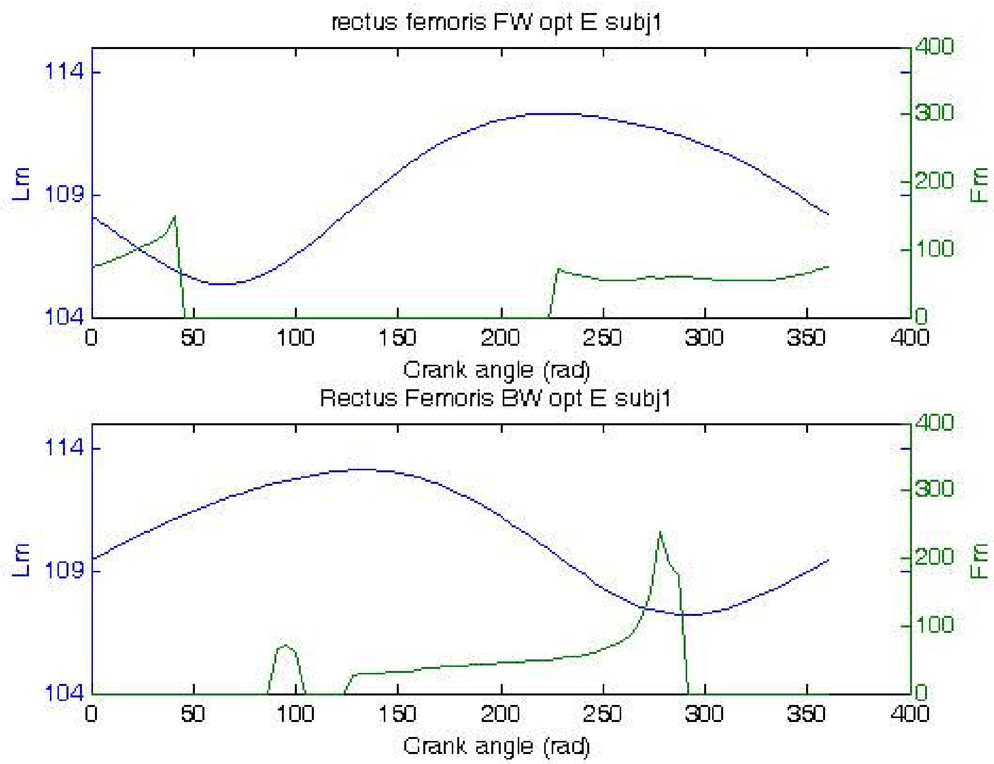

b) The corresponding force and length over the cycle of the rectus femoris. Again the upper figure shows forward and the lower figure shows backward cycling.

The individual muscle work loop patterns showed similar tendencies for both subjects. Moreover, similar tendencies were found when comparing the two objectives. The only difference found in efficiency between the optimal peak activation and optimal energy expenditure was seen during forward cycling for the soleus of subject 2. The work-loop showed for this particular situation a larger working length range for the optimal peak activity configuration. Nevertheless, work-loop patterns were similar for both objectives. Subject 2 also showed negative efficiencies for the tibialis anterior. The work-loops showed that muscle contraction in the tibialis anterior was a very short isometric contraction. This was found for both objectives and both subjects.

The efficiencies of the relevant muscles that showed no difference between the two pedalling techniques were expected to keep similar tendencies in their work-loops and subsequently keep similar functions. As expected, these resulted in relatively similar work-loops in forward and backward cycling. Although lengths at which force is delivered and force levels differ slightly between forward and backward cycling, patterns per optimal configuration are quite similar. The rectus femoris, gluteus maximus, semimembranosus, biceps femoris and vastus medialis, only showed small differences in peak force patterns mainly found at the minimum and maximum muscle lengths. The peaks were mainly found around the dead centres, which are demonstrated for the rectus femoris in figure 33.

The muscles which were expected to show differences in work-loops for forward compared to backward cycling, based on the findings in efficiencies were the gastrocnemius, the soleus and the tibialis anterior. The work-loops indeed showed major changes for these muscles. In figures 34-36 these are illustrated.

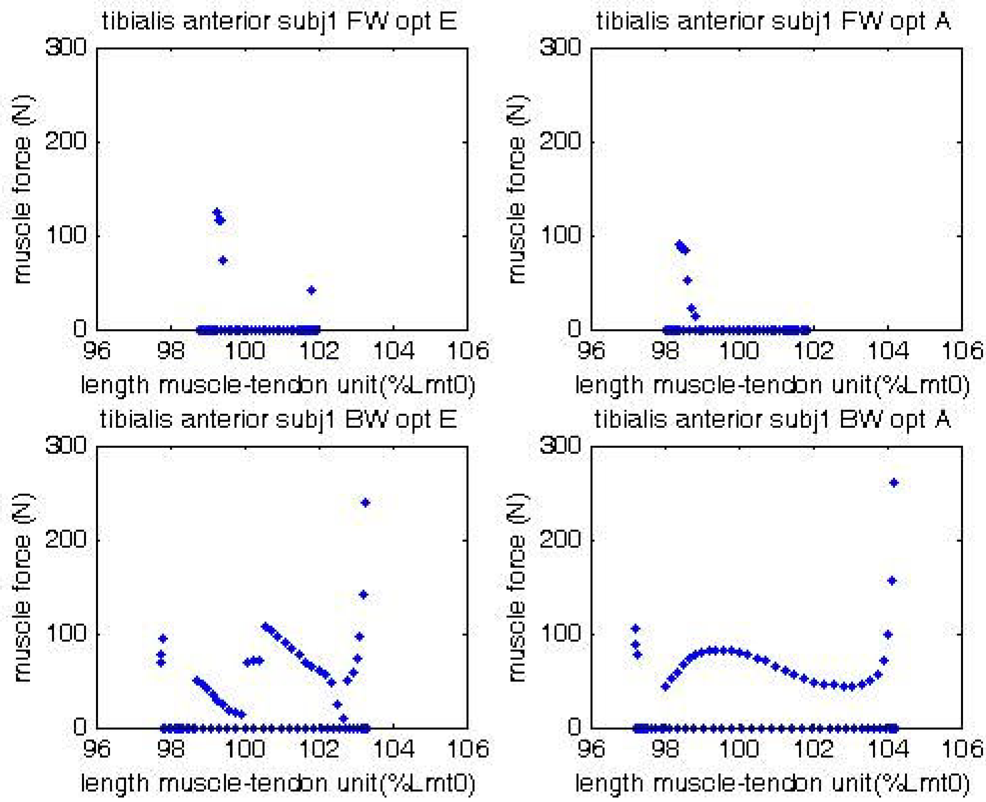

Figure 34 *Work-loops of the tibialis anterior. The upper work-loops are the loops for forward cycling and the lower figures are the loos for backward cycling. The left figures are the loops for optimal energy expenditure and on the right are the loops of optimal peak activation.*

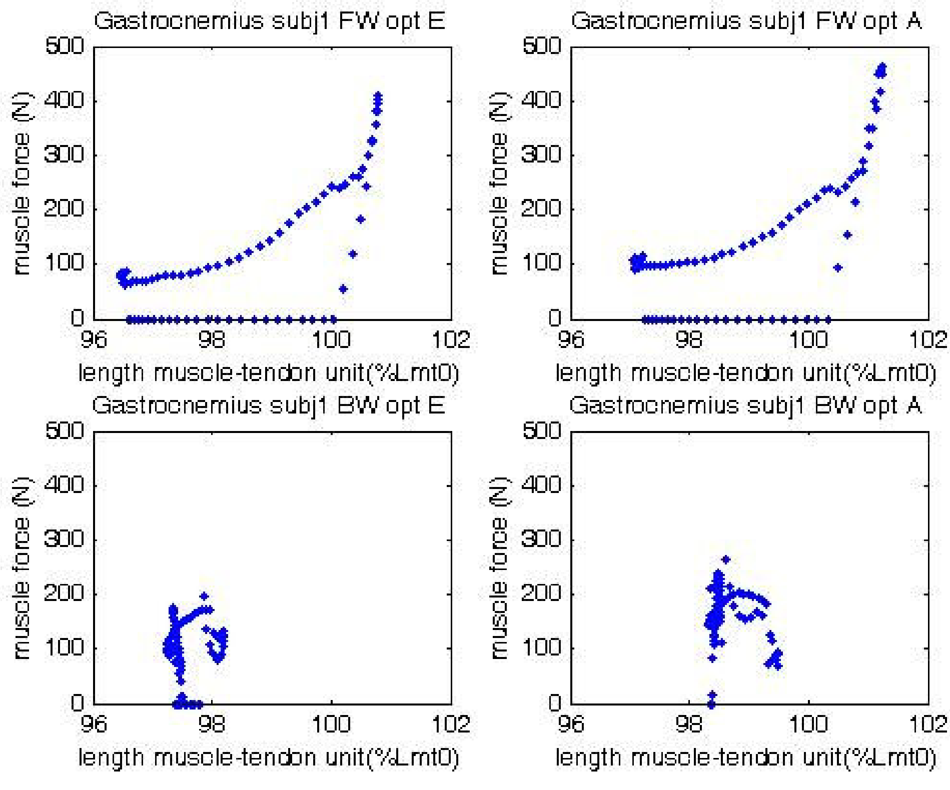

Figure 35 *Work-loops of the Gastrocnemius. The upper work-loops are the loops for forward cycling and the lower figures are the loos for backward cycling. The left figures are the loops for optimal energy expenditure and on the right are the loops of optimal peak activation.*

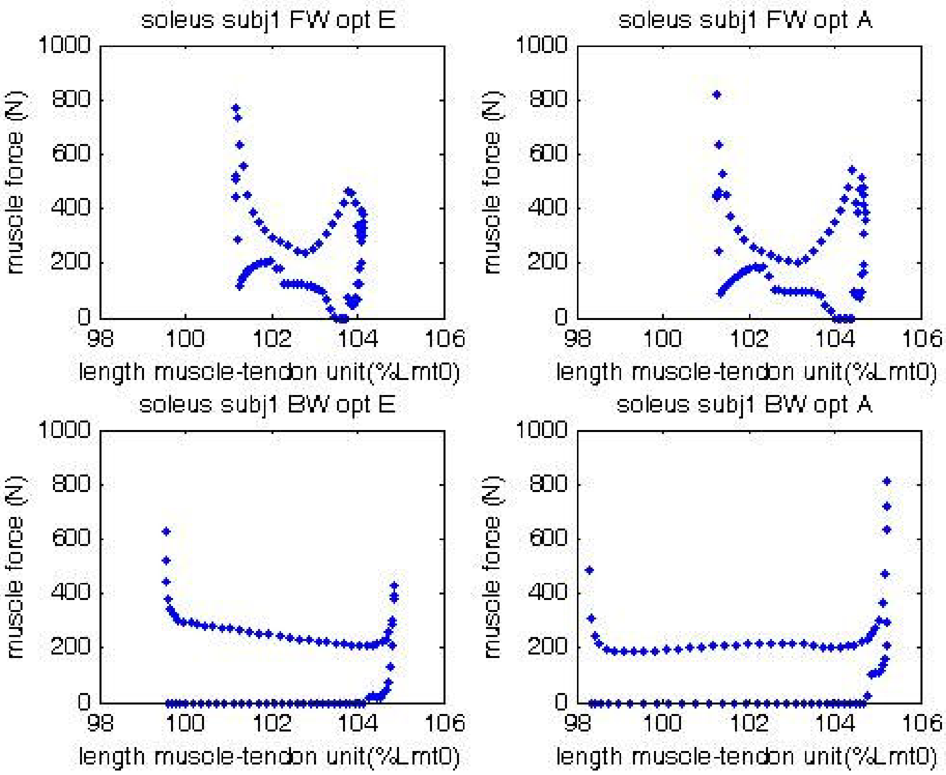

Figure 36 *Work-loops of the soleus. The upper work-loops are the loops for forward cycling and the lower figures are the loos for backward cycling. The left figures are the loops for optimal energy expenditure and on the right are the loops of optimal peak activation.*

First the tibialis anterior is studied. Whereas the tibilais anterior showed mainly isometric contractions during forward cycling, both work length and work delivery increased markedly during backward cycling.

The opposite was found for the gastrocnemius. During forward cycling work was decreasingly delivered during shortening, whereas the range of length at which work was delivered during backward cycling was decreased from 4% around the optimal fibre length to 1% for subject 1 and from 5% to 2.5 % for subject 2. This made the gastrocnemius' work delivery almost isometric during backwards cycling.

The last muscle that was expected to change work-loops when forward cycling was compared to backward cycling was the soleus. Like the tibialis anterior, the soleus increased working length range as well, with up to 7%. During backward cycling, force delivery is almost constant during shortening. However, in forward cycling force is delivered during almost the complete cycle, concentric as well as eccentric contraction was seen.

In the next section, results as found for optimal objective values, variable sensitivity, configurations, efficiencies and work-loops will be thoroughly discussed.

3.7 Discussion

The aim of the optimisation study was to find an optimal configuration with minimal energy expenditure and an optimal configuration with minimal peak activation level. Moreover, the model gave the opportunity to study the individual muscle behaviour at these optimal configurations. The optimum was searched for a combination of design variables, namely seat distance, seat height and cadence. The crank torque phase and ankle offset are directly influenced by these design variables and are therefore optimised as well. As expected, for the optimal energy expenditure configuration, the golden section optimisation method resulted in lower energy levels for each subject per pedalling technique, in comparison to the optimal peak activation configuration. In turn, the peak activation levels were lowest for the optimal peak activation configuration.

The most striking result of the variable analysis was that the objective peak activation was more sensitive to variable changes in comparison to energy expenditure. Since the activation level is of direct influence on the energy expenditure, it was expected that sensitivities would be of the same order for both objectives. Nevertheless, sensitivity of the peak activation in comparison to sensitivity of energy expenditure is at least twenty-five percent higher for cadence, offset and crank torque phase. A closer look at the activations shows that an increase in peak activation did not result in a similar increase in integrated activation. For example, a comparison of the two objectives in forward cycling for subject 2 shows a 15% higher peak activation for optimal energy expenditure, whereas the integrated activation was lowest for the energy expenditure. This explains the different order of sensitivity to the objective E, since the integrated activation determines the energy expenditure and peak activation shows no direct relationship to the integrated activation level.

After optimisation of peak activation, multiple muscles reach the new peak activation level. From this, it follows that optimisation of peak activation resulted, as hypothesised, in a minimised peak activation level of only one or a few muscles. This supports the theory that minimizing peak activation is a good objective function, since it prevents a single muscle to become the bottle neck during long exercise. From these findings it can be concluded that optimisation of peak activation level decreases high activation of a single muscle. However, integrated activation can be increased in this situation as followed from the integrated activation, which implies earlier whole body fatigue. A combination of integrated activation and peak activation might therefore be a good alternative objective to prevent premature fatigue.

To check whether the energy model showed reasonable results, efficiencies were studied. Gross efficiencies of the complete lower limb resulted in efficiencies in the order of 25% that were also found in literature [44]. When looking more closely, the individual muscle efficiencies look relatively high, with values up to approximately 40%. Nevertheless, the study of Umberger [8] also found peak efficiencies of this order for the individual muscles during aerobe exercise and indicated that the origin of these high values could have several causes. First of all, the model does not take into account contraction recovery heat. Secondly, they refer to an article of Stienen [45], which shows a higher economy for human muscles compared to rodent muscles, on which individual muscle peak efficiencies in the order of 25% are based. Isolated muscle efficiencies have not yet been studied for human muscles. Furthermore, a previous study [46] shows efficiencies for human muscles of approximately 30% to 56%, which are also very high. Since these individual muscle efficiencies are found in the same order as in the Umberger model, the peak efficiencies are considered reasonable. Isolated human muscle efficiency measurements would be helpful to identify the maximal human muscle efficiencies.

As explained in chapter 1, muscle force delivery depends on muscle length, contraction velocity and activation level. Almost all optimisation results can be explained by the principles of the force-length and force-velocity relationships. The sensitivity study showed that the objectives were most sensitive to seat distance, which directly affects the effective muscle operating length during the pedalling cycle. A displacement in distance affects the joint angles much more in comparison to a similar displacement in height. As a consequence, the muscle operating lengths change more at a different seat distance, which explains the higher sensitivity over seat height.

The next most sensitive variable was cadence. Since force delivery also directly depends on contraction velocity, this seems plausible. Per optimisation a unique optimal cadence was found, which differed from the preferred cadences found in literature [6, 13, 14], however, these studies were based on conventional cycling. Moreover, optimal cadence was searched for at a single seat position. Most of the studies did not mention the subjects' seat position. In some of these studies seat position was mentioned, but it was mainly determined as the height preferred by experienced cyclists or 100% TH for non-cyclists [6, 17]. From the variable study in this report, however, it could be seen that optimal cadence depends on seat position. The optimisation study also showed a relationship between optimal seat position and optimal cadence; whereas optimal cadence decreased as optimal seat position was found further away from the crank. Since seat position affects muscle working length, it changes the individual muscle contributions as a consequence. When seat position is changed, other muscles will lie more closely to their optimal working length and will consequently contribute more to the pedalling cycle. The origin of the lower cadence at further seat positions can be explained by the relation between force-length en force-velocity curves. For example, at a further seat position, the quadriceps will be working at a longer than optimal fibre length. This reduces the maximal force that can be delivered, which directly affects the reach of the force-velocity curve. Subsequently, only a smaller range (lower range) of cadences is capable to fulfil the required force. In summary, it can be said that optimal cadence will be affected by seat position and it is therefore important to study optimal cadence along with an optimal seat position.

The sensitivity study also showed that for both objectives, sensitivities to offset are of similar order as cadence. Ankle offset directly affects working length of the soleus, tibialis anterior, and gastrocnemius. Thus, these muscles affect the activation level needed to reach the required force level. Subsequently, they have a high influence on the optimal configuration. Also crank torque phase appeared to be of essential influence on peak activation level. Crank torque phase also affects the muscle lengths at which force is delivered. Since crank torque phase and ankle offset have an essential influence on optimal cycling, it is important to test whether these are automatically adapted during experimental human cycling. Otherwise, it might be helpful in future studies to train for the optimal secondary variables.

Force-length curves could also be helpful to explain why backward cycling resulted in higher peak activations compared to forward cycling. Since the power stroke is directed the other way around, force is also delivered at different muscle lengths. However, for backward cycling it was seen that pedal forces were very high around the dead centres. To achieve these high levels, muscle forces need to be high as well, which were determined by activation level. Closer studying is needed to find the cause of the high peak activation levels.

The optimal configurations of the subjects showed different results, despite limited variations between subjects. Peak activation levels of subject 2 are all higher compared to subject 1. The origin of this difference must lie in the scaling of the muscle masses, since the only variations between the two subjects is their segment length and the ratio between the segment lengths. Subject 1 has a thigh:shank ratio of 1:0.9, whereas subject 2 shows a 1:1 ratio. Furthermore, subject 1 has longer segments in comparison to subject 2. These longer segments might have resulted in muscles masses that were scaled to too high values, making subject 1 relatively too strong. Subject 1 has a higher maximal isometric force of 6.13% compared to subject 2. Overestimation of muscle mass of subject 1 might have been the cause of its lower peak activations. The scaling method therefore needs closer studying.

Scaling might also be the cause of the difference in seat position of the two simulated subjects. The optimal seat positions with respect to the trochanter of subject 2 were further in comparison to the optimal seat positions of subject 1. In addition, these positions were also further than optimal seat positions reported in the literature [2]. However, these data were based on findings in conventional cycling. The different optimal configurations between the two subjects might have been caused by the scaling method, resulting in different optimal fibre lengths.

The work-loops showed no differences when efficiencies were equal for two configurations or pedalling techniques. The only differences seen, were the peak forces in the maximum and minimum length of the muscles, which occurred in the regions of the dead centres. Since the model already showed that it has difficulties around these regions in the pedal forces, these muscle peak force changes were not studied more closely. The muscles (soleus, tibialis anterior and gastrocnemius) that were expected to change work-loops, based on their efficiencies, indeed showed remarkable changes. Since the gastrocnemius reduced work tremendously during backward cycling and soleus and tibialis anterior showed the opposite results, this implies that these last two muscles take over the gastrocnemius function. This was inconsistent with experimental findings from Neptune Kautz [21], who found a decrease in muscle work for both the tibialis anterior and gastrocnemius during backward cycling. Like in the current study they did find a synergistic relation for these three muscles.

It can be concluded that with this optimisation study a good start has been made on finding the optimal recumbent cycling configuration and cadence. No information was available in literature on the recumbent cycling configuration or cadence. Therefore, the current recumbent seat positions are only based on practical experience of the cyclists. The search for the combined optimal seat position and cadence appeared to be very important, because it was shown that they depend on each other. The energy model provided efficiency results that seem very plausible and peak activation seemed to minimise protruding activation levels of a single muscle, as expected. Individual muscle efficiencies and work-loops gave the opportunity to study their contribution per configuration and highlighted differences in pedalling technique. An experimental study will be helpful to validate the current findings. The next chapter will describe the start that has been made for model validation.

Chapter 4: Experiment

4.1 Introduction

Each optimal configuration as found in the previous chapter was tested in this part of the study. In the simulation study, predictions were made for a combined seat position with cadence of least energy expenditure and of minimum peak activation level. At the optimal configuration cadence and secondary variables, the model calculated tangential forces, radial forces and muscle activation levels. These will be closely looked at in this chapter to observe the predictive characteristics of the model.

The main question of the experimental study is whether the recumbent cycling model can predict human movement adequately, so that the simulation model can be used for predictive purposes to find the subject specific optimal variables. By means of the experimental study, a start will be made for the validation of the computer model. The experimental research question therefore is:

- Do the configurations and secondary variables predicted by the AnyBody software lead to the corresponding experimental pedal forces, activation levels, energy expenditure trends and peak activation trends?

The main hypotheses are 1: the configuration at minimal energy expenditure in the simulation model will cost less total body energy expenditure compared to the corresponding configuration at minimised peak activation. Hypothesis two is that the configuration at minimal peak activity will result in lower maximum values for the EMG data, since it was seen that for the optimal configurations, multiple muscles determined the peak activation. The most relevant muscles also showed to reach the peak activation levels. Therefore, it was expected that lower EMG levels would be found for the optimal peak activation configurations. In addition, backward cycling simulations resulted for both subjects in higher peak activations during the exercise, which is also hypothesised to occur in experimental recumbent cycling.

4.2 Participants

Two male recreational cyclists were asked to volunteer for this study. They were the same subjects as simulated in chapters 2 and 3. Their anthropometric data can be found in section 2.5. The current two were chosen because their difference in height would be useful in studying more extreme measures in the model as well. Both subjects were without leg pain or impairments to active limbs. Before taking part in this study, participants read informed consent form outlining purpose and methods of the experiments.

4.3 Experimental set-up

For this experiment, a conventional cycle ergometer (Jeager, ER 800) is placed vertically on a steel frame. The height of the crank can be regulated by shifting the complete ergometer up and down the steel construction. Figure 37 demonstrates the experimental recumbent cycle.

Figure 37 *Recumbent cycle experimental setup*

Power is set to 175 W which is equal to the experimental data used for creating and optimising the recumbent model. Cadence can be read by the subject from the ergometer screen. The seat of the recumbent cycle construction is placed on the horizontal part of the steel frame which prevents tilting of the construction. The seat is a cybex chair on wheels, with back support. The chair's trunk angle is set to 26^{o} as explained in section 1.3. Horizontal distance adjustments can be made by shifting the chair backward and forward over the steel frame.

The clip less pedals used are of the Shimano pedalling system (SPD). In the right pedal, a force measuring device is implanted in the spindle. The device measures force magnitude and force direction by means of a strain gauge. The resulting force, which is measured, can be split into tangential forces and radial forces.

Video analysis is applied to determine segment lengths and to analyse kinematics of the lower extremity in time. Reflective markers are placed on the Sias, trochanter major, condylus lateralis, maleolus and on both sides of the pedal for this purpose. A reference balk of 56 cm was used to determine the exact measures in the image. The video recording frequency is 25 Hz. The camera thus records for 40 ms and then turns off for 40 ms.. Each image displays two spots of a single marker which can be analysed separately, increasing the recording frequency of the camera to 50Hz. The video signal is synchronized with the pedal force measuring device and the electromyography measurements (EMG).

EMG measurements were used to record muscle activity. Differences in electric potential of muscle membrane when activated are measured by the EMG. Bipolar surface electrodes each measure the electrical changes in the muscles, reducing ambient noise [35]. For this study the EMG signals of the following muscles are captured:

- biceps femoris longus
- gluteus maximus
- semitendinosus
- rectus femoris
- Tibialis anterior
- Gastrochnemius lateralis
- Soleus
- Vastus lateralis

In the previous chapter, energy expenditure has been used as an objective to find the optimal configurations. Subsequently, energy expenditure needs to be measured experimentally as well. Unfortunately, measuring energy consumption of the leg solely is impossible, which is why complete body energy expenditure has been chosen to measure by use of indirect calorimetrics (Oxycon beta, Mijnhardt). This open circuit system compares the compounds O2, CO2 and N of inspired ambient air (%O_2= 20.93, %CO_2= 0.03, %N_2= 79.04) to expired percentages. During exercise, oxygen is increasingly used for aerobe metabolic reactions, and carbon dioxide is increasingly produced in the expired breath. With the measured CO_2 production and O_2 consumption, the respiratory quotient (RQ) can be calculated. The RQ value approximately indicates the nutrient mixture being catabolized. By means of the RQ value and oxygen consumption, energy expenditure can be calculated [44].

$$\text{energy exp.}\,(\mathrm{W}) = \dot{\mathrm{V}}_{O2}\,(l\,/\,\min)\cdot \text{caloric equivalent at given RQ}(\mathrm{kcal/L_{O2}})\cdot \frac{4.187}{60} \qquad \textit{eq(35)}$$

$\dot{\mathrm{V}}_{O2}$= Volume of oxygen consumed in time

The nutrient compounds catabolised at specific RQ and the corresponding caloric O_2 values are shown in Appendix B [44].

4.4 Procedure

The experimental design of this study required each participant to pedal on a recumbent cycling position in 3 different configurations cycling forward and 2 different configurations backward. The three different forward configurations are configurations:

1. at optimal predicted energy expenditure
2. at optimal predicted muscle activation
3. at preferred distance and cadence at the predicted optimal energy expenditure height

For backward cycling only two configurations will be measured, which are the configurations at optimal energy expenditure and at optimal muscle activation. The measurements are schematically drawn in figure 38.

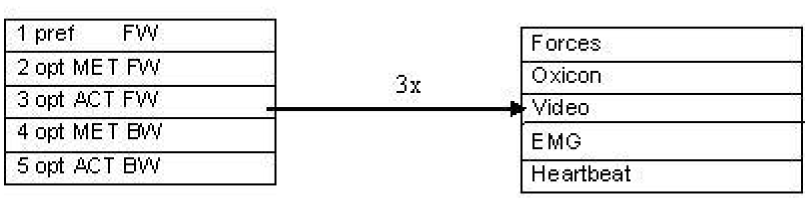

Figure 38 *Schematic overview of the experimental set-u, with pref =preference distance and cadence at metabolic optimal height, MET= optimal metabolic configuration, ACT= optimal peak activation configuration, FW= forward, BW= backward.*

The optimal variables are shown in tables 6 and 7 of the previous chapter. The secondary variables will be used for control purposes only.

Measurements were performed three times each configuration after reaching steady state. EMG, Video analysis, and pedal forces were measured for nine seconds. Oxycon data were registered every half minute during the complete exercise. The time between two measurements in one session was approximately three minutes. After each session of three measurements per configuration, rest was given until heartbeat decreased to 100 BPM and at the same time the new configuration was set. Between the forward and backward measurements, half an hour of rest was given.

4.5 Results

Configuration

The design variable values as found in the optimisation study were translated into experimental settings coming close to them. Nevertheless, it appeared difficult to achieve the correct seat positions. The ergometer on the vertical frame is very heavy and needs to be set by hand. The weight of the ergometer makes it difficult to achieve high accuracy. Distance was difficult to set because it is set as trochanteric distance while the subject is not pedalling. A perpendicular is dropped from the trochanter to the seat lower frame and a line is drawn. This line lies next to the horizontal frame on which the seat is placed and on which a flexible steel rule is attached. During pedalling and between experiments the subject has changed it position on the seat, which is the reason why vertical distance showed inaccuracies. Below in Table 8 the predicted seat position is set next to the experimentally achieved seat positions.

Table 8 *Predicted values of the simulations versus achieved variablesin the experimental setting*

Subject 1	FW exp E	FW sim E	FW exp A	FW sim A	BW exp E	BW sim E	BW exp A	BW sim A
Distance (m)	-0.87	-0.86	-0.89	-0.87	-0.90	-0.85	-0.95	-0.91
height (m)	-0.23	-0.20	-0.19	-0.16	-0.15	-0.11	-0.16	-0.12
Cadence (rpm)	74	74	75	74	80	81	72	68
ankle offset (rad)	1.24	1.15	1.19	1.18	1.07	1.01	1.21	1.18
T phase	2.57	1.79	2.47	2.00	-0.26	-0.74	-0.21	-0.73

Subject 2	FW exp E	FW sim E	FW exp A	FW sim A	BW exp E	BW sim E	BW exp A	BW sim A
Distance (m)	-0.74	-0.74	-0.78	-0.80	-0.80	-0.79	-0.82	-0.81
height (m)	-0.07	-0.09	0.03	0.03	-0.09	-0.10	-0.03	-0.07
Cadence (rpm)	88	88	71	72	68	68	64	64
ankle offset (rad)	1.17	1.21	1.06	1.10	1.23	1.01	1.16	1.12
T phase	-1.70	-1.82	2.10	2.40	-0.43	-0.16	-0.01	-0.16

It can be seen that for subject 1 accuracy was less compared to subject 2. Seat distance during backward cycling was set 4% (opt A) and 6% (opt E) further compared to the predicted seat distance. Also the height of the crank was higher than the predicted value. This resulted in seat positions during backward cycling of 104% TH (opt E) and 109% TH (opt MA), instead of the predicted 99% TH and 104% TH respectively. For forward cycling, seat distances were better set with distances of only 1% (opt E) and 2% (opt MA) further. It has to be taken into remembrance that from the variable sensitivity analysis it was predicted that subjects are very sensitive to seat distances further than optimal distance. Impact was predicted to be extremely high on both maximal activity and energy expenditure. Cadence was kept closely to the predicted values.

For subject 2, the design variables were better set. In forward cycling seat distance of optimal peak activation was set 2% closer to the crank in comparison to the predicted value. From the variable study it was predicted that subjects were much less sensitive to seat distances closer to the crank in comparison to further away. Also the experimentally set height, differed from the predicted simulation height, but the variable studies showed very little sensitivity to changes in height. Cadence was also for subject 2 found very close to the predicted value, with slight differences of less than a percent for both forward and backward cycling. Seat distance during backward cycling, however, was found slightly further again with 1% for both objectives. For optimal peak activation, seat height was set 57% less high in comparison to the predicted value. These results confirm that it was very difficult to achieve high accuracy in the experimental setting.

The secondary variables also resulted in differences for crank torque phase between experiment and predicted value. However, this could be a direct consequence of the different values of the design variables. Although crank torque phase was found in the variable study to have little effect on energy expenditure, it did affect peak activity with the same order as cadence. In forward cycling for subject 1 crank torque phase increased by 44% (opt E) and 23% (opt MA) with respect to the predicted optimum. For subject 2, these differences were less, with 7% (opt E) and 12% (opt A) respectively. For backward cycling, crank torque phase shifts were large for both subjects with up to 169% (opt E subject 2). Although, these values seem high, it has to be taken noticed that compared to a complete pedalling cycle 2π these differences were relatively small. The largest crank torque phase difference of 169% was represented a crank torque phase shift of only 4%. Therefore, it is useful to study correlations again and visualise the experimental and predicted tangential forces, since these are directly related to the crank torque. It might give a better view on the calculated phases and the experimentally found patterns.

Tangential force correlation coefficients

The correlation coefficients have been calculated similarly as done for the validation study in Section 2.5. The main difference is that instead of implementing the experimental data into the model which calculates the corresponding forces, now the forces were predicted and compared to the its experimental equivalent. The correlation coefficients are shown in table 9. The values are a mean value of the three experiments each compared to the simulated tangential force.

Table 9 *Mean correlation coefficients of the three experimental findings per configuration compared to the predicted simulation pedal forces.*

			Correlation	Corrected correlation
Subject 1	opt E FW	Ftan	0.91	
		Frad	0.93	0.97
	opt MA FW	Ftan	0.94	
		Frad	0.90	0.95
	opt E BW	Ftan	0.92	
		Frad	0.89	0.95
	opt MA BW	Ftan	0.89	
		Frad	0.83	0.92
Subject 2	opt E FW	Ftan	0.92	
		Frad	0.90	0.94
	opt MA FW	Ftan	0.93	
		Frad	0.82	0.97
	opt E BW	Ftan	0.92	
		Frad	0.77	0.91
	opt MA BW	Ftan	0.97	
		Frad	0.81	0.94

The correlation coefficients are very high, values were found between 0.89-0.94 for subject 1 and even 0.92-0.97 for subject 2 in both pedalling techniques. In figure 39 an illustration of the three experimental force patterns of a single configuration versus the AnyBody tangential force is shown.

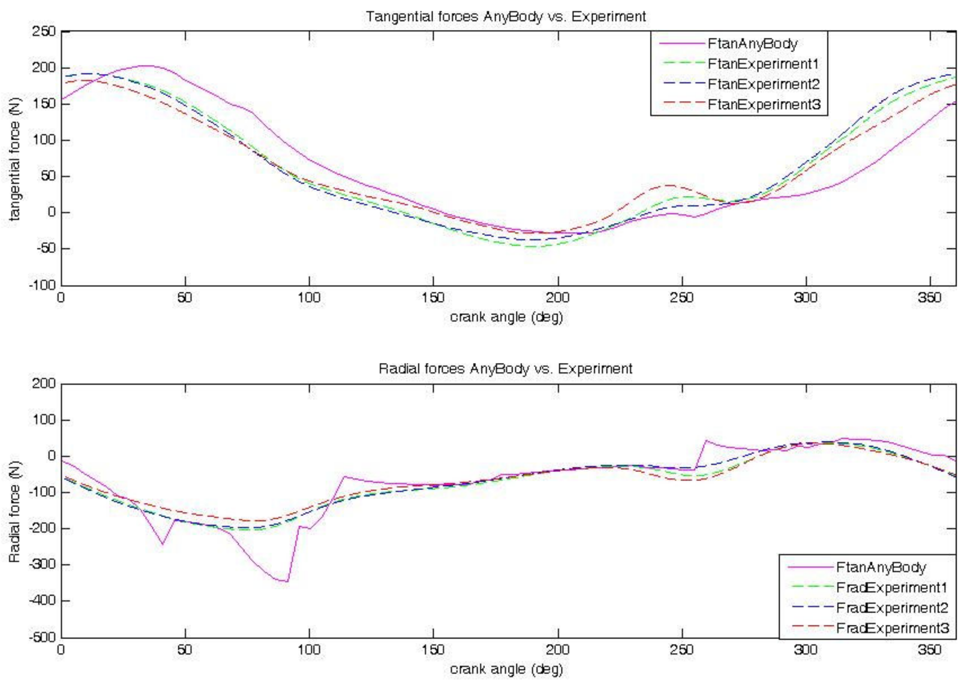

Figure 39 *above) The tangential force during forward cycling of three measurements in a single configuration versus the predicted tangential force of the model. below) A similar comparison of the radial forces.*

In this figure it can also be seen that the high phase change of 43.6% for subject 1 during forward cycling, represents only a relatively small phase shift and still leads to high correlations. The correlation coefficients show that the tangential forces are very well predicted with values in the same order as in the validation study.

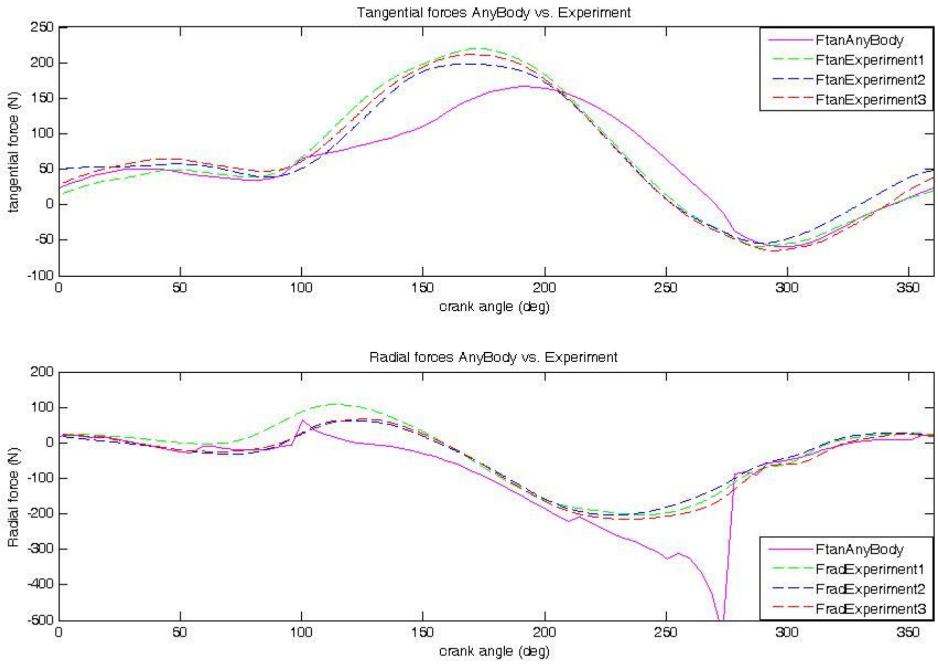

Figure 40 *above) The tangential force during backward cycling of the three measurement in a single configuration versus the predicted tangential force of the model. below) A similar comparison of the radial forces.*

For backward cycling, correlation coefficients were also very good, but in figure 40 it can be seen that the peak force is phase shifted in comparison to the experimental data. The peak shifts for both subjects for approximately 60 degrees, with exception of subject 2 in the optimal maximal activity configuration in which no peak shift was seen.

Overall it can be said that the predicted tangential forces show good correlation in both subjects. With the prediction of tangential forces in forward cycling being stronger compared to backward cycling.

Radial force correlation coefficients

The correlation coefficients of the radial forces might support these findings. The correlation coefficients before correction were again higher for forward cycling compared to backward cycling. For subject 1 the correlations in forward cycling were 0.93 (opt E) and 0.90 (opt MA) and for subject 2 these were 0.90 (opt E) and 0.82 (opt A). These values were even higher than the uncorrected values in the validation study in Section 2.5. After correction, which was again performed by a 9th degree polynomial fit, these values increased to 0.97 (opt E) and 0.95 (opt MA) for subject 1 and 0.94(opt E) and 0.97 (opt MA) for subject 2.

For backward cycling the uncorrected values lie in the same order as the validation study with 0.89 (opt E) and 0.83 (opt MA) for subject 1 and 0.77 (opt E) and 0.81(opt MA). After correction these values increase again, all to values in between 0.9-1. For subject 1 the correlations increased to 0.95(opt E) and 0.92(opt MA), and for subject 2 to 0.91(opt E) and 0.94(opt MA).

The lower pictures of figure 39 and 40 are examples of the predicted and experimentally found radial forces. The correlations of the radial forces indeed support that the model can predict forces on the crank delivered from a specific seat position and cadence very well.

Comparison of pedal forces between configurations in the experiments versus the simulations

The effect of change in the pedal forces was subtle when changing seat configuration. Variations between experimental pedal forces and simulated pedal forces were larger than the variations between the individual pedal forces between experimental configurations. Nevertheless, the model patterns did seem to follow the subtle trends between configurations as seen between experiments for both subjects in forward cycling. Below in figure 41 the measured tangential forces of the experimental setting in each configuration compared to their simulation equivalents are shown. Figure 42 shows a similar illustration for the radial forces. It can be seen that in both force patterns, the forces of the predicted optimal peak activation configuration diverge by a similar trend in both experiment and simulation.

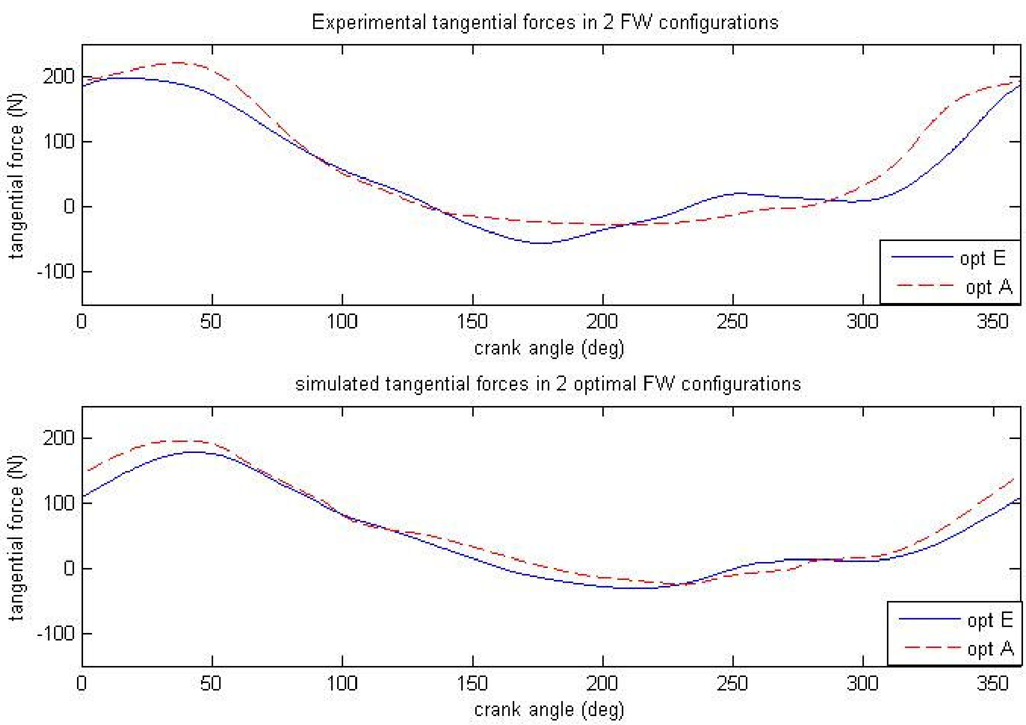

Figure 41 *A comparison of tangential forces for two configurations, the predicted optimal peak activation configuration versus the predicted optimal energy expenditure configuration Above) the experimental tangential force. Below) the simulated tangential force.*

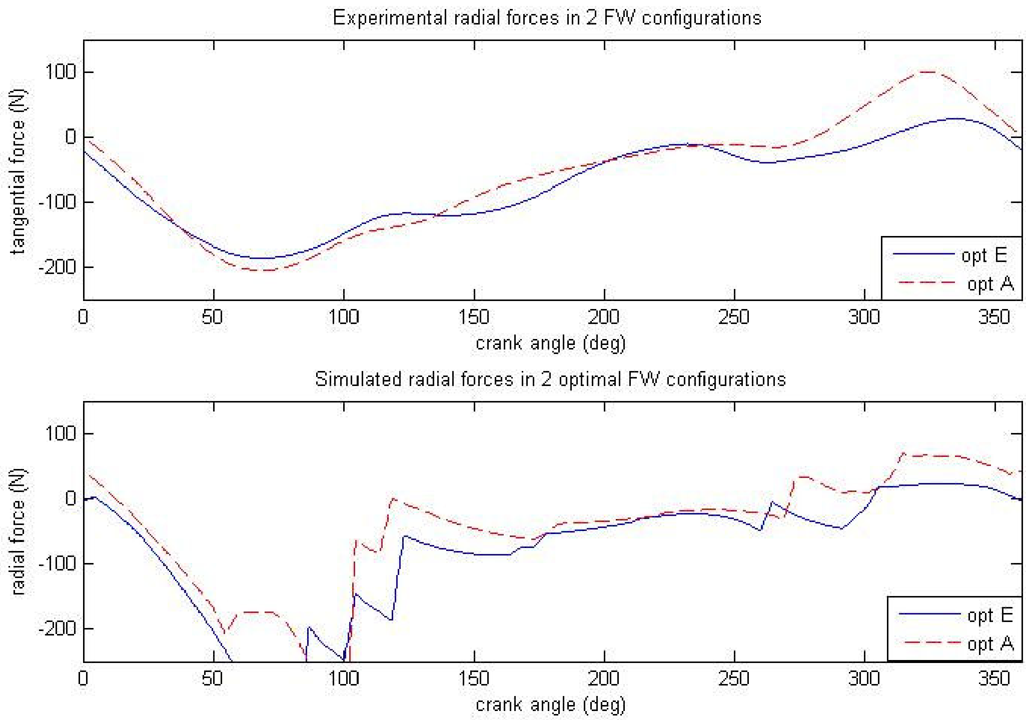

Figure 42 *A comparison of radial forces for two configurations, the predicted optimal peak activation configuration versus the predicted optimal energy expenditure configuration. Above) the experimental tangential force. Below) the simulated tangential force.*

For backwards cycling these similarities were also found for the radial forces in subject 2, however tangential forces did not show a similar trend. For subject 1 the exact opposite was found during backwards cycling. Trends were similar for tangential forces but not for radial forces. These variances were ascribed to inaccurate setting of the experimental seat position in backward cycling.

Activation times

Another comparison between the model and the experiment is made for the muscle activation times. The EMG activation times were each compared to the predicted activation times in the same way as explained in Section 2.5. Threshold was again set to 0.2·(maximal activation in the EMG per muscle) and 0.1·(maximal activation per muscle for the model). The mean values of the three experiments per configuration versus the model activation times are shown in table 10. The mean overlap of all muscles at a single configuration is in the same order as was shown in the validation study.

Table 10 *mean values of the three experiments per configuration versus the model activation times*

Subject 1	FW (%) E	FW (%) A	BW (%) E	BW (%) A
biceps femoris	84.7	80.9	50.0	45.7
gluteus maximus	74.7	76.6	65.7	70.3
semitendinosus	87.9	92.0	59.5	67.8
rectus femoris	82.7	86.1	74.0	73.5
vastus lateralis	83.5	82.7	67.7	72.2
tibialis anterior	54.1	54.1	84.3	87.4
gastrocnemius lateralis	78.9	80.1	83.7	86.7
soleus	98.0	94.4	76.8	82.9
Mean	80.6	80.8	70.2	73.3
SD	12.7	12.4	11.9	13.5

Subject 2	FW (%) E	FW (%) A	BW (%) E	BW (%) A
biceps femoris	84.6	76.0	48.5	16.4
gluteus maximus	71.5	69.0	62.8	76.5
semitendinosus	80.4	83.0	55.3	56.6
rectus femoris	62.9	77.1	69.5	61.1
vastus lateralis	81.2	89.9	78.4	77.1
tibialis anterior	26.3	42.0	51.2	81.1
gastrocnemius lateralis	66.7	78.3	88.5	75.1
soleus	87.5	87.9	75.0	76.2
Mean	70.1	75.4	66.2	65.0
SD	19.7	15.1	14.2	21.4

Subject 1 had an overlap during forward cycling between the predicted activation times per muscle and the measured EMG activation times of 80.6 (opt E) and 80.8 (opt MA). These values were 70.1(opt E) and 75.4(opt MA) for subject 2. In figure 43 the overlaps of subject 1 during forward cycling at the predicted optimal energy expenditure configuration are illustrated.

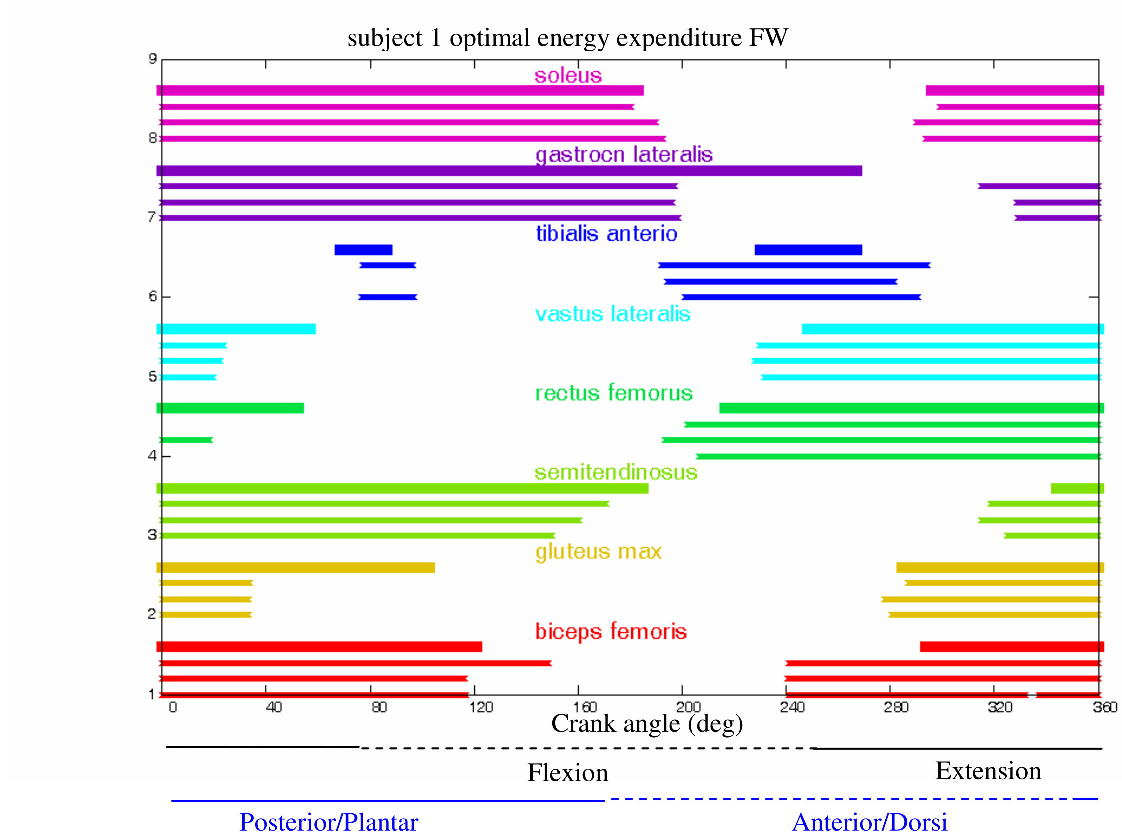

Figure 43 *Predicted activation times (fat lines) vs. the three measurements (small lines) for the predicted optimal energy expenditure configuration during forward cycling. Below the predicted biomechanical functions have been sketched. Plantar= plantar flexion of the ankle and Dorsi-= dorsi flexion of the ankle. Flexion/extension and posterior/anterior are movements with respect to the displacement of the lowest point of the leg.*

The muscle of which activation times deviated most, appeared to be tibialis anterior in both subjects. It showed least overlap between predicted times and experimental activation times. For subject 1 overlap was 54% for both objectives and for subject 2 overlap was less with 42% (opt MA) to as little as 26% (opt E). The validation study already showed little overlap for this muscle during forward cycling. Taking into account all the assumptions as described in section 2.5 regarding EMG data, the overall predictions for the experimental activation times during forward cycling were considered very acceptable.

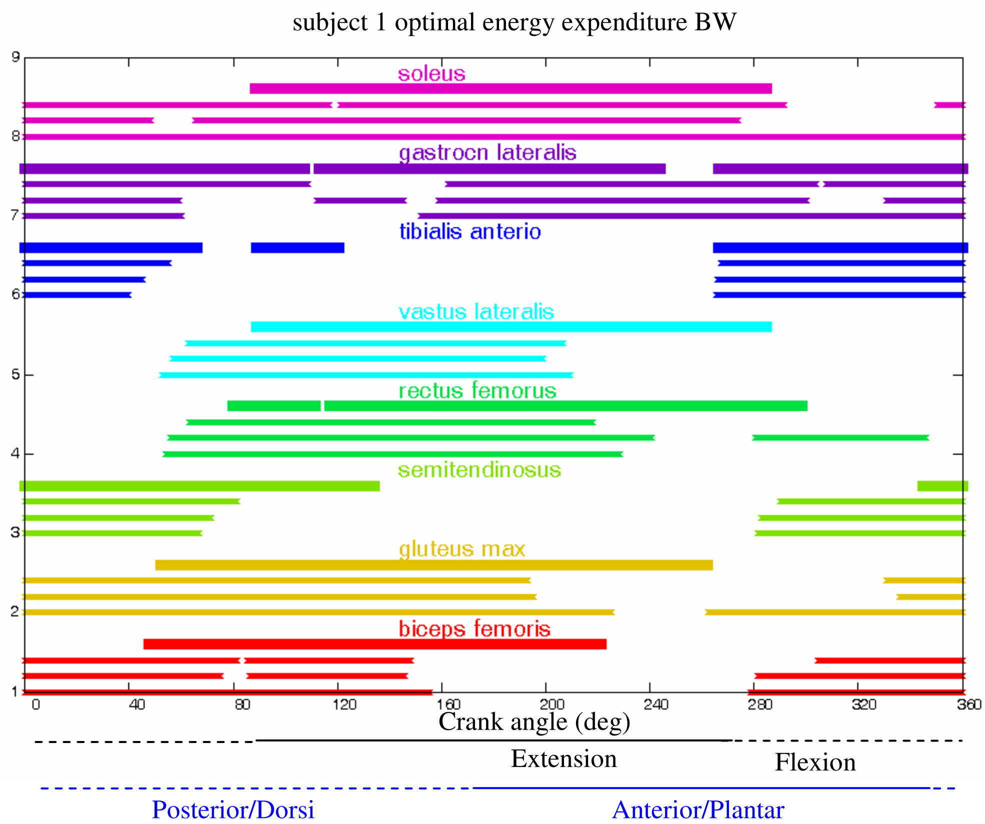

Figure 44 *The predicted activation times (fat line per muscle) versus the three experiments (small lines) at the optimal energy configuration during backward cycling. Below the biomechanical functions have been sketched.*

For backwards cycling, mean overlaps were less well compared to forward cycling. Subject 1 resulted in overlaps of 70.2% (opt E) and 73.3% (opt MA), which were 66.2% (opt E) and 65.0% (opt MA) for subject 2. These smaller overlaps seem to be the result of a phase shift between the predicted model activations and the experimental activations. In figure 44 an example of these overlaps is shown of subject 1. The phase difference appears to be approximately 60 degrees for all muscles except for the soleus and the gastrocnemius lateralis. Activation times for the tibialis anterior showed much more overlap between simulation prediction and experimental activation times compared to forward cycling as was also seen in section 2.5. Overlaps increased to the order of 80% in all cases with exception of subject 2 at optimal energy expenditure which was 51.2%. For backward cycling it appeared to be the biceps femoris that showed least overlap between predicted activation times and experimental activation times as shown in figure 44. The predicted activation times seem phase shifted in comparison to the experimental data.

In addition, the biomechanical functions have been sketched into the activation time figures 43 and 44. During forward cycling, each muscle functioned as predicted in Section 1.3. The soleus contributes to both the plantar function and the extension function. The gastrocnemius functions as a flexor as well as a plantar flexor. The tibialis anterior is active during the dorsal flexion phase and during the flexion phase, whereas the vastus lateralis and the gluteus maximus extend the leg. The rectus femoris extends the leg as well and is responsible for the anterior movement of the leg. The semitendinosus flexes the leg and contributes to the posterior movement together with the biceps femoris, which also contributes to the extension.

For backwards cycling, the angle definition was reversed, which resulted in a switch of all functions except for anterior and posterior function as explained in section 1.3. All muscles were experimentally activated in the periods expected in this pedalling technique as well. In addition to extension function, the gluteus maximus was found to contribute to the posterior movement of the leg. This seems plausible, since contraction of this muscle leads to the backward movement of the thigh. The soleus was found to be active during the extension phase as expected and as predicted by the model. However, soleus activation was also seen during the flexion phase of the experiments in both subjects. Since this was neither predicted by the model, nor logically explainable, this might have been caused by cross talk, since patterns look relatively similar as for the gastrocnemius.

Energy consumption

As shown, all design variables as well as torque phase were different from the predicted optimal values. Moreover, the data used as input for the optimisation study appeared to have discrepancies on segment length data. The shank length of subject 1 was currently measured to be 0.49m instead of the 0.43m which was abstracted from the previous data. Since the former data that was used to model recumbent cycling did not contain energy expenditure data, validation was not done for the energy model in section 2.5. For this reason, to make a proper comparison between model and experiment, a new calculation of the model energy expenditures with the new input values and correct segment lengths of the subjects has been performed. The new model energy expenditure values and the experimentally measured data are shown in figures 45 and 46 for subject 1 and subject 2 respectively. All measured energy expenditure levels are higher compared to the simulated values, because the simulations calculate only the energy expenditure of the legs, whereas in the experimental setting whole body energy expenditure is measured. Since the energy expenditure of the legs seems most important in recumbent cycling, it is expected to see similar trends for energy consumption in both calculated and measured data. The reliability of the oxycon is 5%, which means that a similar measurement can vary five percent due to internal variation of the Oxycon. Furthermore, subjects' also vary between measurements of a single condition. This variability is estimated of another five percent. Therefore, differences in energy expenditure were not taken into account when variation is less than ten percent.

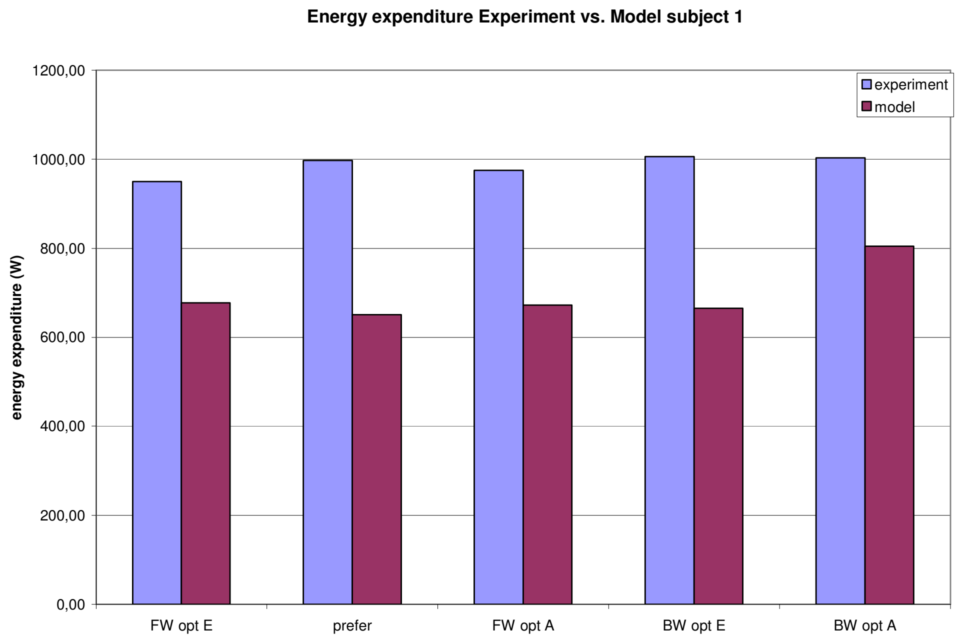

Figure 45 *Energy expenditure of the experiment next to the predicted energy expenditures of subject 1 at each configuration during forward as well as backward cycling.*

First, subject 1 is considered. No differences (< 4%) were found for the recalculated energy expenditures in the model comparing each configuration in forward cycling. Experimentally, differences in the energy expenditures were also negligible (< 5%). For backwards cycling the experimental data were also equal (difference <1%). However, according to the simulated energies a difference was expected between these two configurations. The simulation study showed an energy expenditure of 21% less for the optimal energy configuration compared to the optimal peak activation objective.

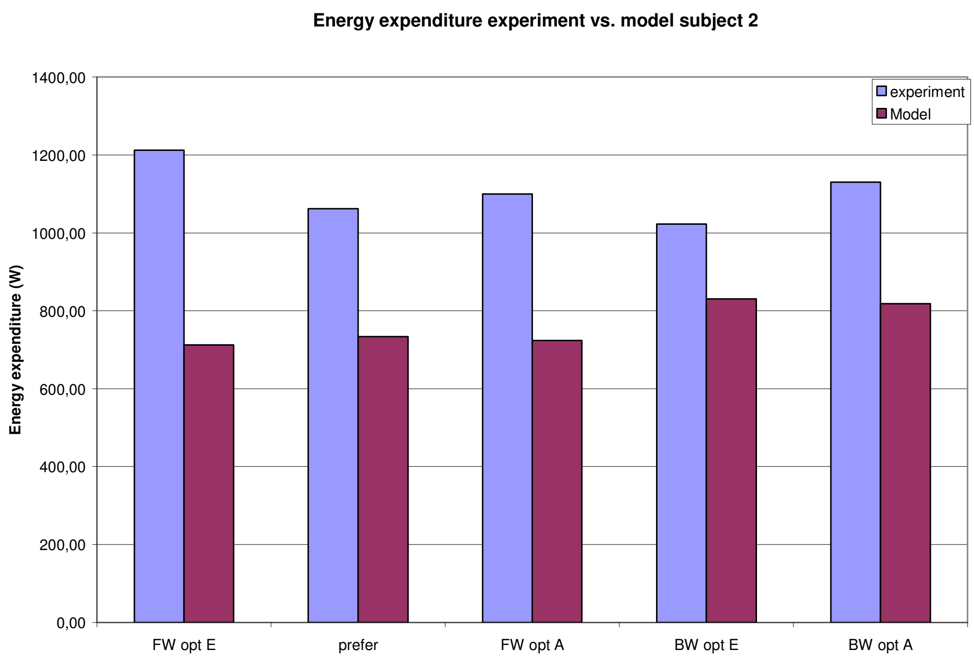

Figure 46 *Energy expenditure of the experiment next to the predicted energy expenditures of subject 2 at each configuration during forward as well as backward cycling.*

Subject 2 also showed little differences for the recalculated predicted energy consumptions, with less than 3%. However, for the experimental setting, preferred distance and cadence led to a reduction of energy consumption of 12.4% in comparison to the optimal energy expenditure configuration. Also the optimal peak activation configuration cost 9.2% less energy in comparison to the optimal energy configuration. For backwards cycling, the simulation predictions were considered equal with less than 2% difference. Again, the experimental energy consumptions did show a difference, with an increase of 10.4% for the optimal maximal activation configuration. In addition, for backwards cycling the calculated energy consumptions were 16.5% opt E and 11.5% opt A higher in comparison to forwards cycling. This trend was not seen in the experimentally measured energy expenditures.

Peak activation versus Maximal EMG

In section 2.5, it was explained that the amplitudes of the individual muscles EMG's cannot be directly compared to each other or to the simulated activation amplitudes. This is for example caused by the EMG amplitude being sensitive to the depth at which the measured muscle is located and the position of the electrodes with respect to the muscle belly. Nevertheless, to make comparisons for the predicted peak activations to the experimental setting, amplitudes need to be taken into account.

In Section 3.6 it was shown that peak activation in the optimal configuration is determined by multiple muscles. For this reason, it was hypothesised that a change in the modelled peak activation leads to a similar trend in the maximum activation of the eight measured EMG amplitudes. This could be done, since the electrodes were not replaced between setting the separate configurations. During forward cycling in the simulation study, the soleus and the tibialis anterior were not found to reach the maximal activation and were therefore excluded from this analysis.

EMG patterns were determined per optimal configuration as the mean of the three measurements. EMG courses were of similar shape between the three measured optimal configurations for forward cycling, and between the two configurations measured for backwards cycling. In Appendix F, the average EMG data per configuration are illustrated. Differences in course were only seen for the gluteus maximus of subject 2 in the predicted optimal peak activation configuration where small bumps were seen within the inactive period of the other configurations. However, the electrodes of this muscle had to be replaced twice. As expected, the main difference between configurations in the EMG patterns was amplitude. In table 11 the difference between the peak values of the experimental EMG are expressed as the relative change with respect to predicted optimal activation configuration. The predicted equivalents are set next to these values.

Table 11 *The relative differences between the peak EMG values expressed as a % of the peak EMG of the predicted optimal peak activation configuration. The right columns show the similar relative differences as found for the simulated peak activation times.*

S1	exp	simu
% E over A	16.35	5.88
%pref over A	30.99	-22.06
% BWE over BWA	-1.05	8.45

S2	exp	simu
% E over A	1.12	-9.88
% pref over A	2.33	-8.64
% BWE over BWA	-10.25	2.41

The maximum values for the individual EMG's will be compared to the peak activation patterns as found in the optimisation study. The patterns for peak activation as found in the optimisation study were not found to occur for the experimental maximum EMG trends.

From the simulation study of subject 1with the corrected segment lengths and inputs, it followed that the optimal energy expenditure configuration results in a 5.9% higher peak activation in comparison to the optimal peak activation configuration, whereas the simulated preferred configuration resulted in a lower peak activation of -22.1%. The experimental values showed 16.3% higher peak activation for the energy expenditure configuration. Although the percentage was much higher for the experimental comparison, both experiment and simulation showed higher peak activation for the predicted optimal energy expenditure configuration. Also the preferred configuration resulted in an increase in peak activation of 31.0% with respect to the predicted optimal peak activation configuration, which was in contrast to the simulated peak force decrease. Simulation and experimental findings also contradicted in backward cycling. The predicted peak activation configuration during this pedalling technique resulted in an 8.5% lower peak activation in comparison to the peak activation in the predicted optimal energy expenditure configuration. Nevertheless, the experimental findings resulted in a lower mean peak activity for the six measured muscles in the optimal energy configuration of -6.2%.

For subject 2, all predicted peak force trends from the simulations differed from the experimental findings. The simulations resulted in the highest peak activation level for the optimal activation configuration after correction for the new experimental inputs. Peak activation was 9.9% higher in comparison to the predicted optimal energy expenditure configuration and 8.6% higher in comparison to the preferred seat distance and cadence. The experimental data resulted in higher mean peak activation level with respect to the optimal activation configuration of 4.6% for the optimal energy configuration and of 5.6% for the preferred configuration. For backwards cycling in the model after correction, the optimal activation configuration resulted in a 2.4% lower peak compared to the optimal energy expenditure configuration. For experimental backwards cycling the found proportional mean peak was lowest for the optimal energy expenditure configuration with -12.4%.

4.6 Discussion

The aim of the experimental study was to test the predictive characteristics of the model optimisation study. Hypothesised was that the predicted combinations for seat position and cadence found for optimal energy expenditure lead to the lowest energy expenditures in the experimental setting and that the configurations of the optimal activation lead to the lowest peak activations. It was assumed that the new configurations led to changes in crank torque phase and ankle offset. The predictions of these variables were used as control. Furthermore, the predicted tangential and radial forces, as well as the activation times were expected to be similar for their experimental equivalent.

The most important result from the experimental study is that the trends as found in the simulation study for energy expenditure and peak activation were not found in the experimental results. There are several explanations for this discrepancy. Firstly, accuracy as achieved in the simulation study could not be achieved experimentally. This was true for both setting seat position as measuring of energy expenditure. Because of low accuracy in seat positioning, energy expenditure and peak activation were recalculated with the experimental values, after which objective values were much less different between configurations. Secondly, peak activation as chosen in the simulation study could not directly be compared to the EMG data, since amplitude of different muscles could not be compared.

The low accuracy of the experiment was caused by several aspects. For this reason, differences in the experimental data smaller than 10% were not considered significant. This is because of measuring variance of the Oxycon (up to 5%) and experimental error (up to 5%). By experimental error it is meant that although steady state was reached, mean energy expenditure was sensitive to the period over which the average was taken. Furthermore, the measurements were not randomised, because setting saddle height was quite laborious and obtaining high accuracy was difficult. Turning around the ergometer for backward cycling was even more laborious. Since the experiments were not randomised, it cannot be excluded that fatigue has influenced the measurements of energy expenditures. Finally, the Oxycon data were averaged over the complete time span of the three measurements per configuration. Therefore, variances of this single measurement are unknown. The 10% threshold should therefore not be considered a strict threshold. For all of these reasons, the differences of 12.4% seen in subject 2 are not convincible, although these are slightly more than the threshold of 10%. It can be concluded that the energy expenditure measurement with the Oxycon was not accurate enough to point out specific trends. Consequently, the differences seen in the experiment can all be considered negligible, which indicates that the measured energy expenditure trends show most plausible resemblance with the predicted energy expenditure trends.

In contrast to forward cycling, energy expenditure results were different between configurations of subject 1 during backwards cycling. Experimentally, however, no variations were found. Subject 2 showed no differences between the simulated configurations, but higher energy levels were found for backwards cycling compared to forward cycling. Neither of these tendencies was found in the experimental setting. The experimental results in this chapter as well as in section 2.5 showed that the simulation model predicted backwards cycling less well compared to forward cycling, especially the pedal forces and activation times were poorly predicted. Since the energy expenditure model is very dependent on activation, the differences found for backward cycling between experiments and simulations can be ascribed to the model predictions. In conclusion, the experimental energy expenditures showed no changes between the different configurations. This can be attributed to shortcomings in the simulation and experimental inaccuracies. Nevertheless, more research is needed to draw more definite conclusions.

As mentioned, it was difficult to compare the simulation findings on peak activation to the experimental EMG data. In section 3.6, however, it was shown that the peak activation in the optimal configurations was determined by multiple muscles. For this reason the assumption was made that trend in peak activation could also be seen in the individual experimental EMG muscle data. Nevertheless, setting the predicted optimal configurations was not achieved accurately in the experiments. This means that the peak activation might have been caused by a single (small) muscle instead of a group of muscles. It is clear that for a more proper comparison between EMG maximum values and simulated peak activations, it should be determined which muscle(s) caused peak activation in the achieved experimental setting. The trend of only this muscle should be compared to indicate similarities between the peak activation of the simulation and the maximum EMG value. Again this is difficult to achieve if the peak activation is caused by another muscle than the ones that are mostly contributing to the pedalling transition. Other muscles than these were not chosen to be measured by EMG and might not be easy to be measured if it concerns a small muscle close to or beneath larger muscles. Therefore, it was chosen to take the average of the trends. The current comparison does not allow for drawing any definite conclusions. As mentioned, the objective peak activation should be combined with integrated activation. In the current study muscle activation is considered as a measure for fatigue and therefore a combined objective for peak activation with total activation might result in a better prediction of the optimal configuration preventing premature fatigue. The combination would also increase the opportunities to compare the simulated findings to the experimental findings.

The validation of the simulation results could be improved on several aspects. Alternatives for a better experimental set-up are outlined in chapter 5. Mainly experimental variation of one variable per experiment when sitting in the optimal configuration would be helpful for a better validation of the energy model.

Although predictions of the objectives in the experiments were not convincing, the model appeared to be a good predictor for pedal forces and muscle activation. Tangential forces and radial forces were very well correlated in forward cycling, even though high accuracy for setting seat position was not achieved. These results show that the recumbent model is very capable of predicting pedal forces at a specific combination of seat position and cadence. However, comparing the different configurations in the experimental setting to their simulation equivalents, it was seen that pedal forces lie closer to each other compared to their simulation equivalents. Nevertheless, the subtle trends that were seen in the experimental setting were also found in the simulated pedal forces. The high correlation values imply that the joint moments were predicted well, subsequently muscle activation was expected to be predicted well by the min-max criterion. Overlaps between experimental results and simulation results during forward cycling were indeed very reasonable. The next step is to compare the model predictions to the biomechanical functions. Hakansson et al. [24] found that the biomechanical functions changed from upright to recumbent cycling with the same angle as the change in seat angle. The data of this study are consistent with these findings. Both the experimental data and the simulation data showed activation times during the predicted biomechanical function phases after correction for seat angle. Only the activation times of the tibialis anterior were less well predicted in forward cycling. However, looking back at the work loops in Section 3.6, it could be seen that the work delivered during forward cycling was very little. The tibialis anterior only showed very short isometric contraction. This might be the reason for the less well predicted activation time of this muscle. This is supported by the much better prediction of the activation time of this muscle in backward cycling, during which the tibialis anterior was predicted to deliver more work.

Backwards cycling showed similar results for pedal forces and activation times as forward cycling. Radial forces and tangential forces were again well predicted. However, in both of the configurations of subject 1 and in one configuration of subject 2, a peak force phase shift was noticed. The underlying cause of this shift could be of two kinds, a modelling cause or an experimental cause. First, the data on which the simulations were based contained discrepancies. Second, segment length was incorrectly measured. Nevertheless, this could not be the cause since the phase shift occurs in both subjects and wasn't noticed during forward cycling. Probably, setting the seat position inaccurately was of bigger influence. This tangential force peak shift is also expected to be the cause of the shifted activation times between the experimental and simulation data. The activation times seem phase shifted to later in the crank cycle with a similar angle as found for the shift in tangential peak force. To study the origin of the phase shift more closely, the biomechanical functions were studied. The identified functions were similar in both the simulated data and the experimental data. For backwards cycling, the posterior and anterior biomechanical functions were inverted, as was demonstrated in the research of Ting et al. [11] during upright cycling. When taking into account both the change in seat angle as well as the inverted biomechanical functions, the current data apply to the correct biomechanical functions. Subsequently, the current study is consistent with previous findings [10, 11]. The difference in seat position in the experiment with respect to the corresponding simulated configuration resulted in a seat angle shift of approximately 2^{o}. Taking into remembrance the theory of Hakansson [24], a seat angle phase shift of this size would result in a similar phase shift in activation times. However, phase shifts of up to 60^{o} were found. Since the change in seat position does not have such a large effect on the seat angle, the activation times would not change much. Thus the activation time phase shift could not be caused by the change in seat position solely. Tangential forces and activation times could also be improved by implementing the alternative support, as mentioned before. A better support could result in a better prediction of pedal forces and decrease the large phase shift found between simulated and experimental findings. Alternatively, experience with the task may have played a role in the shift of the peak pedal force. Even though it is only recreationally, the subjects are used to forward cycling. During backward cycling the muscle lengths at which force is delivered, differ from forward movement. Training could change the optimal muscle length and thereby deliver tangential force at a different phase [47, 48].

In summary it can be said that the model predicted pedal forces and muscle activation times adequately despite discrepancies in the segment lengths model input and low accuracy for the experimental setting. Activation times and biomechanical functions were consistent with previous studies of translating conventional cycling into recumbent cycling and for conventional backwards cycling [10, 11, 24]. However, substantial differences between the experimental setting and the simulation study were found in energy expenditure and peak activation. Nevertheless, the current study made a proper start for searching the optimal configuration in recumbent cycling. Following steps to deepen the search for finding an optimal recumbent pedalling technique are recommended. These will be outlined in the next chapter.

Chapter 5: Recommendations & conclusive remarks

With the current study a start has been made on finding a subject specific optimal configuration for recumbent cycling. Research on recumbent cycling was until now restricted to research on change in biomechanical functions in comparison to conventional cycling [10, 11, 24], and ergonomics [23]. The current optimisation of the recumbent position seems adequate and opened a whole new area for future research. In this chapter the openings for future study will be looked at in more detail. Future research following from the current study can be divided into three groups, namely model additions and improvements, experimental improvements and general additions.

First of all it should be noticed that the current study is based on only two subjects. It is therefore difficult to draw definite conclusions. Only trends per subject could be investigated. An increase in the number of subjects studied will be important to elucidate possible trends. Even more important is that it increases reliability of predicted and measured variables. It is clear that both the experimental as well as the simulation part needs to be expanded with a larger subject pool that varies in age, weight, length, and training level to represent the average male.

Model additions and improvements

For the group of model additions and improvements a start would be to closer study the current objectives. As mentioned, the chosen objective peak activation would be improved when combined to minimal integrated activation. This follows from the finding that peak activation might prevent local fatigue but at the same time integrated activation was increased. Fatigue is a very difficult aspect to include into a simulation model, for example lactate building, but this would be very useful.

Also the second objective, energy expenditure, can be improved. The current model gives plausible results expenditure consistent with Umberger's findings. Further validation is, however, needed. Activation dynamics are not taken into account for the prediction of energy expenditure in the current energy model. The assumption is made that stimulation does not have a large effect and therefore activation was equalled to stimulation. However, Casius and Soest [49] showed that activation dynamics had a big influence on maximal power output and on the simulated optimal cadence. Therefore, activation dynamics would be useful to include in the energy model.

A major benefit of the current energy model is that it is applicable to every AnyBody inverse dynamic model. A good validation of this model is therefore very welcome. To do so, a maximum efficiency study for human muscle would be of great. In addition, a study for determining proper values for fractions of fast twitch fibres in the individual lower limb human muscles is also of great use. Since the energy expenditure model is dependent on these fractions, the effect of changes in these fractions might be helpful for understanding the differences between the simulated values and the experimentally found energy expenditures.

The current model seems to predict pedal forces as well as muscle activations very reasonable and even captures subtle differences between two different configurations. However, there are still sizable differences between simulated and experimental data. The first step to be made is adding trunk muscles to the simulation model. These are needed for two reasons. The first reason is that with these a more proper support can be modelled including back support. As was seen, the recumbent model predicted pedal forces and activation times during forward cycling adequately, however, during backward cycling slightly less. The currently chosen support did not allow for hip movement in the seat. Nevertheless, in the experimental setting hip movement was seen. For this reason, the alternative support that allows for hip movement might be a more proper support. To achieve a good alternative support, the trunk angles are needed.

The second forward step by introducing trunk muscles is that it gives opportunities to optimise the trunk angle. Trunk angle also affects the lengths of muscles that have important contributions to the pedalling cycle. Therefore, optimisation of the trunk angle can be helpful for both energy expenditure minimisation as well as minimisation of peak activation level.

Another opening for future model improvements would be the introduction of a proper scaling method. The current method seems to predict a too high muscle mass for the larger subject, making him relatively too strong. The current method scales for all directions with the same factor. A more proper method includes fat percentage, but the currently mentioned length-fat-mass method as explained in section 2.3 seems inappropriate for people with low BMI's. Adaptation of this method would therefore be welcome.

Furthermore, a separate test for the secondary variables would be helpful. In the current experimental results it is impossible to ascribe the variations in these variables to a slightly different experimental setting or to the fact that the body does not automatically adjust for them. A solution to this problem would be a separate optimisation of the crank torque and ankle offsets at a known experimental setting.

A final remark on the simulation study future research possibilities is with an eye to alternative design variables. For subject specific optimisation, it might be interesting to optimise crank length and bracket length. Since each individual has a different pelvis width and leg length, these variables might also influence maximum performance.

Experimental adjustments

The second group of improvements concerns experimental adjustments. The current experimental set-up only shows in great lines the effects of changes in configuration and cadence. The experimental setting was a reasonable set-up to test the predictions on pedal forces, muscle activations, and major differences in energy expenditure between the individual optimal configurations. Adaptations to this experiment could help in drawing more definite conclusions on whether the found variable values indeed represent the optimal configuration. In addition to multiple subjects, results on energy expenditure and peak activation would be clearer if the optimal configurations were varied per variable. For example, setting all optimal design variables and than vary between a lower cadence, optimal cadence and a higher cadence. This would also give the opportunity to compare sensitivities per variable in the experimental setting to those found in the simulation study. In the current research problem, variation per variable was not applied since it would be to exhausting for the subjects to cycle at three cadences, three heights, three distances and to do this for both objectives and for both pedalling techniques. For this reason it was chosen to only compare the individual optimal configurations on the major differences. Separate experiments, testing the effect of a single variable at a time are in the optimal setting is recommended.

Another issue is that the subjects in this study were not used to recumbent cycling. For this reason, closer studying of training effects would be useful to study. Since training has been shown to affect optimal muscle length [48], the direction of the pedal forces might be influenced by training. Since pedal forces directly influence muscle activation and thus energy expenditure, training effects might be useful to increase accuracy in for the current optimisation study.

Another issue is the effect of fatigue in the current experimental set-up. Randomisation of the trials would be very helpful in exclusion fatigue effects. However, the current vertical ergometer is very heavy and difficult to set accurately. To include backwards cycling, re-placement of the vertical ergometer is even more laborious. Consequently, to achieve randomisation, a more handy adjustable setting is needed.

Objectives as chosen in the present study appeared difficult to validate. Although it needs further validation, the energy expenditure objective, still seems to be a proper objective to search the optimal configuration and cadence for. It minimizes premature fatigue as well as heat production in the human powered aircraft. Mainly peak activation level occurred to be almost impossible to validate for. For this reason as well as for those mentioned for the simulation study, a combination of peak activation and integrated activation would be a better objective. For total activation, it is easier to compare experimental and simulation results by means of the integrated EMG and activation, but still true values cannot be compared.

An alternative possibility to make a more proper comparison between simulation and experiment would be optimisation of net joint moments. For conventional cycling, net joint moments appeared to be a plausible objective for searching optimal cadence. Redfield et al. [50] found optimal cadence close to preferred cadence by means of this objective. For this reason, optimisation of joint moments might be a goof alternative to search the optimal configuration in combination to the optimal cadence.

General additions

The last group of additions would be general additions. The occasion for the current research subject was the design of a proper human powered aircraft. For the pilot it means that duration exercise in a small cabin needs to be delivered. Optimisation of the recumbent configuration and cadence are only a few of the aspects to create a good environment for the pilots during the flight. Factors like training, nutrition, fluid balance and thermoregulation all determine the optimal human performance. Cooling of the pilots is a major aspect during the flight since, as mentioned, the heat production in the small cabin will be major. But a too large ventilation opening will be a disadvantage for air resistance. Since the flight will endure for at least four hours, nutrition and hydration are also of great importance. However, the weight of the HPA needs to be as low as possible and storage capacity is low. Subsequently, a balanced diet is necessary. Furthermore, an alternative pedalling technique that increases pulling force during the returning phase is compared to conventional recumbent cycling techniques and trained for. In addition to increase pilot performance, research is performed on the optimal build of the plain as well. The best bicycle chain and least air resistance of the wings are all factors that have been separately studied by other members of 'Team Icarus'.

Overall conclusion

The overall conclusion of the current study is that a proper start has been made on searching the optimal recumbent cycling configuration in combination with cadence. Although trends as found from the simulation study were not found in the experimental setting for energy expenditure and peak activation, the model appeared to be a good predictor for pedal forces and activation times. It even captured the subtle differences in pedal forces between configurations. Furthermore, a relation between optimal configuration and optimal cadence has been demonstrated. Biomechanical functions were illustrated to change with seat angle and pedalling technique, similarly as shown in previous studies. Therefore it can be said that a good foundation for a recumbent simulation model has been laid. The energy model resulted in plausible values, but closer studying is necessary. The added energy model has the advantage that it is applicable to all AnyBody models. The current study resulted in many future challenges as have been outlined in this report. Therefore, as a first search for optimal recumbent pedalling, the current study is considered as a succeeded pilot study.

Epilogue

A Medical Engineering student is supposed to do a nine months graduation project. The graduation project should contain a scientific research problem that should be solved quantitatively by experimental research and by computing software in a medical environment. Experimental research means creating a measuring protocol, measuring and data analysis. In the ideal situation a predictive computational model will be developed as well.

All this sounds very clear, but previous to starting this graduation project I went through a long search to find my ideal project. I wanted it to be on a sports subject and I wanted to participate in a team working together to reach a common goal. Since my study medical engineering was meant to graduate in a medical environment and not a sports subject, it was difficult to find supervisors within sports subjects which were familiar with capacities and requirements of a medical engineering student. Nevertheless, I found what I searched for at the movement science department of Maastricht University: a sports subject, participation in "Team Icarus" and a supervisor familiar with biomedical engineering. Thanks to the support professors Wagemakers and Hilbers I was able to start the project.

As soon as I sent my decision to Kenneth to accept this graduation subject, he sent me to Aalborg in Denmark to become familiar with the AnyBody software. My Aalborg supervisor Mark de Zee accommodated me and taught me all ins and outs of the AnyBody software in a high speed course. In these six weeks not only did I study the AnyBody software, but I also made a start on getting familiar with biomechanics. Moreover, I had to overcome my fear for the Matlab software. After a short struggle, Matlab decided to give me a second chance. I took this opportunity with both hands and Matlab and I have become close friends now.

Back in Maastricht I gained more in-depth knowledge on the multi-body model, optimisation methods and muscle physiology. On my new computer, I started to run the optimisation routines. These were very time-consuming, so that there was enough time to make fun in our lab-playground with my lab-mates.

After the optimisations, it was time for validation. So instead of making fun with my lab-mates I let them know what endurance recumbent cycling was. Since the measuring equipment wasn't really working along, endurance became very long endurance exercise and my subjects' patience was thoroughly tested. Therefore, I would like to say thank you Wouter and Pijke for your patient co-operation in my research. Neither could I have fulfilled the optimisations and experiments without Harry and Paul who had to act as mediators between me and my computer and measuring equipment many times.

Although this graduation project did not take place in a medical environment, it did fulfil all other requirements of creating a subject specific predictive model, and validate this experimentally. The benefit of creating a predictive model is that instead of finding a subject specific optimal configuration by experimental research alone, is that it is less sensitive to environmental factors, as well as it costs less effort of subjects. Moreover, it is higher accuracy can be reached with a good predictive model. This is why the research problem of making a start on finding an optimal recumbent cycling configuration requires modelling, which was also a start on creating a predictive model. In addition to the modelling part, measuring for validation and data analysis was required. In this project, biomechanics as well as mathematics formed a great part of solving the research problem for both the modelling part as well as the data analysis. For all of these reasons, I find that the current assignment fits well for students with a (Bio) Medical engineering profile, since these have knowledge on both modelling and physiology needed to create and validate simulation models and to interpret experimental results. The combination of using experimental data to formulate a good recumbent model with adding an energy expenditure model has been very instructive. Moreover, to expand this model with an optimisation study and an experimental validation and interpretation have made this assignment a real challenging one.

Because of this challenge, there were also times I felt frustrated. At these times, my parents, sister and friends were always there to cheer me up. I would like to thank them for their support and diversion. Special thanks go out to Marian, Nicole and Marthe who have helped me to make this report readable for others.

Finally, I would like to thank the person who has the biggest contribution in the realisation of my report, Kenneth Meijer. Kenneth taught me to put things into perspective and now I am starting to believe that ghosts really don't exist. Moreover, he has drawn my attention to the vacancy of my new job, in which I can apply all that I have learned over the last year.

It was a year in which I have learned a lot, and made a lot of new friends, as well human as new software friends. I am positive that of the projects I was able to choose from, this was the most fun, interesting and instructive one. I hope that you have enjoyed reading the report.

Pamela de Jong

Appendix A:

Categorisation of lower extremity Muscles

Table 1.1 Overview of the most important muscles in recumbent cycling

Function	Monoarticular	Bi-articular
Hip Extensors	Gulteus Maximus	Semitendinosus, Semimembranosus, Biceps Femoris Caput Longum
Hip Flexors	Iliopsoas	Rectus Femoris, Sartorius
Hip Abductors	Gluteus Maximus, Gluteus Medius, Gluteus Minimus	Tensor Fasciae Latae
Hip Adductors	Adductor Magnus, Add. Longus, Add. Breve	Gracilis
Hip Exorotator	Piriformis	
Knee Extensor	Vastus Lateralis, Vastius intermedius, Vastus lateralis	Rectus Femoris, Tensor Fasciae Latae
Knee Flexor	Biceps Femoris Caput Breve	Gastrochnemius, Gracilis, Sartorius, Biceps Femoris Caput Longum, Semitendinosus, Semimembranosus
Medial rotator		Gracilis, Sartorius, Semitendinosus, Semimembranosus
Ankle Dorsi Flexor	Tibialis Anterior, Peroneus Tertius, Extensor hallucis Longus, Extensor Digitorum Longus	
Ankle Plantair Flexor	Soleus, Flexor Hallucis Longus, Flexor Digitorum Longus, Tibialis posterior, Peroneus Longus	Gastrochnemius
Ankle inversion	Tibialis Posterior, Tibialis Anterior	
Ankle Eversion	Peroneus Longus, Peroneus Breve	

Appendix B

Energy expenditure per litre oxygen at specific RQ

Table 12 *Caloric equivalents and corresponding nutrient compounds catabolised at specific RQ's [44]*

Nonprotein RQ	kcal per LO_2	Percentage kcal derived from: Carbohydrate	Percentage kcal derived from: Fat	Grams per LO_2: Carbohydrate	Grams per LO_2: Fat
0.707	4.686	0.0	100.0	0.000	0.496
0.71	4.690	1.1	98.9	0.012	0.491
0.72	4.702	4.8	95.2	0.051	0.476
0.73	4.714	8.4	91.6	0.090	0.460
0.74	4.727	12.0	88.0	0.130	0.444
0.75	4.739	15.6	84.4	0.170	0.428
0.76	4.750	19.2	80.8	0.211	0.412
0.77	4.764	22.8	77.2	0.250	0.396
0.78	4.776	26.3	73.7	0.290	0.380
0.79	4.788	29.9	70.1	0.330	0.363
0.80	4.801	33.4	66.6	0.371	0.347
0.81	4.813	36.9	63.1	0.413	0.330
0.82	4.825	40.3	59.7	0.454	0.313
0.83	4.838	43.8	56.2	0.496	0.297
0.84	4.850	47.2	52.8	0.537	0.280
0.85	4.862	50.7	49.3	0.579	0.263
0.86	4.875	54.1	45.9	0.621	0.247
0.87	4.887	57.5	42.5	0.663	0.230
0.88	4.899	60.8	39.2	0.705	0.213
0.89	4.911	64.2	35.8	0.749	0.195
0.90	4.924	67.5	32.5	0.791	0.178
0.91	4.936	70.8	29.2	0.834	0.160
0.92	4.948	74.1	25.9	0.877	0.143
0.93	4.961	77.4	22.6	0.921	0.125
0.94	4.973	80.7	19.3	0.964	0.108
0.95	4.985	84.0	16.0	1.008	0.090
0.96	4.998	87.2	12.8	1.052	0.072
0.97	5.010	90.4	9.6	1.097	0.054
0.98	5.022	93.6	6.4	1.142	0.036
0.99	5.035	96.8	3.2	1.186	0.018
1.00	5.047	100.0	0	1.231	0.000

Appendix C

Fractions Fast twitch fibre types [31]

	%FT
Soleus	0,25
Gastrochnemius	0,52
FlexorDigitorLongus	0,50
FlexorHallucisLongus	0,50
TibialisPosterior	0,50
PeroneusBrevis	0,38
TibialisAnterior	0,27
ExtensorDigitorumLongus	0,53
ExtensorHallucisLongus	0,50
VastusLateralis	0,52
VastudMedialis	0,53
VastusIntermedius	0,50
RectorFemoris	0,62
Semitendinosus	0,50
Semimembranosus	0,50
Bicepsfemoriscaputlongum	0,33
BicepsfemoriscaputBreve	0,33
Sartorius	0,50
Gracilis	0,50
Iliopsoas	0,51
Gluteusminimus1	0,50
Gluteusminimus2	0,50
Gluteusminimus3	0,50
GluteusMedius1	0,50
GluteusMedius2	0,50
GluteusMedius3	0,50
GluteusMaximus1	0,48
GluteusMaximus2	0,48
GluteusMaximus3	0,48
TensorFasciaeLatae	0,50
Piriformis	0,50
AdductorLongus	0,50
AdductorMagnus1	0,47
AdductorMagnus2	0,47
AdductorMagnus3	0,37

Appendix D

Maximal activities of muscles in the optimal configurations.

right leg	subj 1 FW A	subj 1 FW E	subj 2 FW A	subj 2 FW E	subj 1 BW A	subj 1 BW E	subj 2 BW A	subj 2 BW E
soleus	0,50	0,50	0,54	0,48	0,59	0,71	0,72	0,75
gastrochnemius	0,51	0,55	0,63	0,74	0,59	0,71	0,72	0,85
flexordigitorumlongus	0,50	0,50	0,58	0,48	0,59	0,59	0,73	0,85
flexorhallucislongum	0,50	0,50	0,58	0,48	0,59	0,71	0,73	0,77
tibialis posterior	0,50	0,50	0,58	0,48	0,55	0,59	0,73	0,85
peroneusbrevis	0,51	0,56	0,63	0,74	0,59	0,71	0,72	0,77
tibialis anterior	0,46	0,50	0,58	0,44	0,59	0,68	0,73	0,85
extensor digitorumlong	0,51	0,56	0,63	0,74	0,59	0,71	0,71	0,77
extensor hallucis longu	0,46	0,50	0,62	0,64	0,59	0,71	0,73	0,85
vastus lateralis	0,51	0,56	0,63	0,74	0,59	0,71	0,73	0,77
vastus medialis	0,51	0,56	0,63	0,74	0,59	0,71	0,73	0,77
vastus intermedius	0,51	0,56	0,63	0,74	0,59	0,71	0,73	0,77
rectures femoris	0,51	0,56	0,63	0,74	0,59	0,71	0,72	0,85
semitendinosous	0,51	0,55	0,63	0,74	0,59	0,71	0,73	0,77
semimembranosous	0,50	0,55	0,62	0,67	0,55	0,50	0,73	0,77
bicepsfemoriscaputlon	0,51	0,55	0,62	0,73	0,57	0,68	0,73	0,77
bicepsfemoriscaputbre	0,51	0,55	0,63	0,74	0,59	0,71	0,71	0,85
sartorius	0,51	0,55	0,63	0,74	0,59	0,71	0,71	0,85
gracilis	0,51	0,55	0,63	0,74	0,49	0,35	0,67	0,66
iliopsoas	0,51	0,55	0,63	0,74	0,59	0,70	0,71	0,85
gluteusminimus1	0,50	0,50	0,63	0,72	0,59	0,71	0,71	0,77
gluteusminimus2	0,50	0,51	0,63	0,74	0,59	0,71	0,71	0,77
gluteusminimus3	0,51	0,56	0,63	0,74	0,59	0,71	0,71	0,85
gluteusmedius1	0,50	0,50	0,52	0,44	0,52	0,65	0,70	0,77
gluteusmedius2	0,50	0,50	0,62	0,64	0,49	0,48	0,59	0,76
gluteusmedius3	0,50	0,50	0,63	0,66	0,46	0,43	0,55	0,76
gluteusmaximus1	0,51	0,55	0,63	0,74	0,59	0,71	0,73	0,77
gluteusmaximus2	0,51	0,55	0,62	0,74	0,59	0,71	0,73	0,77
gluteusmaximus3	0,50	0,55	0,62	0,74	0,59	0,71	0,73	0,77
tensorfasciaelatae	0,51	0,55	0,63	0,74	0,59	0,59	0,67	0,85
piriformis	0,51	0,56	0,63	0,74	0,59	0,71	0,73	0,77
adductorlongus	0,51	0,50	0,62	0,67	0,59	0,30	0,70	0,64
adductormagnus1	0,50	0,55	0,62	0,74	0,59	0,71	0,73	0,77
adductormagnus2	0,50	0,55	0,62	0,74	0,59	0,71	0,73	0,77
adductormagnus3	0,50	0,55	0,62	0,74	0,56	0,37	0,72	0,77

maximum right leg
maximum left leg
maximum both

Appendix E

Individual muscle efficiencies including delta differences between configurations

FW = forward cycling
BW = backward cycling
E = optimal energy expenditure configuration
A = optimal peak activation configuration

Subject 1	FW E	FW A	∆ FW E-A	∆ FW-BW E	∆ FW-BW A
soleus	0,253	0,268	0,014	0,053	0,046
gastrochnemius	0,105	0,096	-0,010	-0,084	-0,089
flexordigitorumlongus	0,184	0,183	-0,001	-0,339	-0,314
flexorhallucislongum	0,328	0,319	-0,009	-0,017	0,053
tibialis posterior	0,191	0,176	-0,015	-0,515	-0,357
peroneusbrevis	-0,031	-0,026	0,005	0,050	0,112
tibialis anterior	0,164	0,176	0,012	0,133	0,114
extensor digitorumlongus	0,175	0,182	0,007	0,121	0,127
extensor hallucis longus	0,139	0,151	0,012	0,151	0,152
vastus lateralis	0,358	0,353	-0,005	0,016	-0,022
vastus medialis	0,375	0,375	-0,001	0,006	-0,028
vastus intermedius	0,367	0,361	-0,007	0,003	-0,030
recturs femoris	0,310	0,307	-0,003	-0,063	0,000
semitendinosous	0,249	0,240	-0,009	0,053	0,034
semimembranosous	0,408	0,400	-0,008	0,028	0,065
bicepsfemoriscaputlongum	0,375	0,368	-0,007	-0,002	-0,001
bicepsfemoriscaputbreve	0,204	0,185	-0,019	-0,001	0,036
sartorius	0,165	0,140	-0,025	-0,027	-0,014
gracilis	0,130	0,115	-0,015	0,071	-0,030
iliopsoas	0,064	0,064	0,000	-0,016	-0,007
gluteusminimus1	0,169	0,190	0,021	0,007	-0,008
gluteusminimus2	0,187	0,205	0,018	-0,014	-0,003
gluteusminimus3	0,205	0,222	0,016	0,008	0,021
gluteusmedius1	0,148	0,162	0,015	0,050	0,014
gluteusmedius2	0,247	0,236	-0,011	-0,010	-0,011
gluteusmedius3	0,227	0,185	-0,042	0,047	0,065
gluteusmaximus1	0,185	0,177	-0,009	0,030	0,033
gluteusmaximus2	0,146	0,130	-0,015	-0,037	0,000
gluteusmaximus3	0,211	0,231	0,020	-0,004	0,010
tensorfasciaelatae	0,059	0,026	-0,033	-0,017	0,081
piriformis	0,123	0,145	0,023	-0,001	0,007
adductorlongus	0,146	0,089	-0,056	-0,010	-0,011
adductormagnus1	0,262	0,284	0,022	0,018	0,038
adductormagnus2	0,244	0,266	0,022	0,044	0,059
adductormagnus3	0,268	0,289	0,022	0,006	0,062

Subject 1	BW E	BW A	∆ BW E-A
soleus	0,3066	0,31398	0,007
gastrochnemius	0,021403	0,007254	-0,014
flexordigitorumlongus	-0,15537	-0,13138	0,024
flexorhallucislongum	0,31066	0,3716	0,061
tibialis posterior	-0,32419	-0,18089	0,143
peroneusbrevis	0,01891	0,085533	0,067
tibialis anterior	0,29649	0,28998	-0,007
extensor digitorumlongus	0,29654	0,30963	0,013

extensor hallucis longus	0,28965	0,30288	0,013
vastus lateralis	0,37424	0,33054	-0,044
vastus medialis	0,38146	0,3464	-0,035
vastus intermedius	0,3705	0,33049	-0,040
recturs femoris	0,2468	0,30697	0,060
semitendinosous	0,3023	0,27427	-0,028
semimembranosous	0,43646	0,46492	0,028
bicepsfemoriscaputlongum	0,37283	0,36708	-0,006
bicepsfemoriscaputbreve	0,20339	0,22096	0,018
sartorius	0,13725	0,1253	-0,012
gracilis	0,20123	0,085135	-0,116
iliopsoas	0,04723	0,056641	0,009
gluteusminimus1	0,17533	0,18179	0,006
gluteusminimus2	0,17313	0,20191	0,029
gluteusminimus3	0,21306	0,24266	0,030
gluteusmedius1	0,19817	0,17658	-0,022
gluteusmedius2	0,23714	0,22483	-0,012
gluteusmedius3	0,27348	0,25027	-0,023
gluteusmaximus1	0,21543	0,20918	-0,006
gluteusmaximus2	0,10875	0,13026	0,022
gluteusmaximus3	0,20769	0,24055	0,033
tensorfasciaelatae	0,04209	0,10704	0,065
piriformis	0,12109	0,15213	0,031
adductorlongus	0,13625	0,078912	-0,057
adductormagnus1	0,28008	0,32195	0,042
adductormagnus2	0,28843	0,32513	0,037
adductormagnus3	0,27359	0,35143	0,078

Subject 2	FW E	FW A	Δ FW E-A	Δ FW- W E	Δ FW-BW A
soleus	0,146	0,258	0,112	-0,126	0,010
gastrochnemius	0,148	0,118	-0,030	0,125	0,110
flexordigitorumlongus	0,129	0,240	0,110	-0,010	0,139
flexorhallucislongum	0,296	0,387	0,092	-0,029	0,068
tibialis posterior	0,192	0,228	0,036	0,188	0,104
peroneusbrevis	-0,040	-0,079	-0,039	0,116	-0,056
tibialis anterior	-0,433	0,011	0,444	-0,630	-0,297
extensor digitorumlongus	0,073	0,176	0,103	-0,247	-0,148
extensor hallucis longus	-0,022	0,149	0,170	-0,251	-0,150
vastus lateralis	0,327	0,325	-0,003	-0,009	0,033
vastus medialis	0,350	0,343	-0,006	0,003	0,031
vastus intermedius	0,340	0,331	-0,009	-0,008	0,017
recturs femoris	0,293	0,282	-0,010	-0,005	-0,050
semitendinosous	0,305	0,221	-0,084	-0,015	-0,070
semimembranosous	0,359	0,347	-0,012	-0,030	-0,018
bicepsfemoriscaputlongum	0,345	0,334	-0,011	-0,012	-0,010
bicepsfemoriscaputbreve	0,240	0,216	-0,025	0,002	-0,028
sartorius	0,200	0,204	0,004	0,061	0,087
gracilis	0,196	0,119	-0,077	-0,036	-0,004
iliopsoas	0,077	0,132	0,055	0,015	0,079
gluteusminimus1	0,187	0,226	0,038	-0,009	0,028
gluteusminimus2	0,205	0,224	0,019	0,004	0,019
gluteusminimus3	0,251	0,248	-0,004	0,024	0,005
gluteusmedius1	0,047	0,121	0,074	-0,173	-0,118
gluteusmedius2	0,301	0,208	-0,093	-0,004	-0,058
gluteusmedius3	0,300	0,216	-0,084	0,008	-0,076
gluteusmaximus1	0,219	0,184	-0,035	0,041	0,017

gluteusmaximus2	0,166	0,142	-0,024	0,028	0,012
gluteusmaximus3	0,211	0,270	0,059	-0,020	0,003
tensorfasciaelatae	0,047	0,061	0,015	0,016	-0,079
piriformis	0,149	0,199	0,051	0,027	0,024
adductorlongus	0,187	0,091	-0,096	0,028	-0,002
adductormagnus1	0,230	0,305	0,075	-0,065	-0,020
adductormagnus2	0,213	0,290	0,076	-0,069	-0,036
adductormagnus3	0,227	0,325	0,099	-0,066	-0,028

Subject 2	BW E	BW A	Δ BW E-A
soleus	0,272	0,248	-0,024
gastrochnemius	0,023	0,008	-0,014
flexordigitorumlongus	0,139	0,100	-0,039
flexorhallucislongum	0,325	0,319	-0,006
tibialis posterior	0,004	0,124	0,119
peroneusbrevis	-0,155	-0,023	0,133
tibialis anterior	0,197	0,308	0,111
extensor digitorumlongus	0,320	0,325	0,005
extensor hallucis longus	0,230	0,299	0,069
vastus lateralis	0,336	0,292	-0,045
vastus medialis	0,346	0,313	-0,034
vastus intermedius	0,348	0,314	-0,033
recturs femoris	0,297	0,333	0,035
semitendinosous	0,320	0,291	-0,029
semimembranosous	0,389	0,365	-0,024
bicepsfemoriscaputlongum	0,357	0,345	-0,012
bicepsfemoriscaputbreve	0,238	0,243	0,005
sartorius	0,139	0,117	-0,021
gracilis	0,232	0,122	-0,110
iliopsoas	0,062	0,053	-0,009
gluteusminimus1	0,196	0,197	0,001
gluteusminimus2	0,200	0,205	0,005
gluteusminimus3	0,227	0,242	0,015
gluteusmedius1	0,220	0,238	0,018
gluteusmedius2	0,305	0,266	-0,039
gluteusmedius3	0,292	0,291	-0,001
gluteusmaximus1	0,178	0,167	-0,011
gluteusmaximus2	0,138	0,131	-0,008
gluteusmaximus3	0,231	0,267	0,036
tensorfasciaelatae	0,031	0,141	0,110
piriformis	0,122	0,176	0,054
adductorlongus	0,160	0,093	-0,067
adductormagnus1	0,295	0,325	0,030
adductormagnus2	0,282	0,325	0,043
adductormagnus3	0,293	0,354	0,061

Appendix F

EMG patterns per subject per configuration, average of three measurements per configuration.

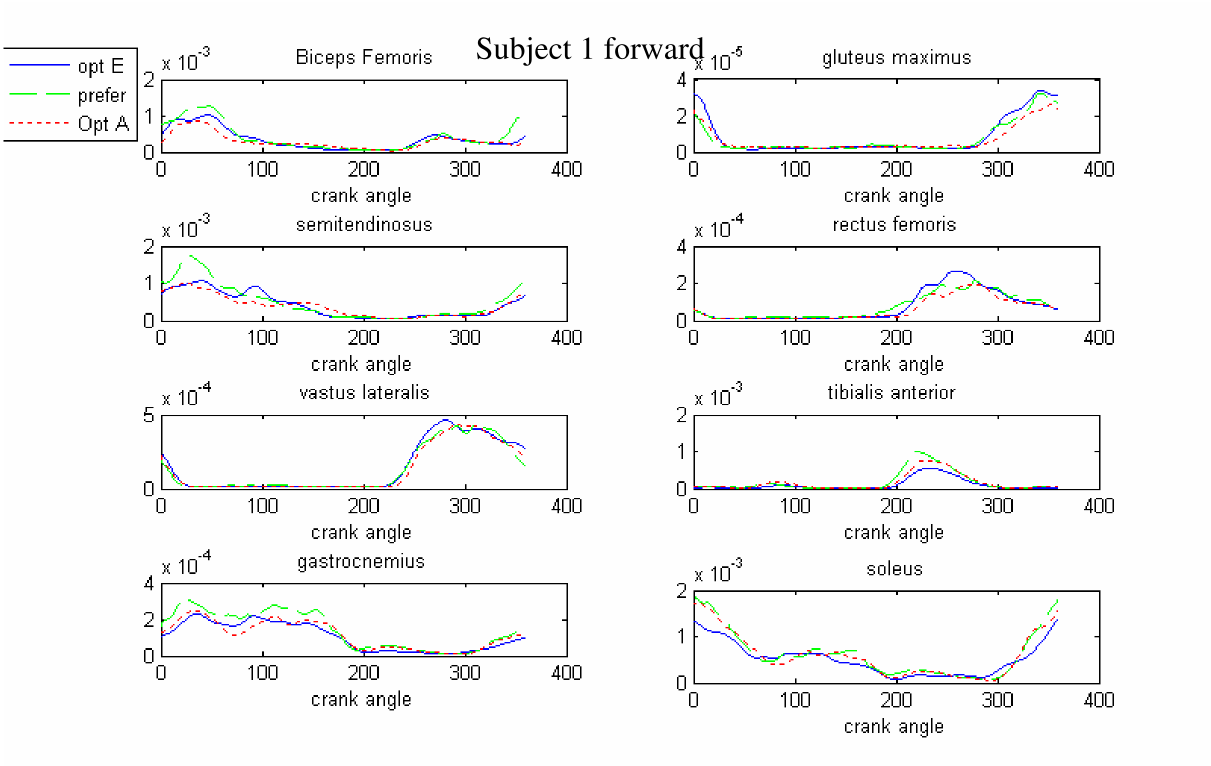

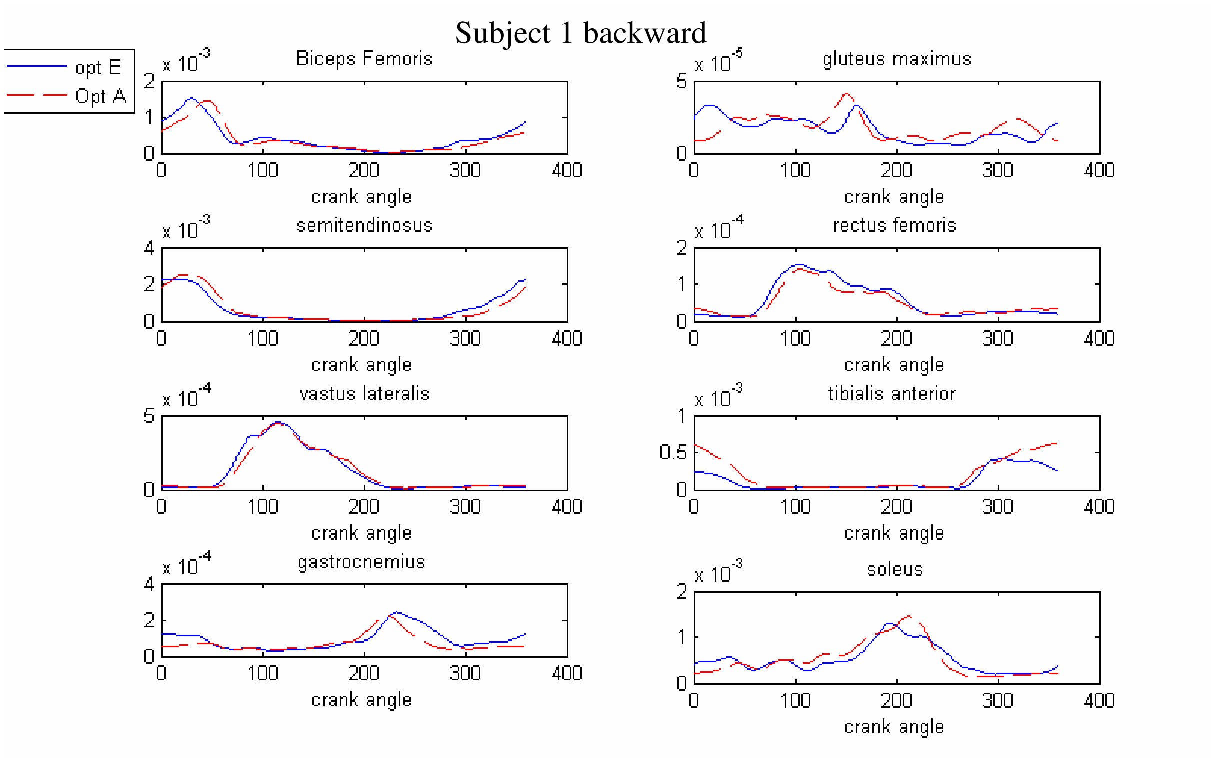

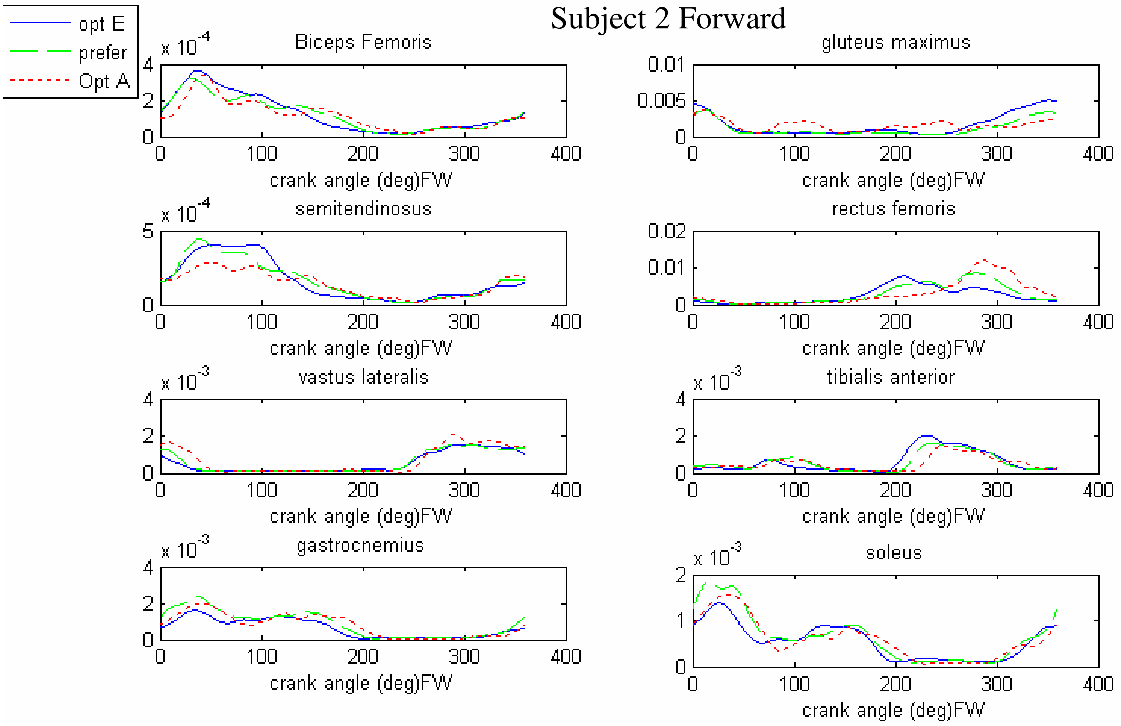

Subject 2 Forward
opt E
prefer
Opt A
Biceps Femoris
gluteus maximus
semitendinosus
rectus femoris
vastus lateralis
tibialis anterior
gastrocnemius
soleus
crank angle (deg)FW

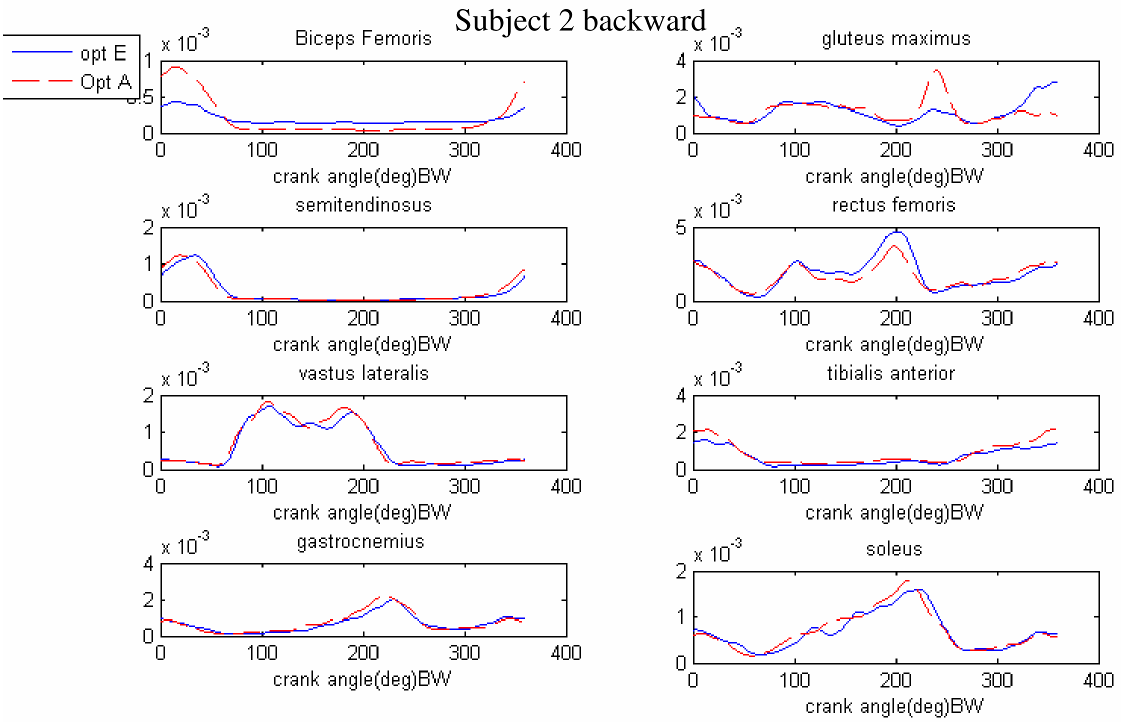

Subject 2 backward
opt E
Opt A
Biceps Femoris
gluteus maximus
semitendinosus
rectus femoris
vastus lateralis
tibialis anterior
gastrocnemius
soleus
crank angle(deg)BW

List of figures

List of Tables

Bibliography

[1-4, 7-11, 13-52]

1. Welbergen E, Clijsen LP: **The influence of body position on maximal performance in cycling**. *Eur J Appl Physiol Occup Physiol* 1990, **61**(1-2):138-142.
2. Price D, Donne B: **Effect of variation in seat tube angle at different seat heights on submaximal cycling performance in man**. *J Sports Sci* 1997, **15**(4):395-402.
3. Ryschon TW, Stray-Gundersen J: **The effect of body position on the energy cost of cycling**. *Med Sci Sports Exerc* 1991, **23**(8):949-953.
4. Gaesser -G-A, Brooks -G-A: **Muscular efficiency during steady-rate exercise: effects of speed and work rate.** . *J-Appl-Physiol* 1975, **38**(6):1132-1139.
5. Sidossis LS, Horowitz JF, Coyle EF: **Load and velocity of contraction influence gross and delta mechanical efficiency**. *Int J Sports Med* 1992, **13**(5):407-411.
6. Marsh AP, Martin PE: **Effect of cycling experience, aerobic power, and power output on preferred and most economical cycling cadences**. *Med Sci Sports Exerc* 1997, **29**(9):1225-1232.
7. Crooijmans, Egdom, Loerakker, Sleutjes: **Voorwaarts versus achterwaarts ligfietsen** In.: University of Maastricht; 2004.
8. Umberger BR, Gerritsen KG, Martin PE: **A model of human muscle energy expenditure**. *Comput Methods Biomech Biomed Engin* 2003, **6**(2):99-111.
9. Rozendal RH, P.A. H: **Inleiding in de Kinesiologie van de Mens**, vol. 6: Wolters Groningen; 1996.
10. Raasch CC, Zajac FE: **Locomotor strategy for pedaling: muscle groups and biomechanical functions**. *J Neurophysiol* 1999, **82**(2):515-525.
11. Ting LH, Kautz SA, Brown DA, Zajac FE: **Phase reversal of biomechanical functions and muscle activity in backward pedaling**. *J Neurophysiol* 1999, **81**(2):544-551.
12. Rasmussen, Damsgaard, Voigt: **Ergonomic optimisation of a bicycle**. In: *Third World Congress of Structural and Multidisciplinary Optimization 1999; Amherst, New York, USA*; 1999.
13. Marsh AP, Martin PE, Foley KO: **Effect of cadence, cycling experience, and aerobic power on delta efficiency during cycling**. *Med Sci Sports Exerc* 2000, **32**(9):1630-1634.
14. Hagberg, Mullin, Giese, Spitznagel: **Effect of pedalling rate on submaximal exercise responses of competitive cyclists**. *Journal of applied Physiology* 1981, **51**:447-451.
15. MacIntosh BR, Neptune RR, Horton JF: **Cadence, power, and muscle activation in cycle ergometry**. *Med Sci Sports Exerc* 2000, **32**(7):1281-1287.
16. Neptune RR, Hull ML: **A theoretical analysis of preferred pedaling rate selection in endurance cycling**. *J Biomech* 1999, **32**(4):409-415.
17. Neptune RR, Herzog W: **The association between negative muscle work and pedaling rate**. *J Biomech* 1999, **32**(10):1021-1026.
18. Savelberg, Port Vd, Willems: **Body configuration in cycling affects muscle recruitment and movement pattern**. *Journal of applied physiology* 2003, **19**:310-324.
19. Gnehm P, Reichenbach S, Altpeter E, Widmer H, Hoppeler H: **Influence of different racing positions on metabolic cost in elite cyclists**. *Med Sci Sports Exerc* 1997, **29**(6):818-823.
20. Raasch CC, Zajac FE, Ma B, Levine WS: **Muscle coordination of maximum-speed pedaling**. *J Biomech* 1997, **30**(6):595-602.

21. Neptune RR, Kautz SA, Zajac FE: **Muscle contributions to specific biomechanical functions do not change in forward versus backward pedaling**. *J Biomech* 2000, **33**(2):155-164.
22. Bressel E, Heise GD, Bachman G: **A neuromuscular and metabolic comparison between forward and reverse pedalling.** . *Journal of applied physiology* 1998, **14**:401-411.
23. Daams: **Een inventarisatie van de ergonomische aspecten van ligfietsen**. *Tijdschrift voor Ergonomie* 1999, **24**(2):42-50.
24. Hakansson NA, Hull ML: **Functional roles of the leg muscles when pedaling in the recumbent versus the upright position**. *J Biomech Eng* 2005, **127**(2):301-310.
25. Gregor SM, Perell KL, Rushatakankovit S, Miyamoto E, Muffoletto R, Gregor RJ: **Lower extremity general muscle moment patterns in healthy individuals during recumbent cycling**. *Clin Biomech (Bristol, Avon)* 2002, **17**(2):123-129.
26. Reiser P: **Backrest influence on recumbent cycling power output**. In: *ASME Bioengineering Conference: 1999; Montana*; 1999.
27. Neptune RR, Kautz SA, Hull ML: **The effect of pedaling rate on coordination in cycling**. *J Biomech* 1997, **30**(10):1051-1058.
28. Christensen, Damsgaard, Rasmussen, Zee d: **Muscle model for inverse dynamic musculo-skeletal models** *not published* 2002.
29. Bhargava LJ, Pandy MG, Anderson FC: **A phenomenological model for estimating metabolic energy consumption in muscle contraction**. *J Biomech* 2004, **37**(1):81-88.
30. Rasmussen J, Damsgaard M, Voigt M: **Muscle recruitment by the min/max criterion -- a comparative numerical study**. *J Biomech* 2001, **34**(3):409-415.
31. Winters JM, Woo SLY: **Multiple muscle systems**. New York: Springer-Verlag; 1990.
32. Rasmussen, Zee d, Damsgaard, Christensen, Clemens, Siebertz: **A general method for scaling musculo-skeletal models**. In: *International symposium on computer simulation in Biomechanics: 2005; Cleveland*; 2005.
33. Frankenfield DC, A. RW, N. CR, S. SJ, D. B: **Limits of body mass index to detect obesity and predict body composition.** *Nutrition* 2001, **17**:26-30.
34. Johnson, Polgar, Weightman, Appleton: **Data on th edistribution of fibre types in thirty-six human muscles: An autopsy study** *Journal of the Neurological Sciences* 1973, **18**:111-129.
35. Winter DA: **Biomechanics and Motor Control of Human Movement**, 2nd Edition edn: Wiley-Interscience; 1990
36. Al-Haboubi: **Modelling energy expenditure during cycling** *Ergonomics* 1999, **42**(3):416-427.
37. Guyton, hall: **Textbook of physiology**, 9 edn: Saunders company 1996.
38. Umberger BR, Gerritsen KG, Martin PE: **Muscle fiber type effects on energetically optimal cadences in cycling**. *J Biomech* 2005.
39. Epstein M, Herzog W: **Theoretical models of skeletal muscle.** . Chichester: John Wiley and Sons; 1999.
40. Landau, Everitt: **A handbook of statistical analyses using SPSS /**: Boca Raton, Fla., [etc.] : Chapman & Hall/CRC; 2004.
41. Li L, Baum BS: **Electromechanical delay estimated by using electromyography during cycling at different pedaling frequencies**. *J Electromyogr Kinesiol* 2004, **14**(6):647-652.
42. Press, Teukolsky, Vetterling, al.] e: **Numerical recipes in C : the art of scientific computing** vol. 2. Cambridge Cambridge University Press; 1992
43. [http://www.shokhirev.com/nikolai/abc/optim/optim/optim.html].
44. McArdle, Katch, Katch: **Exercise physiology : energy, nutrition and human performance** vol. 4. Baltimore: Williams & Wilkins Annotatie: ill; 1996

45. Stienen, Kiers, Bottinelli, Reggiani: **Myofibrillar ATPase activity in skinned human skeletal muscle fibres: fibre type and temperature dependence**. *Nutrition* 1996, **493**(2):299-307.
46. González-Alonso, Quistorff, Krustrup, Bangsbo, Saltin: **Heat production in human skeletal muscle at the onset of intense dynamic exercise** *Journal of Physiology* 2000, **524**:603-615.
47. Rassier, MacIntosh, Herzog W: **Length dependence of active force production in skeletal muscle**. *Journal of applied Physiology* 1999, **86**(5):1445-1457.
48. Savelberg HH, Meijer K: **Contribution of mono- and biarticular muscles to extending knee joint moments in runners and cyclists**. *J Appl Physiol* 2003, **94**(6):2241-2248.
49. van Soest O, Casius LJ: **Which factors determine the optimal pedaling rate in sprint cycling?** *Med Sci Sports Exerc* 2000, **32**(11):1927-1934.
50. Redfield, Hull: **On the relation between joint moments and pedalling rates at constant power in bicycling**. *Journal of Biomechanics* 1986, **19**:317-329.
51. van Ingen Schenau GJ, Boots PJ, de Groot G, Snackers RJ, van Woensel WW: **The constrained control of force and position in multi-joint movements**. *Neuroscience* 1992, **46**(1):197-207.
52. Zameziati K, Mornieux G, Rouffet D, Belli A: **Relationship between the increase of effectiveness indexes and the increase of muscular efficiency with cycling power**. *Eur J Appl Physiol* 2006, **96**(3):274-281.
53. Zamparo P, Capelli C, Cencigh P: **Energy cost and mechanical efficiency of riding a four-wheeled, human-powered, recumbent vehicle**. *Eur J Appl Physiol* 2000, **83**(6):499-505.

[1, 49, 51-53]